



UNIVERSITÀ DEGLI STUDI DI UDINE
DOTTORATO DI RICERCA IN
TECNOLOGIE CHIMICHE ED ENERGETICHE
XXVII CICLO

Distributed generation: prospects for fuel cells based micro-cogeneration systems

Rodolfo TACCANI

COMMISSIONE

Prof. Gianfranco Di Giuseppe	REVISORE
Prof. Andrea Lazzaretto	REVISORE
Dr.ssa Monica Fabrizio	COMMISSARIO
Prof. Piero Pinamonti	COMMISSARIO
Prof. Giuseppe Spazzafumo	COMMISSARIO
Prof. ssa Marta BOARO	SUPERVISORE

Prof. Alfredo SOLDATI	COORDINATORE DI DOTTORATO
-----------------------	---------------------------

To my daughter who has just arrived

SUMMARY

Distributed generation can be an option to reduce energy consumption and facilitate the introduction of bigger amount of electricity produced with renewable energy sources.

In the first part of the thesis an overview on fossil fuels power plants and primary movers for distributed micro-cogeneration systems is given. Then, the effect of renewable energy sources on the operation of the European power plants and grid is discussed.

In the second part of the thesis generators based on PEM fuel cells are considered and analyzed from a theoretical and experimental point of view to what concerns performance and life span.

Experimental data on a micro generator are presented. Control complexity and performance degradation over time are, in particular, studied. Degradation is also studied considering the effect of load cycles profile over performance.

The research is completed with the analysis of the energy saving achievable by fuel cell micro-cogeneration systems.

SOMMARIO

La generazione distribuita di energia è da molti considerata una delle soluzioni per ridurre i consumi energetici e per agevolare l'introduzione di quote sempre più importanti di elettricità provenienti da fonti rinnovabili di energia. Nella prima parte della tesi viene fatta una panoramica sulle tecnologie oggi più adatte alla generazione distribuita e viene fatta un'analisi su alcune delle problematiche che la massiccia introduzione di elettricità da fonti rinnovabili sta comportando nella gestione della rete di distribuzione e delle centrali di produzione, a livello europeo.

Nella seconda parte delle tesi, si va ad analizzare un particolare tipo di impianto per la micro-cogenerazione distribuita: i generatori elettrici basati su celle a combustibile ad elettrolita polimerico.

Si vanno ad analizzare, sia dal punto di vista teorico che sperimentale, le prestazioni, la vita utile ed alcune delle problematiche relative al degrado funzionale nel tempo.

Si presentano dei dati sperimentali su un micro-cogeneratore di piccola taglia e se ne evidenziano le problematiche di controllo e di degrado delle prestazioni nel tempo. In particolare, a questo riguardo, vengono riportati alcuni dati sperimentali atti a valutare l'effetto dei cicli di carico sul degrado delle prestazioni delle celle.

La ricerca si completa con la presentazione di una metodologia per il calcolo del risparmio energetico in funzione delle caratteristiche del generatore e delle scelte di gestione dello stesso.

CONTENTS

Summary	3
Sommario	4
Index of figures.....	7
Index of tables	11
Nomenclature.....	13
Acronyms.....	13
Subscripts and superscripts.....	13
Preface.....	14
Introduction.....	15
1 Generation and Distributed generation: an overview	19
1.1 Introduction	19
1.2 Power generation: facts and figures	19
1.3 Distributed generation	23
1.4 The net benefit of RES DG	29
1.5 Harnessing RES	39
1.5.1 The potential of micro-CHP systems.....	40
2 Micro-cogeneration: the technologies.....	43
2.1 Introduction	43
2.2 Choice of the reference plant.....	43
2.3 Technologies	44
2.4 Reciprocating Internal Combustion Engines (ICE).....	44
2.5 Stirling engines	46
2.6 Micro gas turbine.....	46
2.7 Organic Rankine Cycles.....	47
2.8 Fuel cells	48
2.8.1 Introduction.....	48
2.8.2 Operating principle.....	48
2.8.3 System integration and efficiency.....	50
2.8.4 PEM fuel cells and micro-CHP	51

2.8.5 Costs and applications	54
2.9 Micro-CHP: technologies comparison.....	55
3 Papers and reports presented during the research	58
3.1 Introduction	58
3.2 Literature review and background.....	59
3.3 Simulation models development	59
3.4 Test rig and automation system set up	62
3.5 Experimental characterization of single cells and stack	63
3.6 Experimental characterization of the fuel processor and complete system.....	65
3.7 Experimental degradation analysis	72
4 Conclusions	75
Acknowledgments	81
References	83
Annex 1:	88

INDEX OF FIGURES

Figure 1. World energy consumption, 1990-2040 (quadrillion Btu). Projection according to IEO2013 Reference case [9].	19
Figure 2. World electricity generation by fuel used (billion kilowatthours). Projection according to IEO2013 Reference case [9].	20
Figure 3. Gas turbines and Combined cycle plants BAT efficiency trend over years [10].	20
Figure 4. Combined cycle plants fleet efficiency over years. [10]	21
Figure 5. Cumulative CCGT and OCGT capacity. Gas fired power capacity, particularly CCGT has increased rapidly since 2000 [10].	21
Figure 6. Coal-fired power plants fleet efficiency over years [10].	22
Figure 7. Natural gas spot price over the years. [10]	22
Figure 8. Ratio of average natural gas and coal prices to crude oil prices. Dotted line: forecast. Fuel price is calculated on an energy-equivalent basis [12].	23
Figure 9. Distributed generation technologies [14].	24
Figure 10. Share of renewable energy in gross final energy consumption [18].	25
Figure 11. EU power mix in 2000 (left) and 2013 (right) [19].	25
Figure 12. Energy mix in EU 2013 [20].	26
Figure 13. Evolution of world PV cumulative installed capacity 2000-2012 (MW) [1].	26
Figure 14. Evolution of European new grid-connected PV capacity 2000-2012 (MW) [1].	27
Figure 15. Power plants efficiency as a function of plant size [21].	28
Figure 16. CHP share of total power production in selected countries [23].	29
Figure 17. Germany: electricity production and spot price. February 2014 [25].	30
Figure 18. Germany: electricity production and spot price. February 2014. Negative intraday price on Feb 16th explanation [25].	30
Figure 19. Business as usual and renewable energy sources: competing technologies? [2]	31
Figure 20. Typical electrical load profile and power mix (black). In red the typical PV production in a sunny day.	31
Figure 21. Germany: day ahead price volume weighted and inflation adjusted (price 2014) [25].	32
Figure 22. Germany: plat type utilization over day ahead spot price [25].	33
Figure 23. Power mix and electricity price in Italy. Average monthly values, July 2013. Elaborated from [26].	34

Figure 24. Electricity cost in Italy. Average hourly values on “Mercato del giorno prima” (Day ahead market) [26].	34
Figure 25. Power mix and electricity price in Italy. Day of highest PV production in July 2013. Elaborated from [26].	35
Figure 26. Power mix and electricity price in Italy. Day of lowest PV production in July 2013. Elaborated from [26].	35
Figure 27. Electricity production in Italy: fuel share. Elaborated from [28].	36
Figure 28. CO ₂ per kWh in Italy. The thermoelectric production encompasses biomass, biogas and biofuel. In the total production RESs are included. In the electrical consumption grid losses and electricity import are included. Elaborated from [28].	37
Figure 29. Addressable market for fuel cells in apartment buildings [39].	40
Figure 30. Number of new PV plants in Italy. Data at July 2014. The different colors indicate the different support schemes for PV (Conto Energia). Elaborated from [40].	41
Figure 31. DG and business as usual transition...[2].	42
Figure 32. Micro CHP concept.	43
Figure 33. Typical energy balance for a 1 kW system. Fuel inlet 100%, reference to LHV [21].	45
Figure 34. Part load efficiency of a micro GT [Elaborated from Capstone data [21]].	47
Figure 35. Schematic view of a fuel cell.	48
Figure 36. Schematic view of a fuel cell: from single cell to stack.	49
Figure 37. Typical polarization curve for a PEM fuel cells.	50
Figure 38. Typical efficiency curves for different types of engines with power output higher than 200 kW. a) Low pressure, low temperature fuel cell system. b) High pressure, high temperature fuel cell system. c) Fuel cell system with an on-board reformer. d) Compression-ignition engine (diesel). e) Spark-ignition engine. Elaborated from [7].	51
Figure 39. SEM image of a cross section of a HTPEM MEA before operation (a) and after operation (b).	53
Figure 40. Japan FC sales and subsidy [62].	54
Figure 41. Micro-CHP in Europe, some of the competitors in SOFC and PEM [63].	55
Figure 42. PV cost trend. In ten years the price of residential system has halved [64].	57
Figure 43. Fuel cell and system electrical and thermal efficiencies as function of stack load [VIII].	60
Figure 44. System lay-out [XI].	61
Figure 45. Electric and thermal power load curves assumed for the January typical day [XI].	61
Figure 46. Primary energy saving index for the three considered system configuration [XI].	62
Figure 47. Graphic interface of the data acquisition and control system of the fuel cell based micro-CHP [XIII].	62
Figure 48. Polarization and power density curves measured with the same operating conditions but using different bipolar plates [IV].	63

Figure 49. Stack performance with pure hydrogen, at different operating temperatures. Anode stoichiometry 1.5, cathode stoichiometry 3.0 [I].	64
Figure 50. Influence of CO concentration and operating temperature on the stack current at cell voltage of 0.6 V [I].	64
Figure 51. Simplified schematic of the considered plant [V].	65
Figure 52. Fuel processor startup. Reactors temperature profile over time. Fuel LPG [V].	67
Figure 53. Fuel processor startup. Reactors temperature profile over time. Fuel biogas [XIV].	67
Figure 54. Single cell performance comparison (BioRef = biogas reformat, SimRef = synthetic reformat). Operating temperature: 160 °C [XIV].	68
Figure 55. Stack (22 cells) performance with biogas reformat at different operating temperatures [XIV].	68
Figure 56. Comparison between the stack average cell and single cell performance. Ref-Bio is reformat biogas [XIV].	68
Figure 57. Thermo image of the stack. A temperature difference as high as 25 °C has been measured from stack center to stack end plates.	69
Figure 58. Typical stack voltage distribution at different currents, T=140°C.	70
Figure 59. Biogas, reformat and anode-off gas volumetric composition (vol. dry)	70
Figure 60. Schematic representation of the fuel flows.	70
Figure 61. SAXS scattering intensity curves of MEA_ref, MEA_a) and MEA_b). For each sample, three different areas on the MEA surface have been analyzed (1, 2, 3), as shown in the top right inset of the graph where they has been indicated by colored spots. The intensities of the three sets of samples have been scaled by a factor of 10 to each other in order to resolve better the differences. The arrows indicate the scattering of the Pt particles [XVI].	73
Figure 62. Volume size distributions of MEA_ref, MEA_a, and MEA_b. On the inset, the mean radii with the standard deviations of the distribution are shown. For each sample, three different areas have been analyzed (1, 2, 3) in reference to the inset of Figure 61 [XVI].	74

INDEX OF TABLES

Table 1. Net benefits per year per MW of new electrical capacity: displacement of coal base load production [29].39

Table 2. Main specifications and cost for two micro CHP ICE. Fuel: natural gas [21].45

Table 3. Main specifications for three micro Stirling engine [21].....46

Table 4. Classification of fuel cells according to the electrolyte and main characteristics.50

Table 5. Comparison between LTPEM and HTPEM.....53

Table 6. Comparison of different micro CHP technologies in the range of 1kW.....56

Table 7. Composition of the gas mixtures used in the presented experimental data [I].63

Table 8. System and stack efficiency values72

NOMENCLATURE

Acronyms

AD	Aero Derivative
BAT	Best Available Technology
BOP	Balance of plant
CAES	Compressed Air Energy Storage
CCGT	Combined-Cycle Gas Turbine
CHP	Combined Heat and Power
CSP	Concentrated solar power
DG	Distributed Generation
GT	Gas Turbine
FC	Fuel Cell
HTPEM	High Temperature Proton Exchange Membrane
HD	Heavy Duty
LTPME	Low Temperature Proton Exchange Membrane
MGT	Micro Gas Turbine
NP	Nano-particle
OCGT	Open Cycle Gas Turbine
OECD	Organisation for Economic Co-operation and Development
PES	Primary Energy Saving index
RES	Renewable Energy Source
SMES	Superconducting Magnetic Energy Storage
SNG	Substitute Natural Gas
SW	Software

Subscripts and superscripts

el: electrical

p: peak

PREFACE

Having the chance to complete a PhD after being involved in research for some years, not so say many... is, somehow, a privilege.

It is a privilege in particular if you had the chance to get in touch with young scientists during their PhD years.

It helps make clear how complex is this choice and how challenging is to write a thesis.

As a fresh postgraduate, I was sitting in a car with one well known and charismatic professor who was the PhD supervisor of an Italian researcher I knew well and that we will call Mr. Alpha.

Just talking, I said: "Mr. Alpha has become an assistant professor", and the first reply of the charismatic professor was: "... how many PhD students has he tutored?" meaning that: necessary condition to become a professor is tutoring a certain number of PhD students.

Yes, it is difficult to be a PhD student and to supervise a PhD student. But the thrill to discover something new (or that you think it is new), to share it with colleagues after long months of work ... it is worth the effort.

Nobody tells exactly what it means to enroll for a PhD. The first reason is that, if somebody does, nobody enrolls; the other is that nobody knows exactly... it is a research matter!

INTRODUCTION

A transition from a heavily centralized power grid to one with rooftop solar panels, natural gas generators at homes and businesses, plug-in electric vehicles, and technologies to change the way electricity is produced and used, is clearly underway.

As an example, in Italy, since the introduction of Photovoltaic (PV) incentives in 2007, new PV plants for a total of 17 GW (and rising) have been installed. In a few years, the amount of electricity from solar collectors has jumped from zero to 4% [1]. However, all this has a cost.

Subsidies for renewable energy are running at €7 billion a year in Italy, €16 billion a year in Germany, and in Europe the cumulative cost is around €60 billion [2].

The value of carbon permits and credits traded was down from 62 billion euros in 2012 to 96 billion euros in 2011, a two-year period in which benchmark EU carbon permit prices fell from 18 euros to 5 euros per ton [3]. Due to economy slow growing and availability of natural gas in US, coal is cheap.

High efficiency low polluting power plants (combined cycles gas turbines) are shut down as the price of electricity during peak hours is low and there are no profits when natural gas is used. In these conditions the operation of coal power plants is favored. Coal power plants specific CO₂ production is higher because plant efficiency is lower and fuel carbon content is higher than in natural gas. Thus, the impact of renewable energy sources, in terms of greenhouse gas emissions, is not easy to evaluate.

High flexibility distributed micro-generation / micro-cogeneration and storage seems to be a mean to optimize Renewable energy Sources (RES) utilization [4], [5], [6].

Among distributed generation solutions, fuel cells offer good part-load efficiency, good load following capability and a great flexibility in terms of choice of power output [7].

Objective and methodology

The research question that is addressed in this thesis is:

Can fuel cell based micro-cogeneration systems be a technical and viable option? To what extent these systems can contribute to reduce energy consumption and facilitate the exploitation of RES?

The thesis is organized around the combined use of simulation models and experimental tests in order to assess the potential of a High Temperature PEM Fuel Cell micro-CHP systems.

The research activity includes the following tasks:

Literature review and background

A literature review of DG and micro-cogeneration systems has been carried out, with specific focus on fuel cell systems. An analysis on how micro-cogeneration systems can be integrated into a scenario where RES DG is growing quickly is given.

Simulation models development

A process simulation model has been implemented to design the micro-CHP system. The model has then been used to assess the potential of micro-CHP in combination with distributed electrical storage.

Test rig and automation system set up

A test rig including the necessary equipment to measure the operating variables have been built to characterize the fuel cells both as single units and stacks. In the following phase, a test rig to analyze the performance of the fuel processor and the complete system has also been developed. Such a system encompasses all the necessary automation to operate 24/7 and include all the necessary safety procedures.

Experimental characterization of single cells and stack

Several single cells and different bipolar plate configurations have been tested to identify the right combination of material, components and design that achieve the best performance. On these bases, several stack configurations have been tested with the aim to measure polarization curves, sensitivity to CO and effect of operating temperature.

Experimental characterization of the fuel processor and complete system

A steam reforming reactor (fuel processor) has been used to fuel the stack with natural gas. An extensive series of tests have been carried out in order to measure the efficiency and the effect of fuel composition and operating variable on syngas composition. Tests have then been extended to the fuel processor and stack assembly to study the overall efficiency, the performance degradation over time and to determine the best control strategies that allows avoiding transient conditions that could be detrimental to the system.

Experimental degradation analysis

One of the key issues still open that hamper fuel cells utilization is performance degradation over time. Experimental procedures to perform accelerated degradation tests have been implemented. To have a better insight into catalyst degradation, in the framework of a research project in collaboration with the University of Graz, a procedure to characterize the nano-morphology of the catalyst platinum particles using SAXS (Small Angle X ray Scattering) has been developed. This part of the research is still on-going.

Structure of the present work

In Chapter 1 an overview on how electricity is produced is given. The efficiency trends of the power plants today used are analyzed. The recent introduction of Distributed Generation (DG) based on Renewable Energy Sources (RES) in Europe is discussed and the advantage and not yet resolved problems outlined.

In Chapter 2 emphasis is given on distributed micro-cogeneration (micro-CHP) systems. The technologies today available are presented and the potential benefits of the integration with RES DG are shown.

In Chapter 3 a selection of the published paper is presented in terms of hypothesis, methodology and results. The first part concerns the development of a system energy simulation model that has been used for the development of the system. Then the experimental set up is described and experimental results discussed. In the final part, an experimental study on MEA degradation phenomena is presented.

In Chapter 4 the Conclusions are discussed. The effect of RES is considered and the necessity to improve FC system durability and to reduce costs addressed. Then an outlook on future possible research development is given.

1 GENERATION AND DISTRIBUTED GENERATION: AN OVERVIEW

1.1 Introduction

In the first part of this Chapter, an overview on what is the performance of power plants today available is given. In the second part, distributed generation is defined and discussed. It is pointed out how, in few years, distributed generation has had a widespread diffusion in countries where renewable energy sources have been economically supported.

1.2 Power generation: facts and figures

An accurate source of information on how electricity is generated can be found in the yearly report issued from IEA [8] and the US Department of energy [9]. World energy consumption is growing fast (see Figure 1) and electricity is growing even a faster rate and its demand has doubled in less than 30 years (see Figure 2). Explain projected electricity consumption in Fig 1.

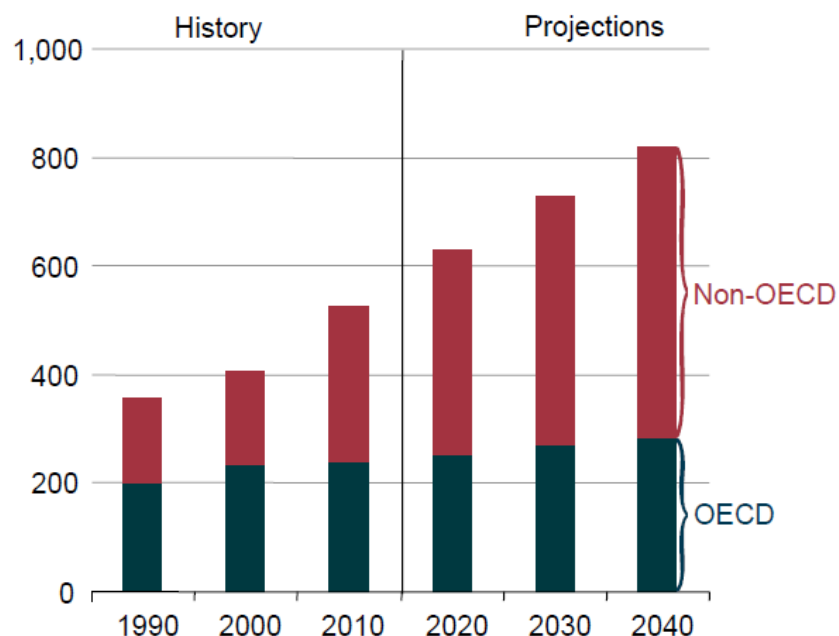


Figure 1. World energy consumption, 1990-2040 (quadrillion Btu). Projection according to IE02013 Reference case [9].

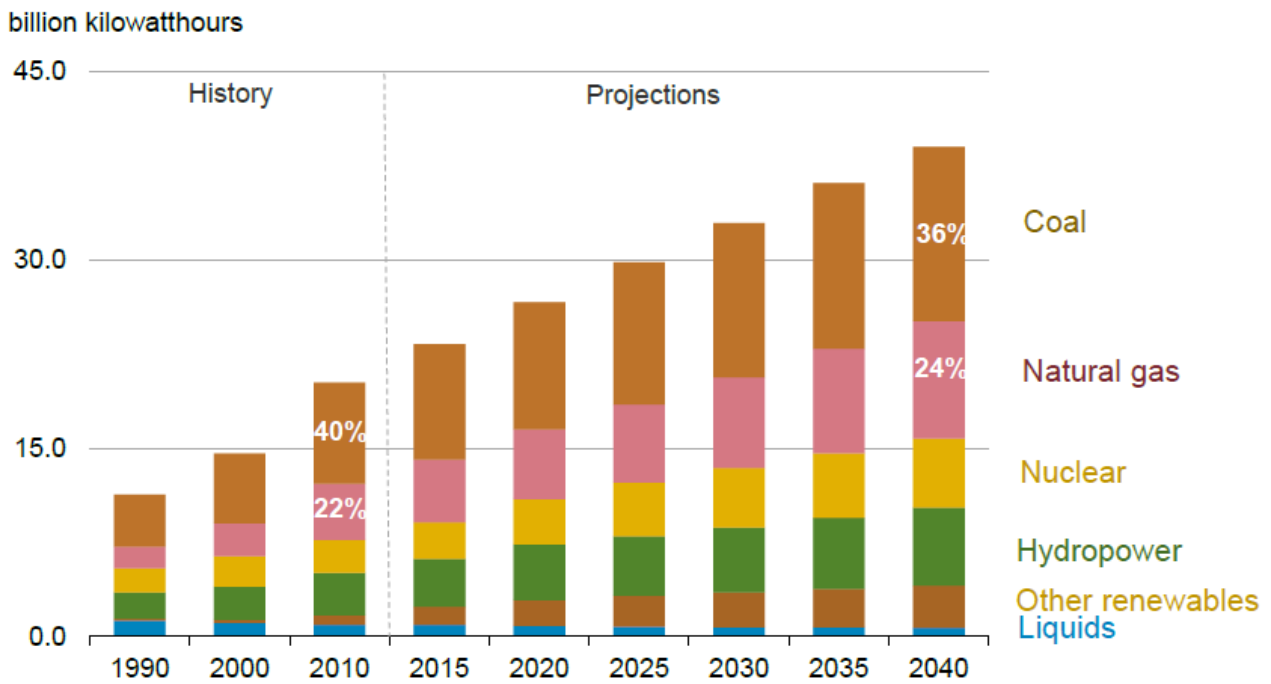


Figure 2. World electricity generation by fuel used (billion kilowatt-hours). Projection according to IE02013 Reference case [9].

In Figure 2 the world electricity generation by different fuel used is shown. The data give an indication of which type of power plant is used from which generation efficiency can be inferred.

For fossil fuels, natural gas is used mainly in gas turbines and combined cycles. Coal is mainly used in steam power plants. Liquid fuels are used mainly in internal combustion engines.

When using natural gas, efficiency can reach 40% in gas turbine power plants and exceed 60% in combined cycles (see Figure 3).

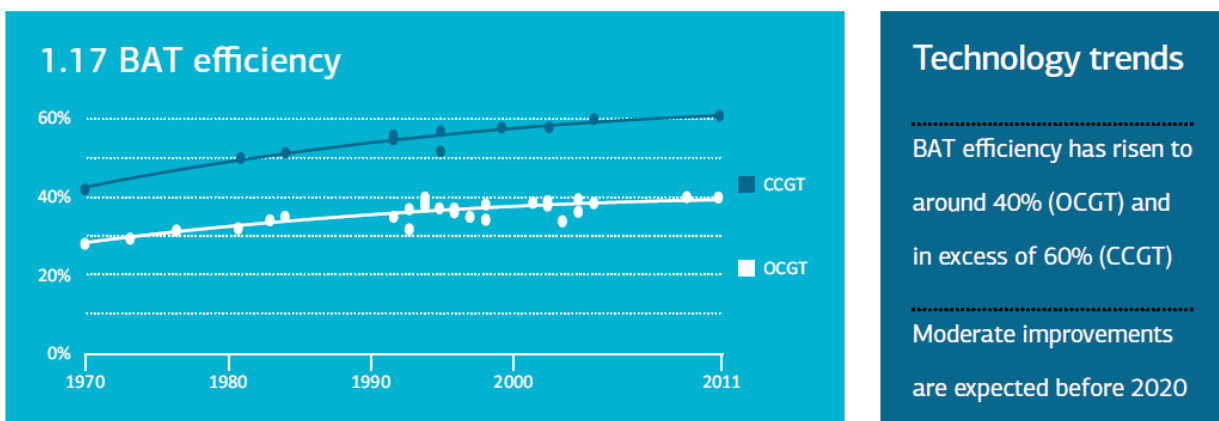


Figure 3. Gas turbines and Combined cycle plants BAT efficiency trend over years [10].

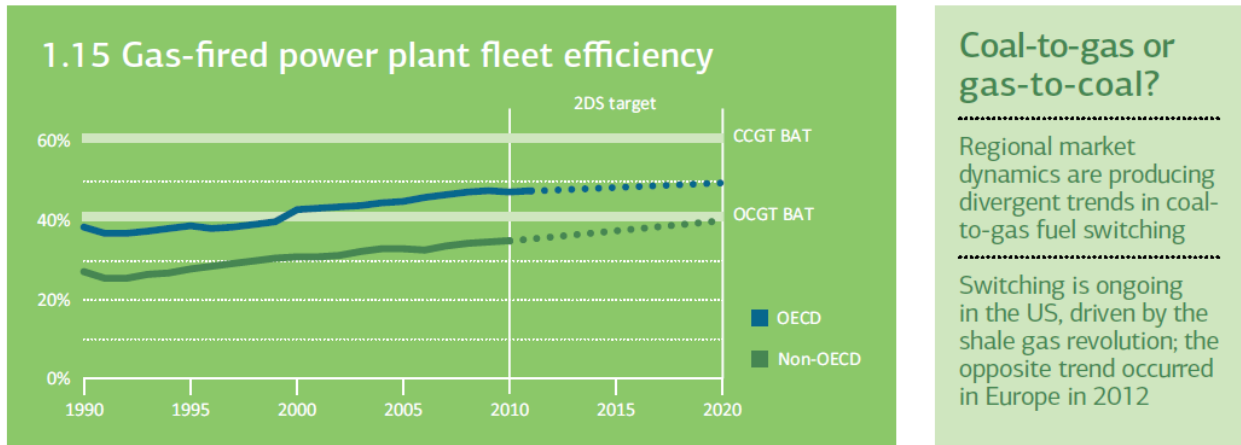


Figure 4. Combined cycle plants fleet efficiency over years. [10]

When world total efficiency of natural gas fired plants is considered (Figure 5), the values are considerably lower: efficiency is 35% in non OECD countries (Organisation for Economic Co-operation and Development) and 49% in OECD countries.

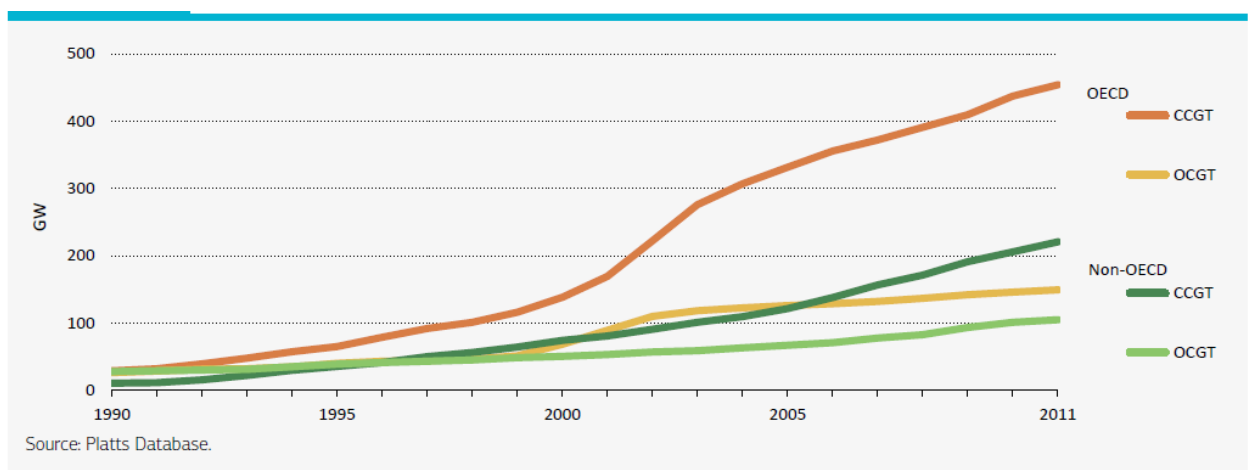


Figure 5. Cumulative CCGT and OCGT capacity. Gas fired power capacity, particularly CCGT has increased rapidly since 2000 [10].

At the end of 90's the availability of cheap natural gas and increasing public concern in environmental issues, including global warming, have favored a rapid increase in CCGT capacity (see Figure 5), allowing a reduction of specific CO₂ production. Nevertheless, the new power generation segmentation has bound some countries to a fuel which has a more complex supply chain.

Coal fired power plants are characterized by lower operating cost as fuel is cheaper but efficiency is lower when compared to combined cycles. Figure 6 shows that in OECD countries fleet efficiency is 38%.

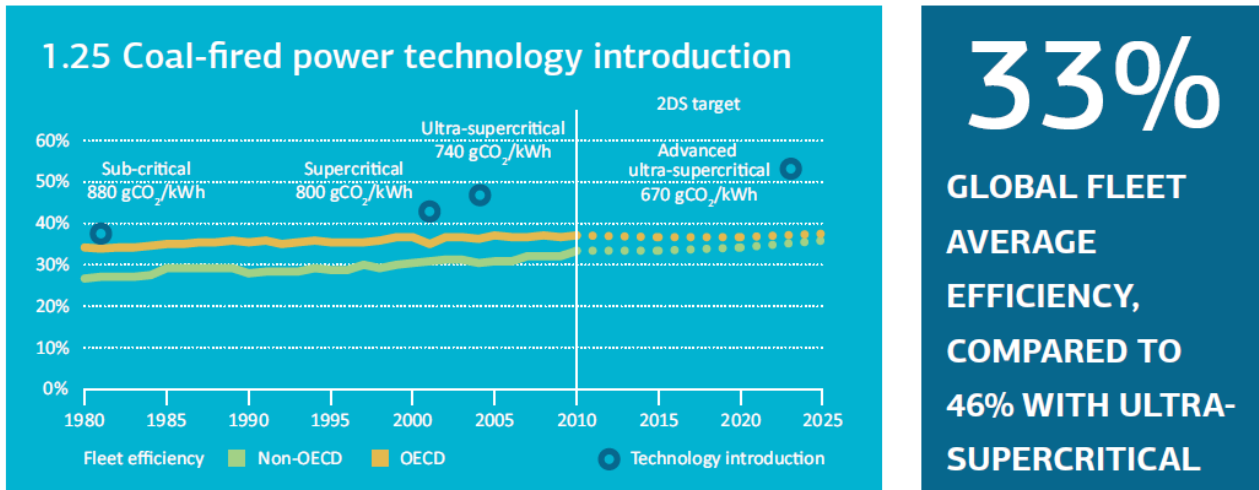


Figure 6. Coal-fired power plants fleet efficiency over years [10].

Liquid fuels are scarcely used as they are expensive. In most cases, they are used in internal combustion engines to provide electricity in remote area or when cogenerated heat can be utilized. The average efficiency of a MW size power plant is 45%.

Nuclear power plants operate on the basis of a steam power cycle as in coal power plants. To increase reliability and availability the operating conditions are kept away from extreme values and cycle efficiency is in the range of 38%. Fuel efficiency is not an issue in this type of plants, because the focus is on radiation losses and fuel availability.

A complete discussion on power plants efficiency and thermodynamics can be found in reference [11].

Utilization of natural gas or coal depends on fuel cost.

Fuel cost has changed considerably in the last years confirming the unpredictability nature of commodity markets.

Figure 7 shows the natural gas spot price over the years. Geographical price differences have increased in recent years, following the revolution in unconventional gas extraction using techniques such as fracking.

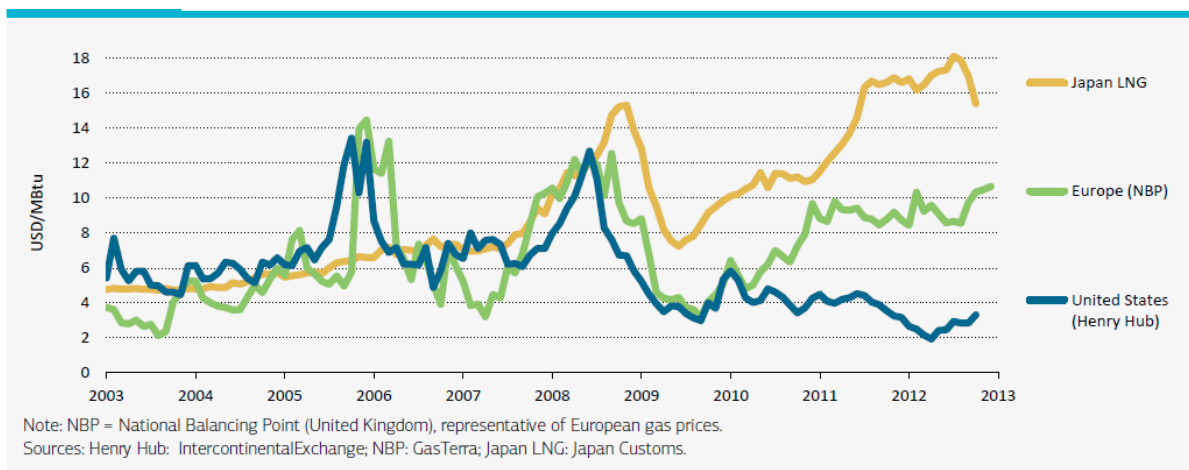


Figure 7. Natural gas spot price over the years. [10]

In Europe, as NG price is rising (Figure 7) and coal price differential is increasing (Figure 8), more electricity is produced with coal instead of NG.

The recent US interest in CCGT can be explained by analyzing Figure 8, where the ratio of average natural gas and coal prices to crude oil prices is shown. In the past, most of the power plants were coal fired, as US was extracting more coal than natural gas. From 2005, after the full scale exploitation of shale gas resources, US is becoming a producer of natural gas and cost is falling close to coal.

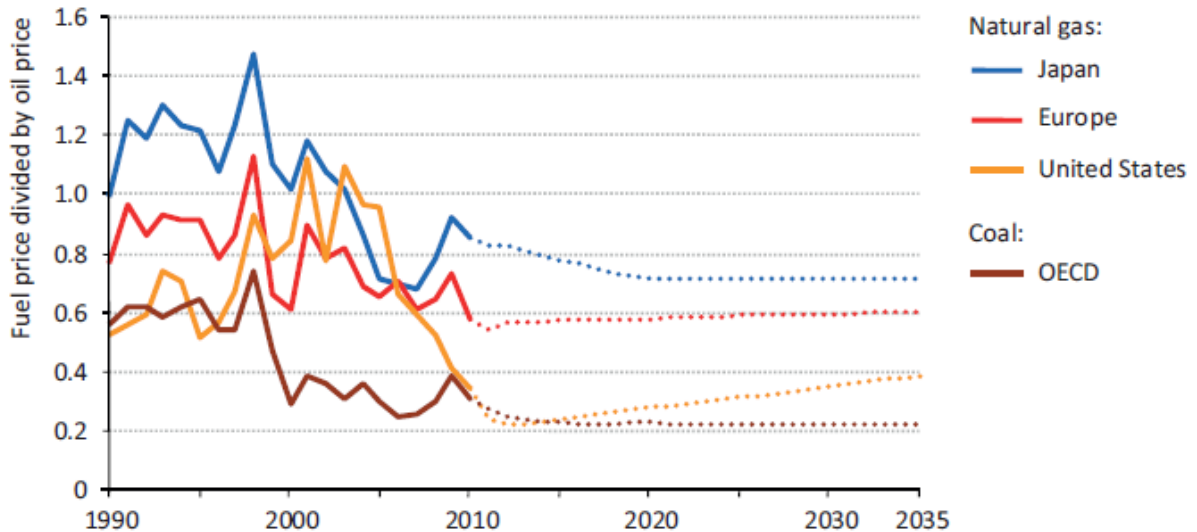


Figure 8. Ratio of average natural gas and coal prices to crude oil prices. Dotted line: forecast. Fuel price is calculated on an energy-equivalent basis [12].

1.3 Distributed generation

More than two decades of discussion have not been enough to find consensus over the definition of Distributed Generation. Recently, some research papers have addressed the issue but without coming to a conclusion [13],[14].

In this research, it has been chosen to use the definition proposed by *Achermann et al.* [15]: “Electric power generation sources connected directly to the distribution network or on customer side of meter”. According only to the capacity, often, the following classification is used:

Micro DG: 1 W-5 kW

Small DG: 5 kW-5 MW

Medium DG: 5-50 MW

Large DG: >50 MW

Technological innovations, changing economic trends and regulatory environment have contributed to a global inclination towards distributed generation. As per the International Energy Agency (IEA) [16], five major factors have significantly increased interest towards distributed generation. These are as follows:

- development in DG technologies;
- constraints on construction of new transmission lines;
- increased customer demand for highly reliable electricity;

- electricity market liberalization;
- concerns about climate change.

DG technologies can be classified as renewable energy based and non renewable energy based. Today, it is frequent to include in DG electrical storage as well.

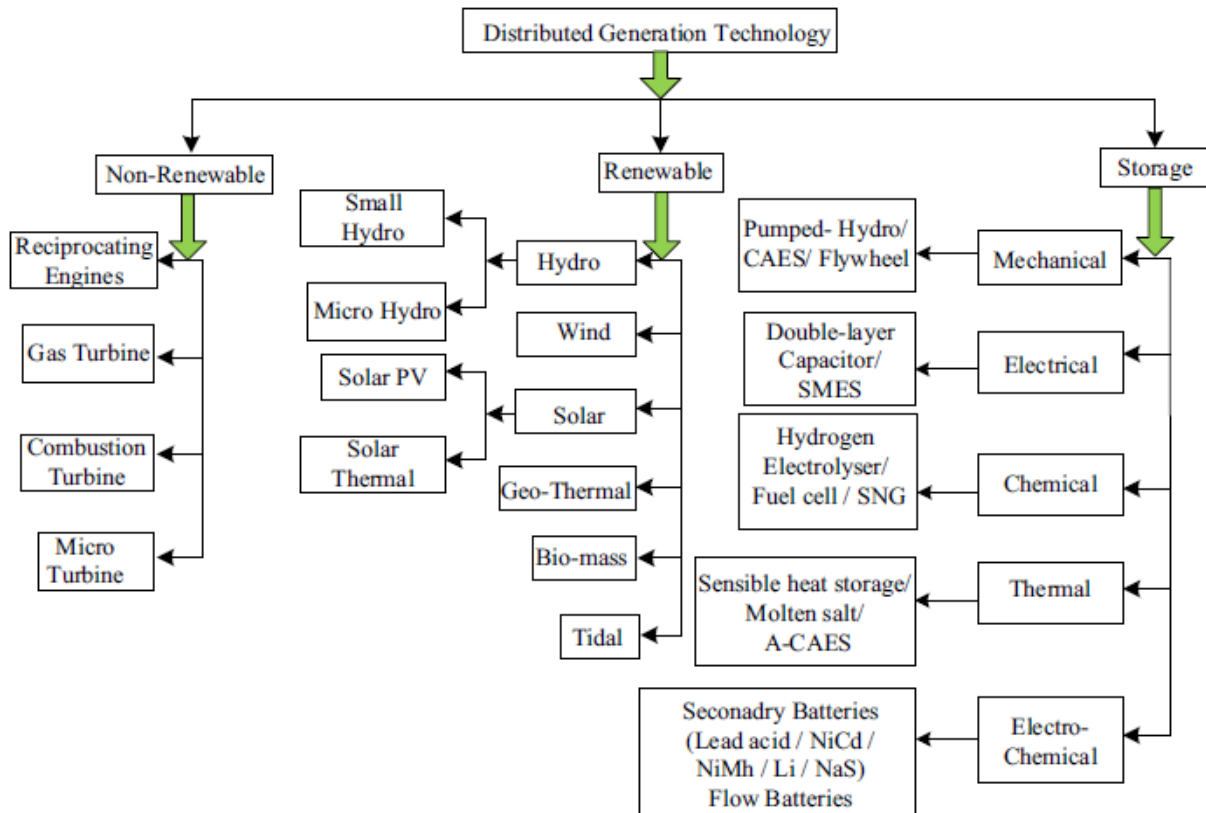


Figure 9. Distributed generation technologies [14].

Recently, many support schemes [17] have been introduced to facilitate the introduction of renewable DG. For example, in the EU, with the Directive 2001/77/CE (Promotion of electricity from renewable energy sources), incentives have been introduced. In Italy such incentives, regulated by the “Decreto Ministeriale 28 luglio 2005) have reached values in the range of 0.40 €/kWh for PV electricity. Figure 10 shows the share of renewable energy in gross final energy consumption in EU. In 8 years the share has increased of 5.4%.

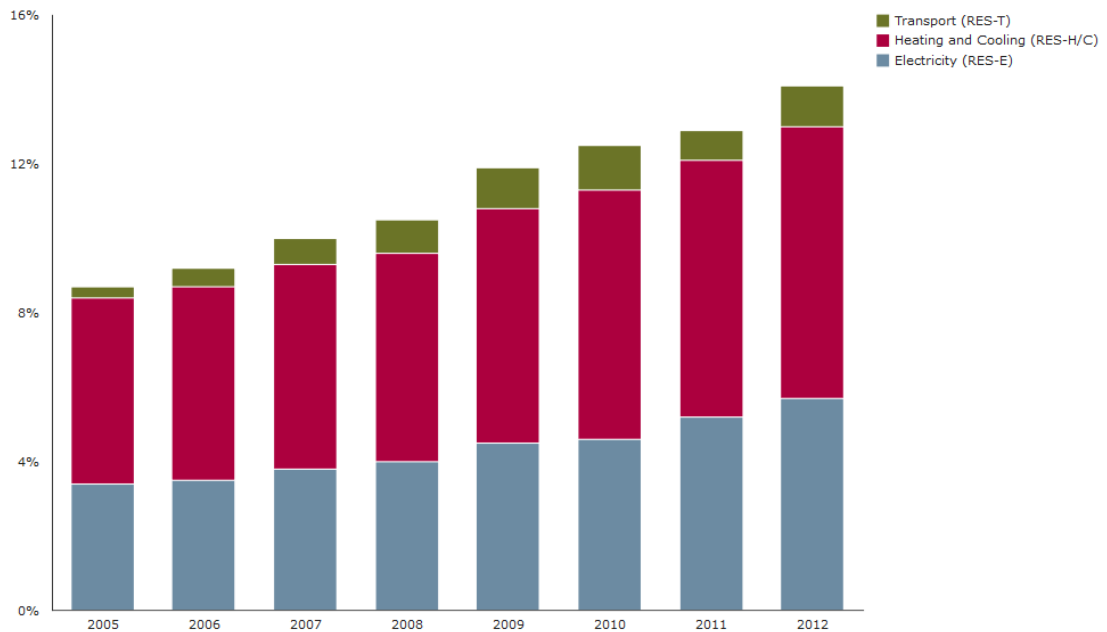


Figure 10. Share of renewable energy in gross final energy consumption [18].

Figure 11 shows the electricity production power mix in EU in 2000 (left) and 2013 (right). In recent years, renewable energy sources such as wind and solar, which are highly unpredictable and variable in terms of power output, have shown the biggest increment, as incentive schemes have been introduced by local and central authorities.

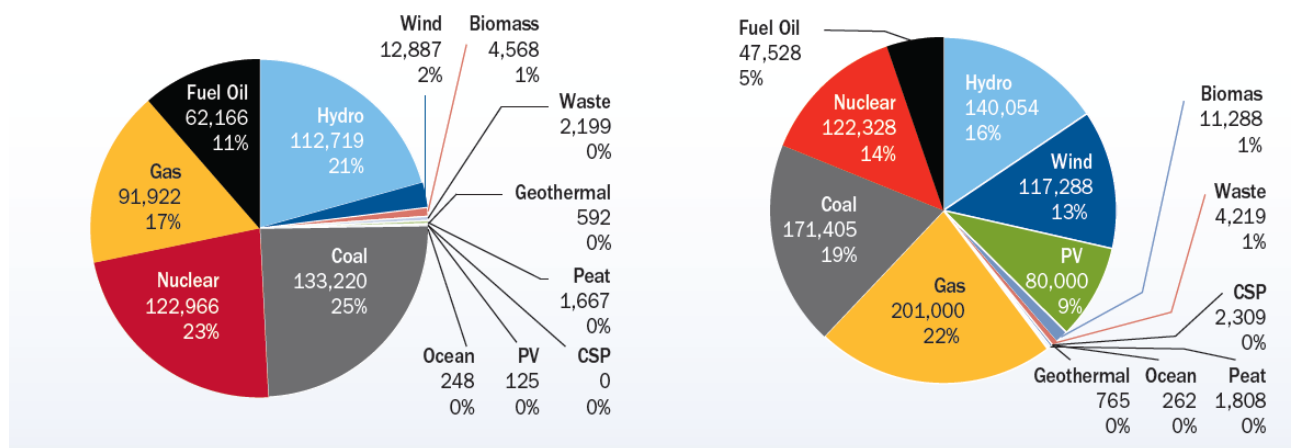


Figure 11. EU power mix in 2000 (left) and 2013 (right) [19].

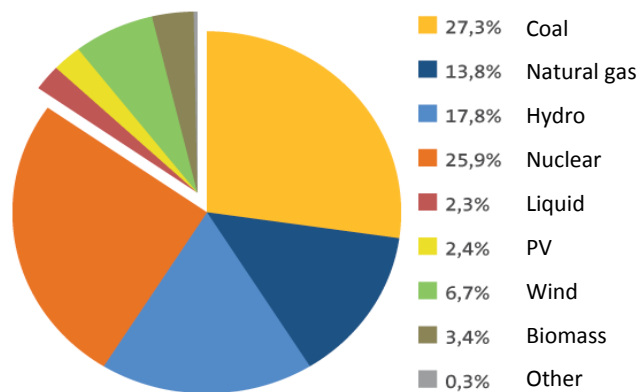


Figure 12. Energy mix in EU 2013 [20].

As for the effect on the existing power plants and distribution infrastructure, it is interesting to note that the PV installed capacity is 9% and wind is 13% but the energy share is 2.4% for the PV and 6.7% for wind (Figure 12). In terms of ratio (PV over wind) is 0.69 for the capacity and 0.35 for the energy.

In Europe (Figure 13) and, especially in Italy (Figure 14), PV has shown a dramatic increase in terms of installed power originating many economic and technical consequences that will be discussed in the next paragraph.

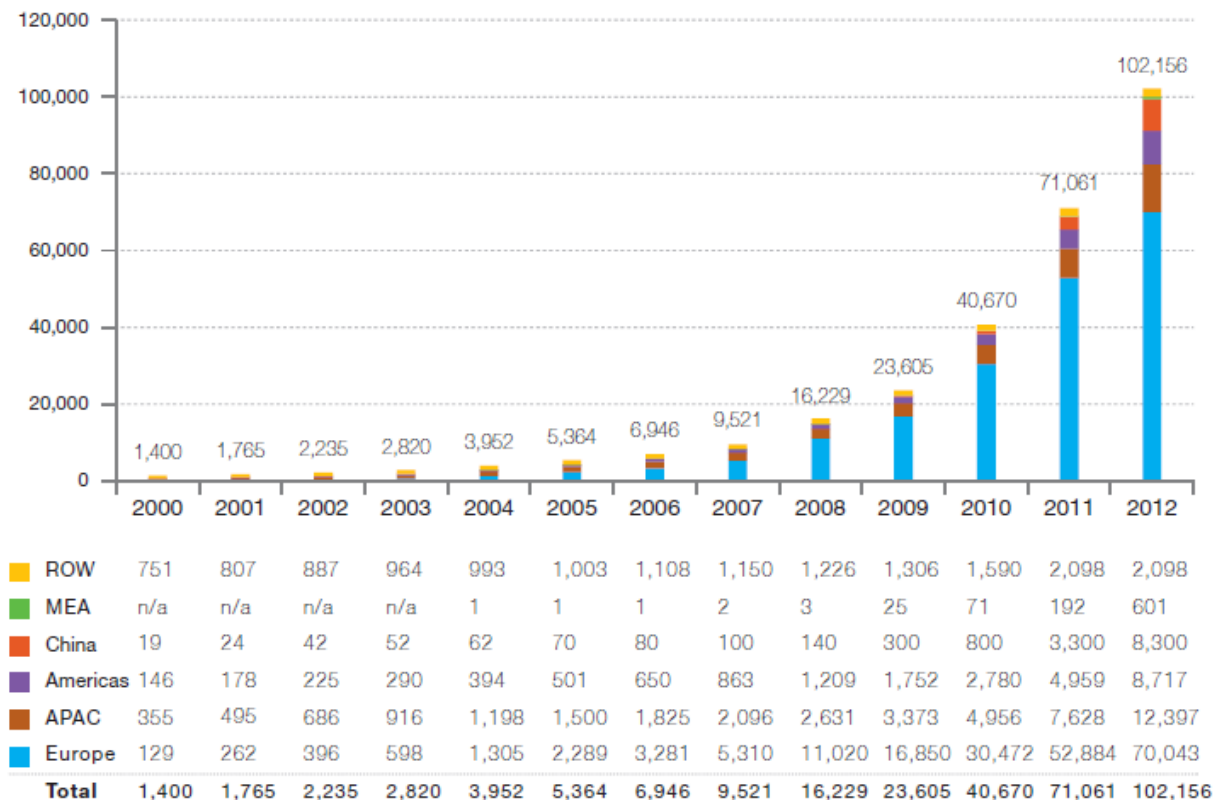


Figure 13. Evolution of world PV cumulative installed capacity 2000-2012 (MW) [1].

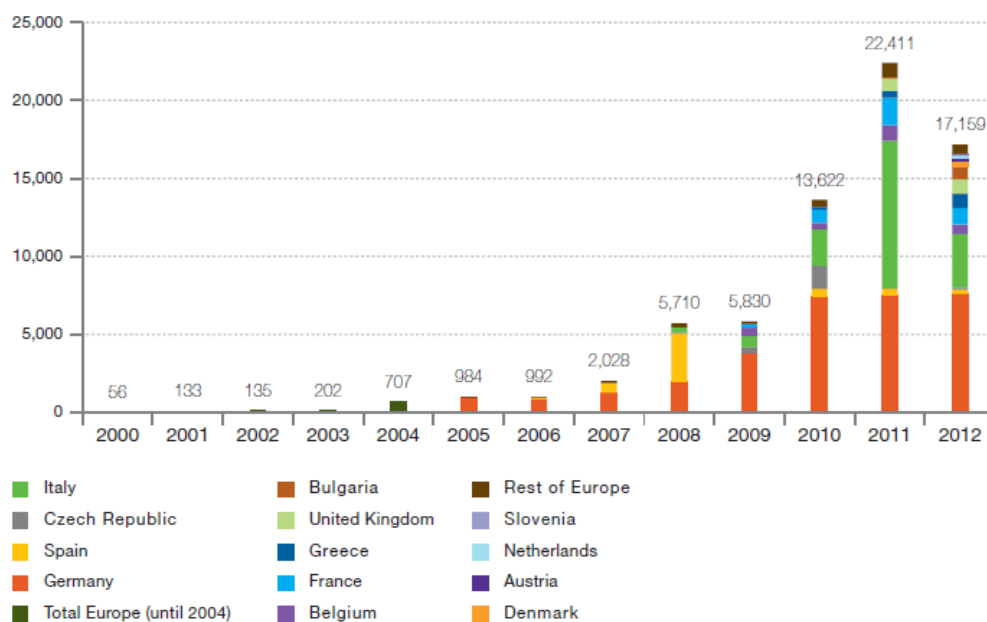


Figure 14. Evolution of European new grid-connected PV capacity 2000-2012 (MW) [1].

As for non RES based DG the most interesting option, today, in term of energy efficiency, is the cogenerative / trigenerative scheme using internal combustion engine (reciprocating internal combustion engines and gas turbine) [14]. Given the proximity to the final consumers, especially where there is a significant and relatively constant demand for heat, DG systems suitable for the combined heat and power (CHP) or combined heat, power and cooling (CHPC) generation may be particularly attractive. In this way local CHP/CHPC may be preferable instead of purchasing electricity from the grid and producing heat/cold separately.

In particular, the so called, natural gas micro-cogeneration, seems to have many advantages and it is addressed as one of the potential breakthrough in power generation [21].

From the fuel utilization point of view the benefits are clear: if the heat is used directly where the electricity is produced the effort, technical and economical, to deliver the thermal energy is at a minimum as are at minimum the losses due to the heat distribution network.

Figure 15 shows efficiency of different power plants as a function of plant size. If a part of the fuel energy not converted in electricity is used as useful heat, the total efficiency (First Law efficiency) is higher.

From the same Figure is also possible to see the efficiency of the most mature technologies already mentioned: reciprocating internal combustion engines and micro gas turbines.

Further details regarding the technologies will be presented in the following Chapter.

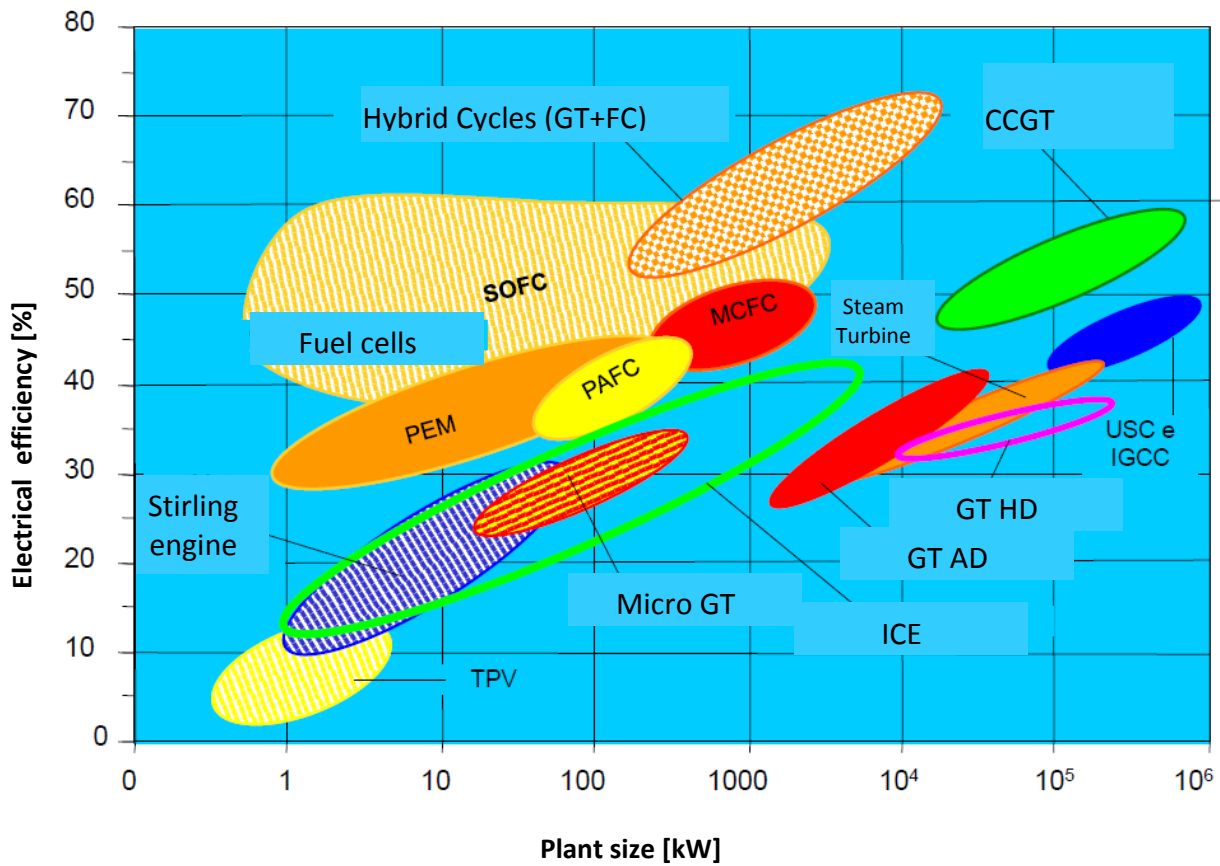


Figure 15. Power plants efficiency as a function of plant size [21].

Nevertheless, the exploitation of non-RES DG remains a small share of total energy production. In Figure 16 the CHP share of total power production is shown. The figure encompasses all the type of plants, including coal power plant and CCGT.

As for the micro-cogeneration systems the European figures are, in 2012, 45,000 units for a total installed power of 52 MW [22].

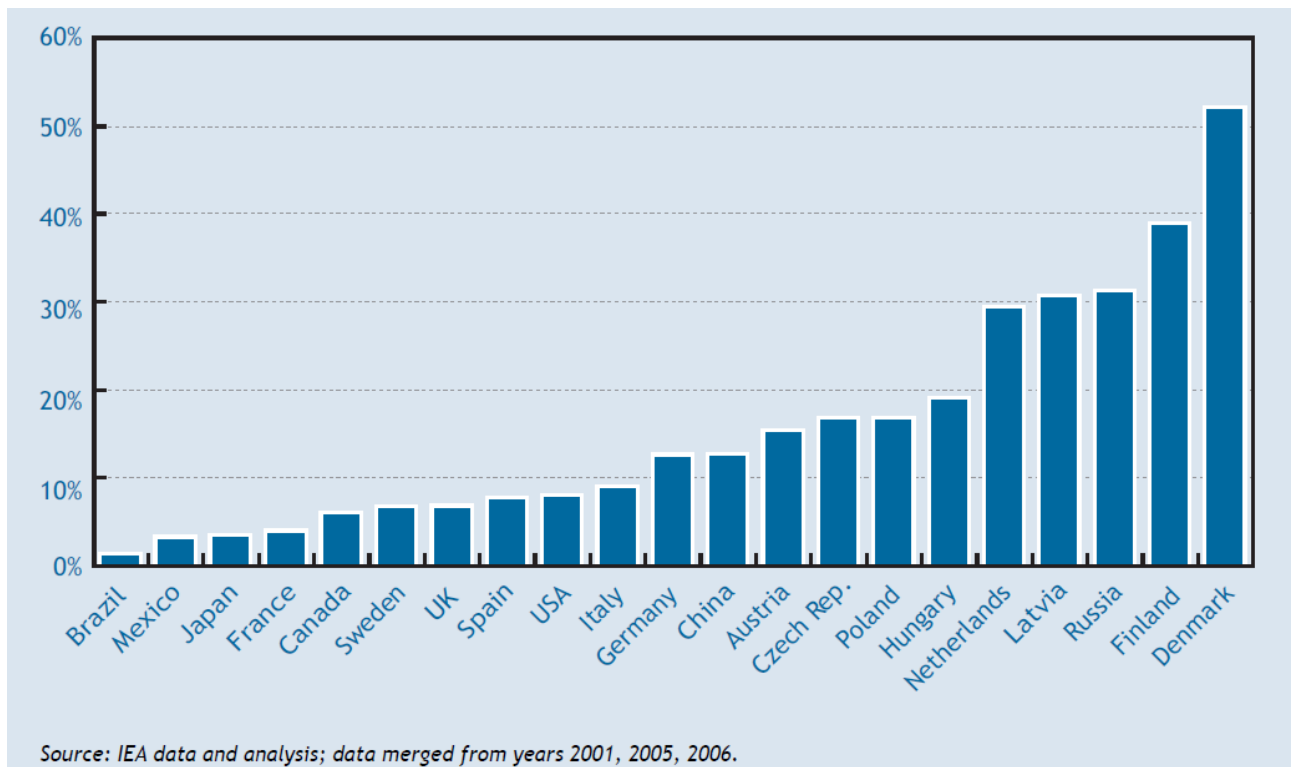


Figure 16. CHP share of total power production in selected countries [23].

1.4 The net benefit of RES DG

The importance of exploiting RES is globally recognized. So far, less attention has been paid to assess the real costs of RES introduction and to assess different alternatives to mitigate fossil fuel exploitation and mitigate associated environmental consequences.

Only recently the media have been addressing the topic, being the issue quite sensitive and very complex both in terms of technical and social implications.

To what concern the European context, an interesting article was published on *The Economist* in October 2013 [2]. The article starts:

“On June 16th (2013) something very peculiar happened in Germany’s electricity market. The wholesale price of electricity fell to minus € 100 per megawatt hour (MWh). That is, generating companies were having to pay the managers of the grid to take their electricity. It was a bright, breezy Sunday. Demand was low. Between 2pm and 3pm, solar and wind generators produced 28.9 gigawatts (GW) of power, more than half the total. The grid at that time could not cope with more than 45GW without becoming unstable. At the peak, total generation was over 51 GW; so prices went negative to encourage cutbacks and protect the grid from overloading.”

Regarding the same day (June 16th) an Italian newspaper, *La Repubblica*, was publishing that for two hours the price of electricity felt to zero [24].

In 2014 negative price were presents as well and, for example, always in Germany, the intraday price was negative on February 16th as shown in Figure 17. The negative price was due to a wrong prediction of solar and wind production as shown in Figure 18.

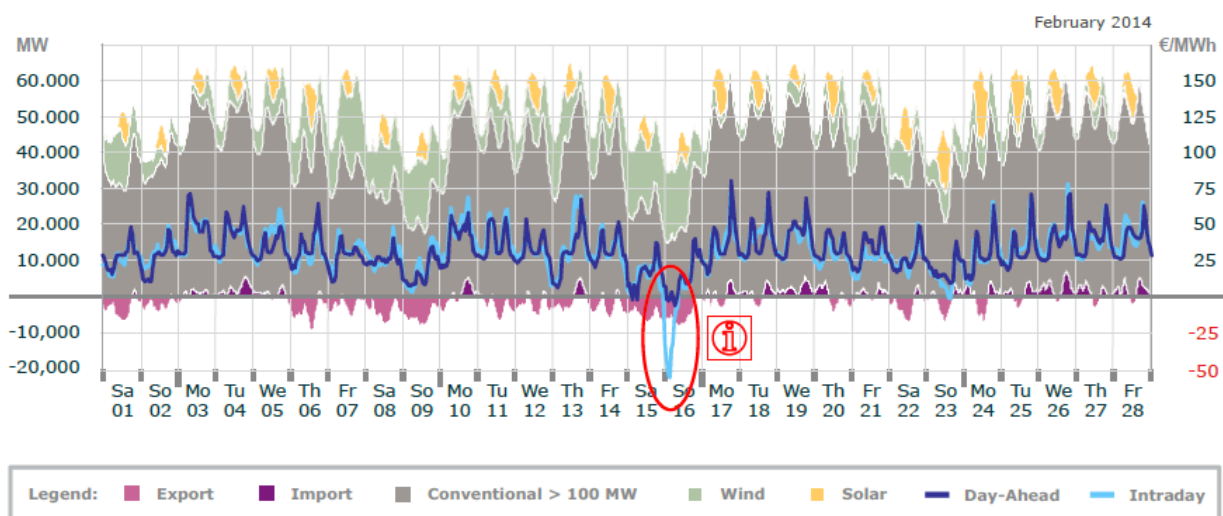


Figure 17. Germany: electricity production and spot price. February 2014 [25].

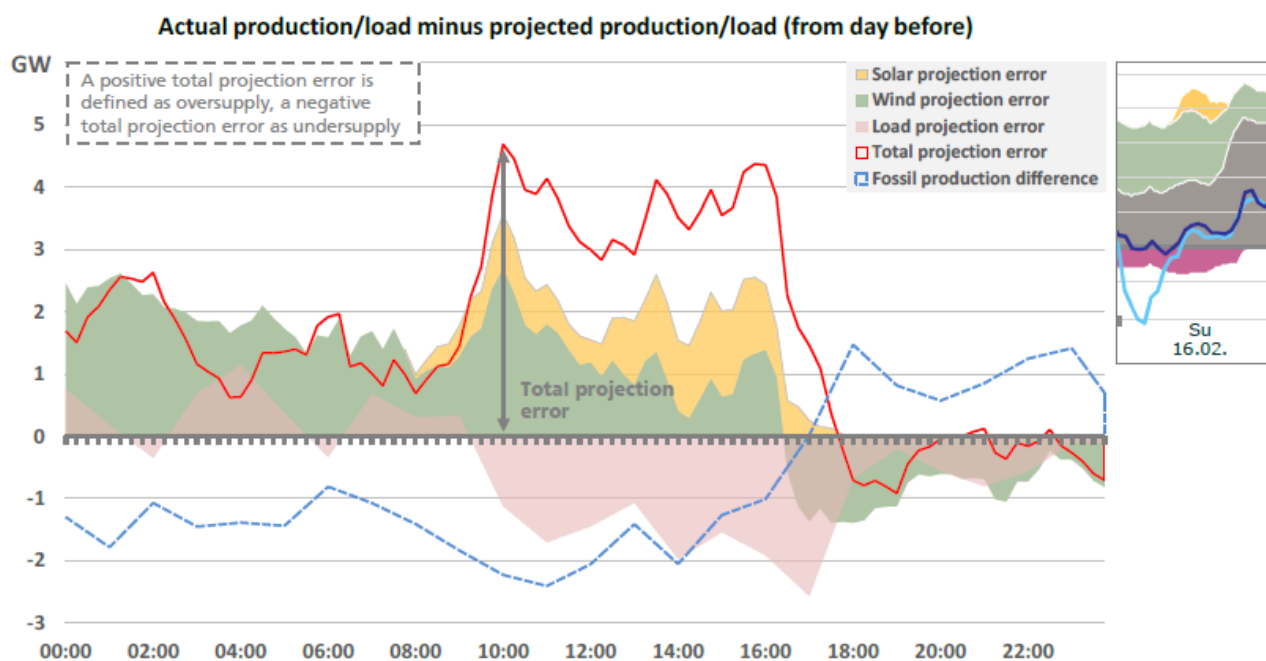


Figure 18. Germany: electricity production and spot price. February 2014. Negative intraday price on Feb 16th explanation [25].

The “negative price” is something peculiar but, it is indeed evident, that the dynamic of electricity price has completely changed in the last year thanks, to large measures, to the introduction on RES DG.

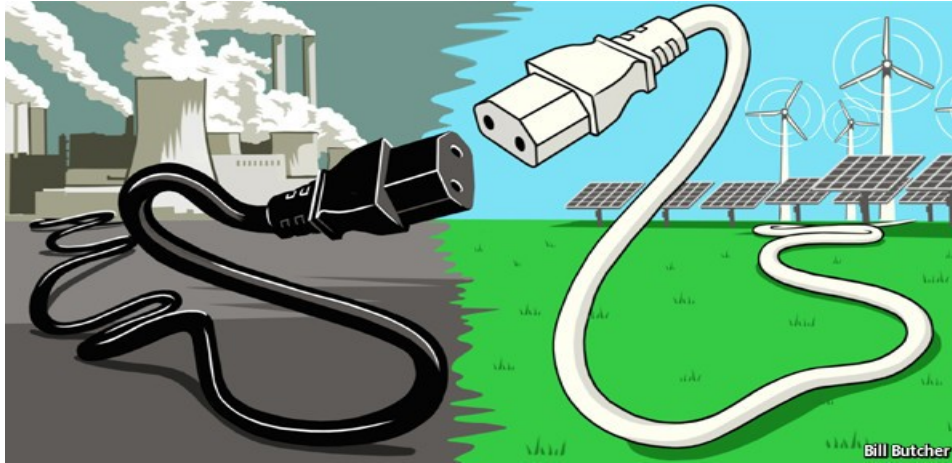


Figure 19. Business as usual and renewable energy sources: competing technologies? [2]

Back in the 1980's, providing electricity was a relatively simple. The base load was supplied by coal plant or, where available, nuclear and "river hydro". For technical reasons these plants had to run at full load or close to full load 24/7. To supply extra electricity at peak times, lunchtime and early evening, more flexible plants were used such as gas turbine or "storage hydro". In the following years, the intermediate load was supplied by GGCC where available. The typical power mix is shown in Figure 20. In the same figure is also shown, in red, the typical profile of the production with PV.

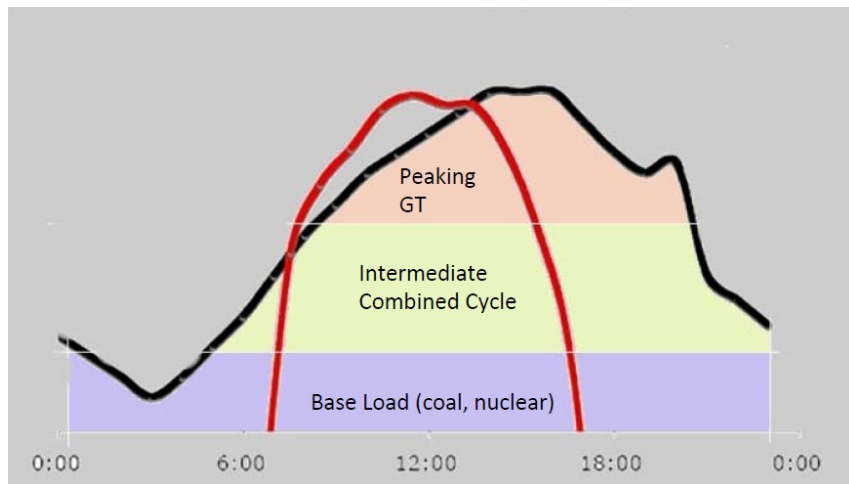


Figure 20. Typical electrical load profile and power mix (black). In red the typical PV production in a sunny day.

When in many countries deregulation was introduced, power plants operation was decided on the basis of the marginal cost of electricity. The changing process was also accelerated as normally, to encourage installation of RES plants, grid has to take their electricity first (grid priority). This priority would be indeed in force even without a specific regulation as, in most cases, RES electricity marginal cost is zero. Therefore, RES electricity remains in the lower part of the load profile graph Figure 23. But, unlike base load plants already in place (nuclear and coal), solar and wind power are intermittent and affected by weather conditions.

When electrical demand fluctuates, it may not be enough just to modulate the load of natural gas generators. Some plants may have to be switched off altogether and it may be necessary to reduce the load on some coal power plants. This happened on June 16th. The process to reduce load on coal power plant is complex and it can introduce volatility on electricity price bringing devastating effects on profit.

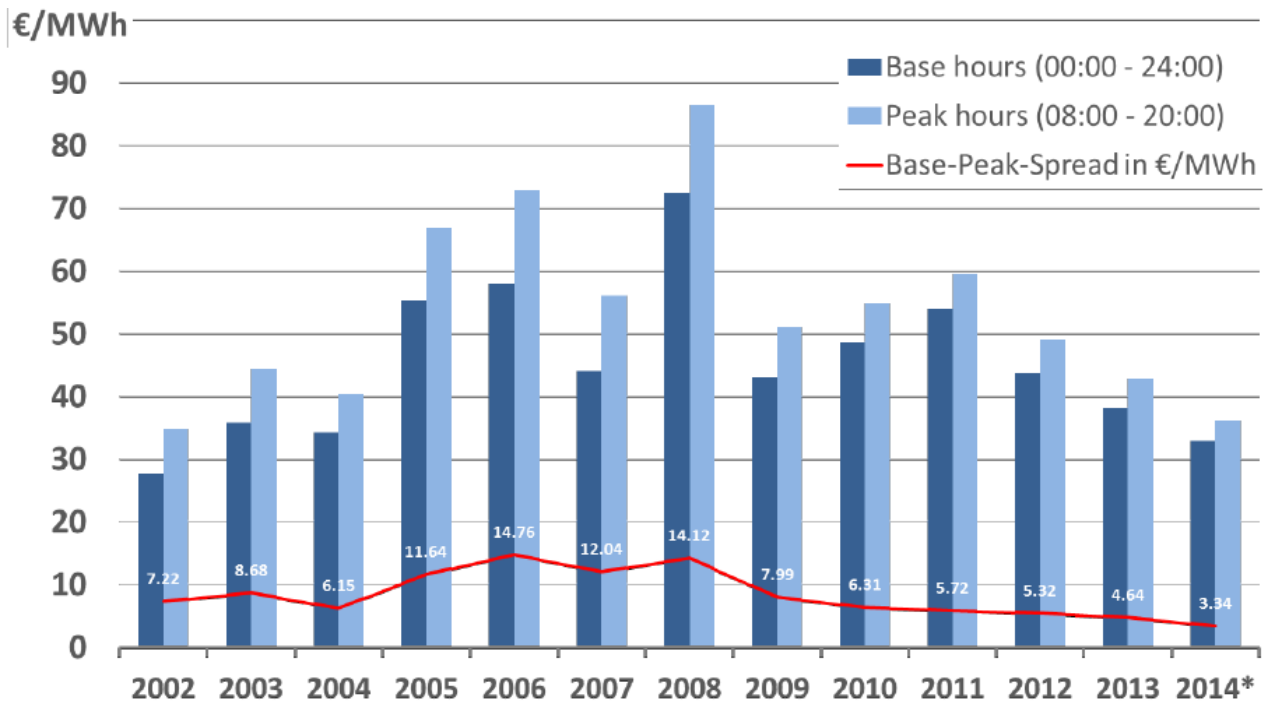


Figure 21. Germany: day ahead price volume weighted and inflation adjusted (price 2014) [25].

Before the introduction of RES, electricity prices spiked during peak hours (the middle of the day and early evening), falling at night. Most of the company's profit came from production during peak hours. But today PV satisfies most of the load during the middle of the day and it has flattened the peak price and squeezed profits. According to the Fraunhofer Institute for Solar Energy Systems [25], in Germany in 2008, peak-hour prices were € 14 per MWh above base load prices. In the first eleven months of 2014, the difference was € 3 (Figure 21). The effect on CCGT is evident in Figure 22. The reduction in electricity price and the in the base-spread is causing serious effect on the companies and utilities that have invested in CCGT, as these plants does not operate enough hours to payback the investment.

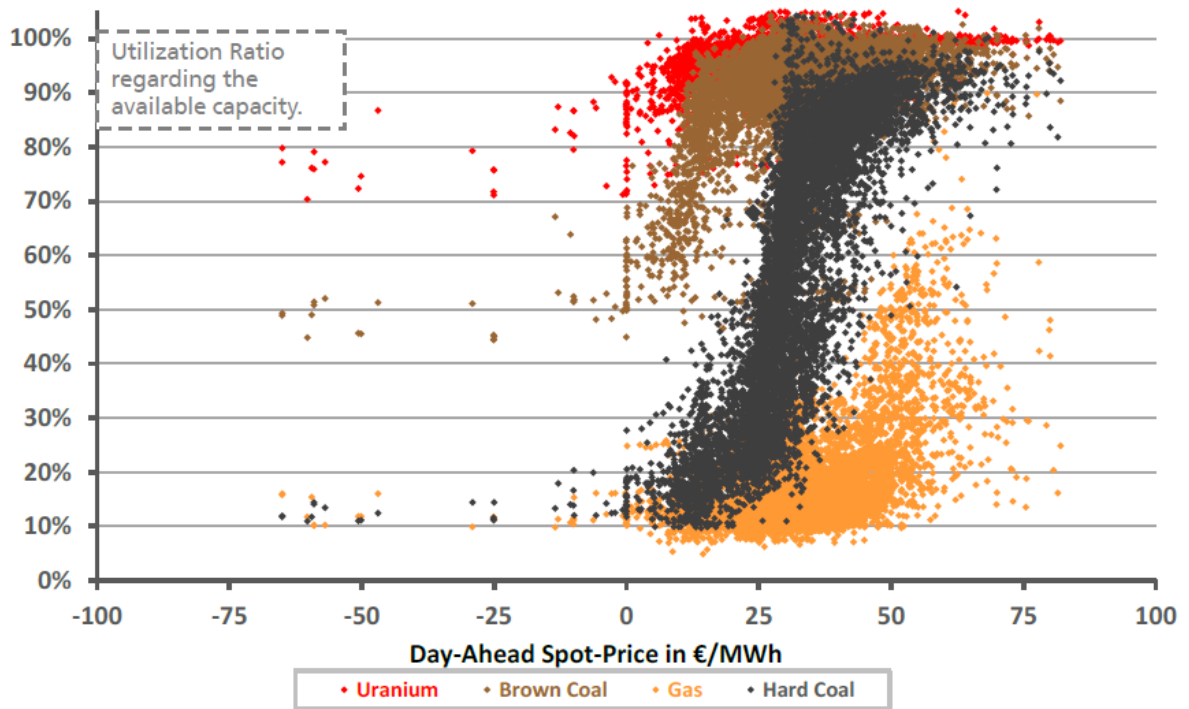


Figure 22. Germany: plant type utilization over day ahead spot price [25].

In Italy the effect of DG RES and in particular of PV can be outlined examining Figure 23 and Figure 24.

In Figure 23 the July 2013 average daily power mix is shown. Starting from the top of the production curve the “programmable” sources are indicated: import, thermal power plant, hydro (storage), and then the “non programmable sources”: PV, wind. On the bottom the “continuous non programmable”: hydro river and geothermal.

It is clear that PV introduces a new element in the power mix as it can reach almost one third of the total demand. Unfortunately, this peak is not programmable and if a low irradiance day happens, Figure 26, the other programmable sources have to support the production. In July 2013 the highest PV production on a working day was on July 31st with a peak of 12.5 GW and an energy share of 10% (102 GWh), Figure 25, and the minimum production, always on a working, day was on July 29th with a peak of 7.8 GW and an energy share of 7% (70 GWh) (Figure 26). Therefore, with only few days of difference, the power plants have to cover a difficult to forecast gap of 4.7 GW due only to a weather conditions change.

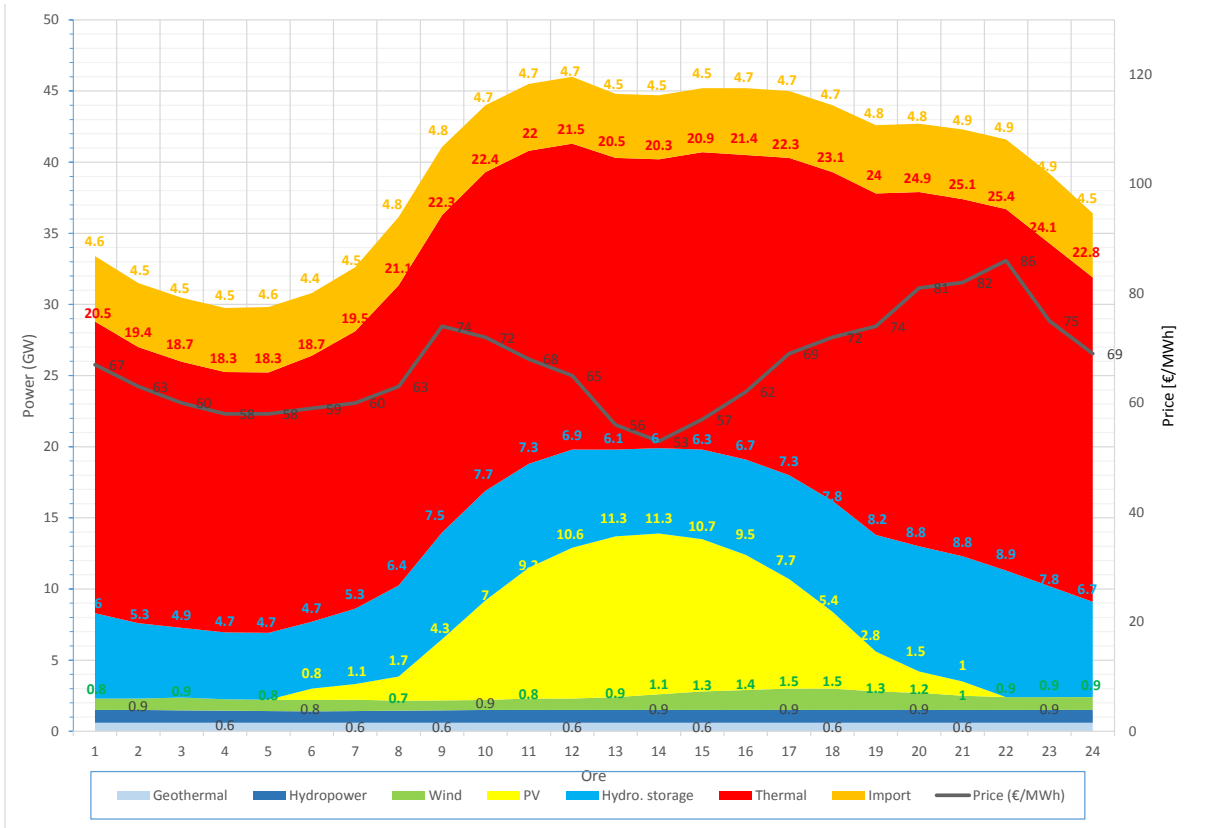


Figure 23. Power mix and electricity price in Italy. Average monthly values, July 2013. Elaborated from [26].

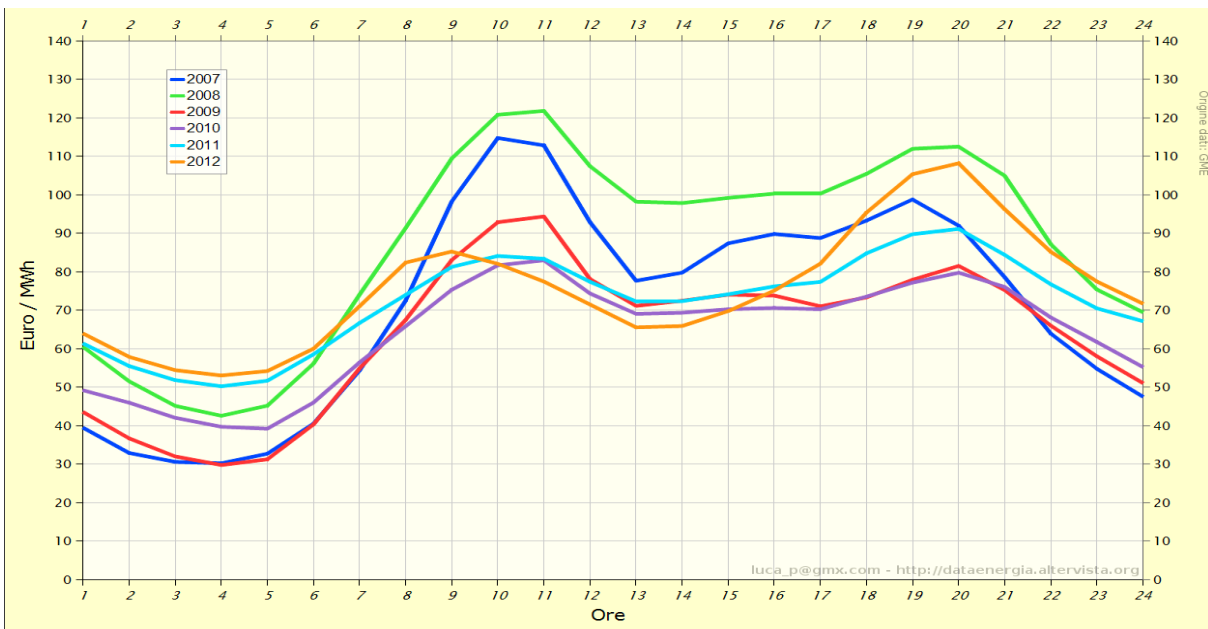


Figure 24. Electricity cost in Italy. Average hourly values on “Mercato del giorno prima” (Day ahead market) [26].

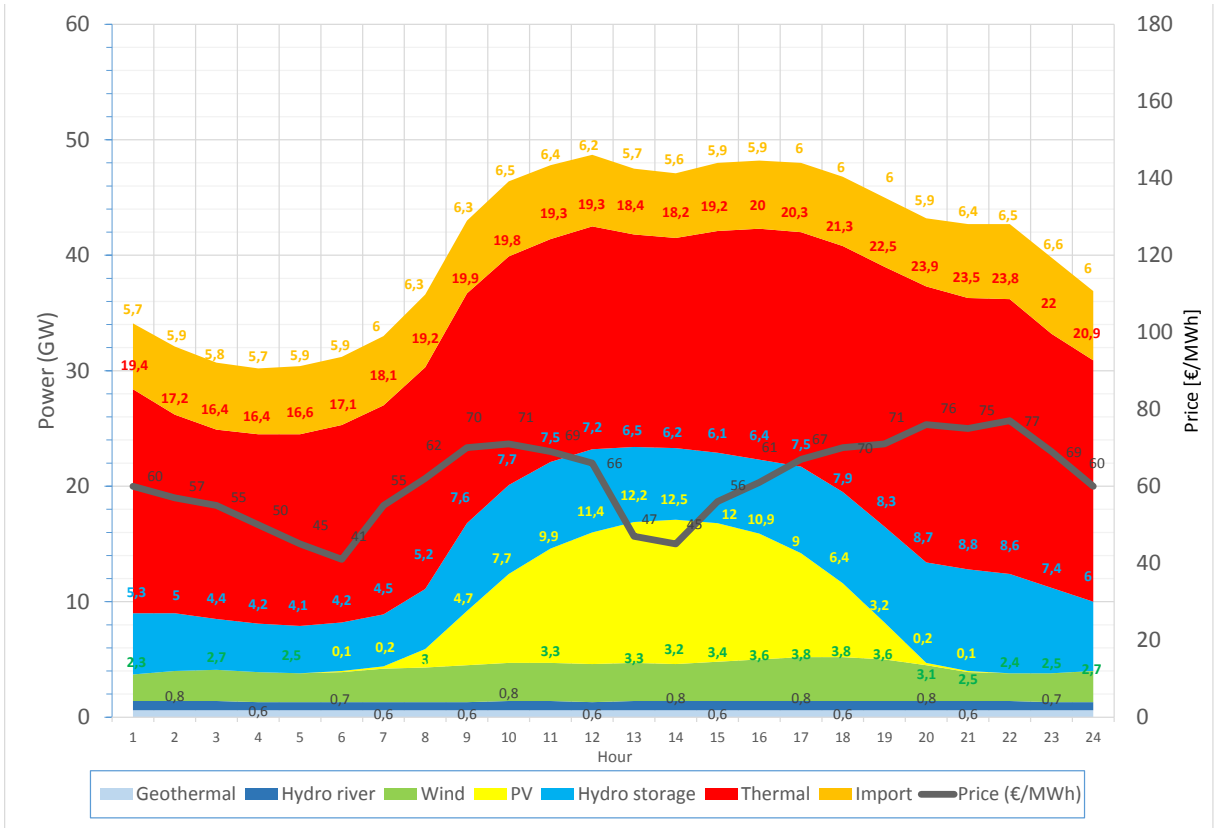


Figure 25. Power mix and electricity price in Italy. Day of highest PV production in July 2013. Elaborated from [26].

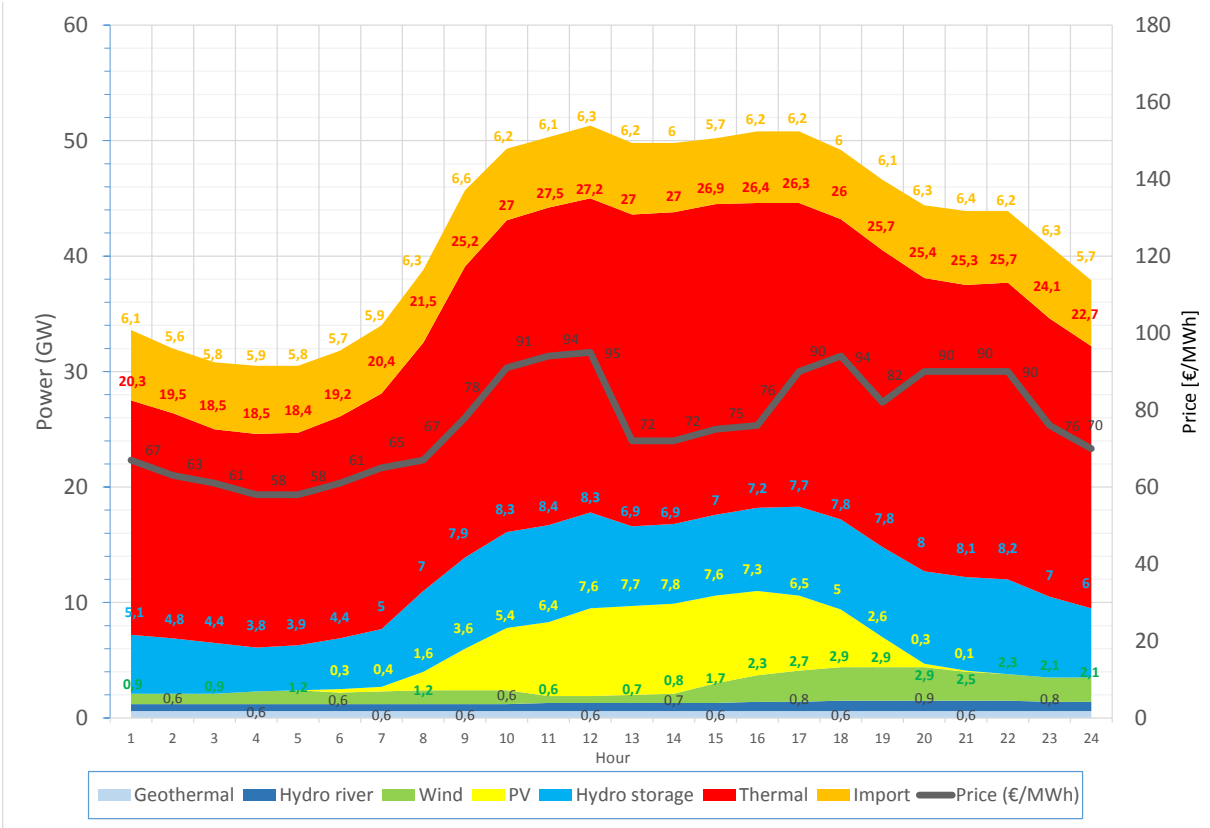


Figure 26. Power mix and electricity price in Italy. Day of lowest PV production in July 2013. Elaborated from [26].

In Figure 23 is also shown the electricity cost during the day. Considering that, in Italy, the intermediate loads were covered by CCGT and these plants are profitable starting at about 60 €/MWh, in most cases it has been decided to shut down these high efficiency plant in favour to low efficiency, but cheaper to run, coal plants (Figure 27).

Indeed, the electricity market is very complex and other variables have to be taken into account, such as EU carbon permit prices that fell to 5 euros per tonne (2012) from 18 euros (2011) [3] and US shale gas revolution [27]. In recent years the extraction of shale gas in US has lowered natural gas price, fostering the utilization of CCGT and introducing on the market coal at a lower price.

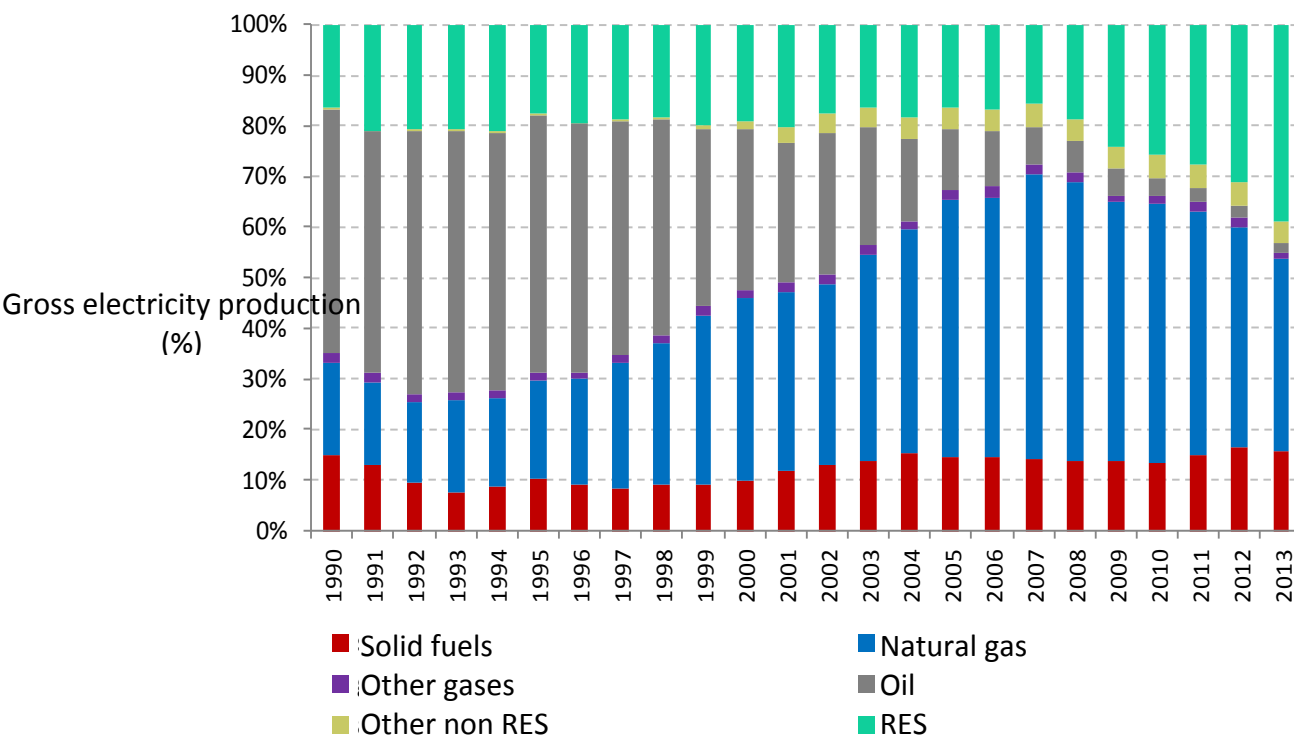


Figure 27. Electricity production in Italy: fuel share. Elaborated from [28].

Coming back to the situation in Italy, the question that could arise is: does RES contribute to lower the CO₂ specific production? The answer can be found in Figure 28, where the CO₂ emissions for kWh produced/consumed is shown.

For fossil fuel power plants, from year 2007 when incentives for PV have been introduced, the specific CO₂ emission after many years of reduction as CCGT have been introduced, has raised again.

But, as mentioned before, the trend inversion, is not only due to RES, but to a series of concomitant factors.

Indeed, if the total production is considered, RES has contributed to a significant reduction in specific CO₂ emissions.

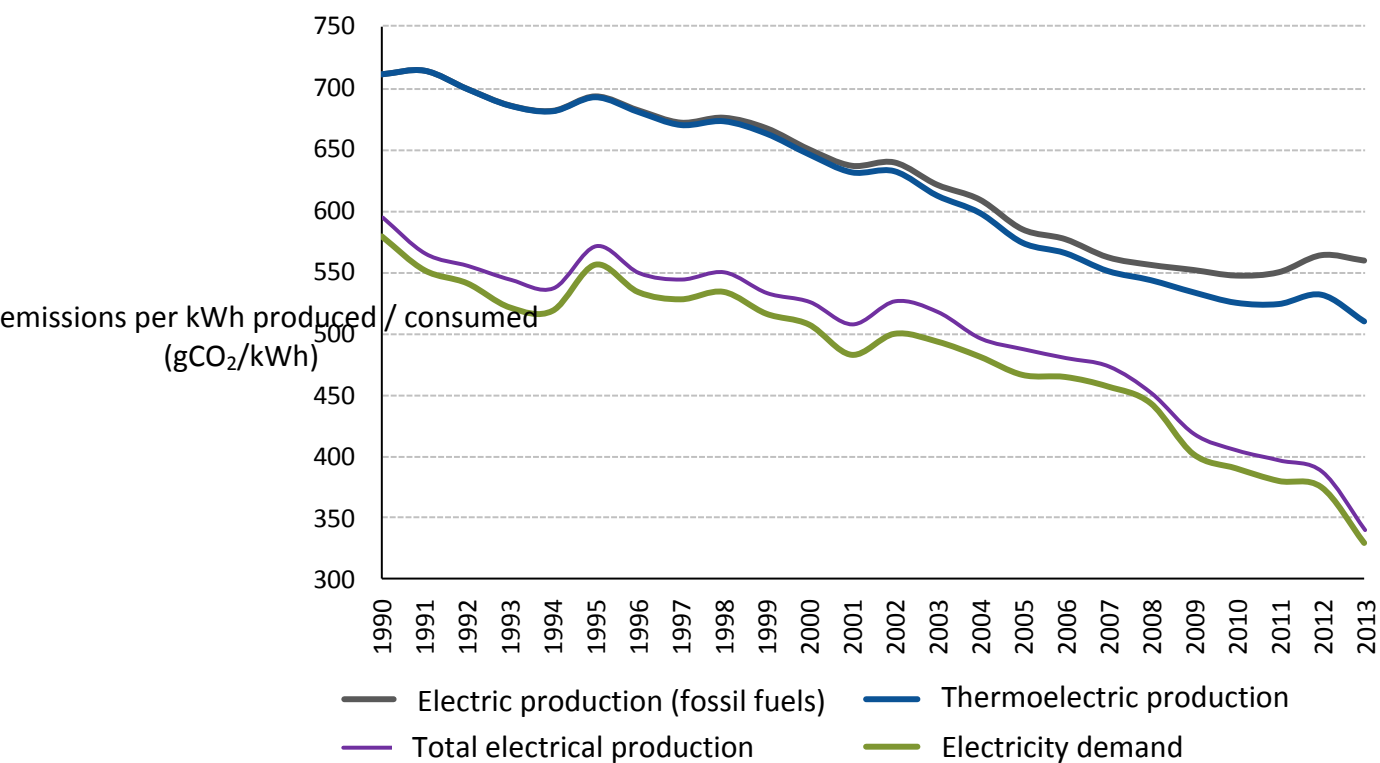


Figure 28. CO₂ per kWh in Italy. The thermoelectric production encompasses biomass, biogas and biofuel. In the total production RESs are included. In the electrical consumption grid losses and electricity import are included. Elaborated from [28].

As for the effect that RES DG can have on CO₂ emissions, an interesting analysis is presented in [29]. The research presents a cost benefit analysis of various RES and non-RES power plants ranking the technology by net benefits delivered per megawatt (MW) of new electrical capacity.

As mentioned in the first part of the paper [29], the most common method for comparing the cost of different electricity technologies is to compute and compare the “levelized” cost of each alternative. However, levelized costs could not be appropriate for ranking technologies. An electricity plant that produces electricity with a relatively high levelized cost may be more valuable than a plant with a lower levelized cost if the plant with a high levelized cost delivers electricity more reliably and more cheaply when the price of electrical energy is high. For example, a high levelized-cost hydroelectric project with ample storage capacity can produce electricity at near zero marginal cost at full capacity during peak periods. While levelized costs might suggest that hydroelectric plants are higher-cost than fossil fuel plants, the hydroelectric plant may in fact be more profitable and valuable if that fossil fuel plant is burdened with a high energy cost during peak hours. Similarly, a solar plant that delivers more power during daytime (when electricity demand is at its peak) may be more valuable than a wind plant that produces more power during the night (when electricity demand is lower).

Thus, rather than using levelized costs to compare alternative technologies, one should compute the annual costs and benefits of each project and then rank those projects by net benefits delivered per megawatt (MW) of new electrical capacity. The benefits of a new electricity project are its avoided carbon dioxide emissions, avoided energy costs and avoided capacity costs. The costs include its carbon dioxide emissions, energy cost, and capacity cost. In addition, there are

costs unique to certain technologies. For example, the decommissioning of a nuclear plant and disposal of its spent nuclear fuel at the end of its useful life can be very costly. Wind, solar and hydroelectric plants produce electricity intermittently and therefore generate additional system balancing and cycling costs that have to be taken into account (described in more detail later).

The cited paper,[29], estimates benefits and costs for five different technologies, though to be used in the U.S.A., on capital costs, operation and maintenance costs and carbon dioxide emissions. While costs can vary geographically, the market for power plant construction, operation and maintenance is global and there are few major differences in such costs among countries.

Similarly, markets for coal and oil are international and major price differences among countries arise largely from government trade policies. Prices for natural gas, however, are highly variable among countries because of the high cost of, and long lead times for, pipelines and liquid natural gas facilities required to transport natural gas over long distances. Also there are large differences among countries regarding capacity factors (or load factors) for renewable energy because of geographical variations in wind and solar intensity and availability of hydroelectric sites among countries.

The results of the research can be summarized in Table 1. On the basis of the research hypotheses it is more convenient to invest in replacing an old coal power plant with a CCGT instead that installing a wind or solar plant. This outcome is mainly due to the so called “avoided capacity cost” (The capacity cost of a fossil fuel plant that would have been incurred had not a new plant using low or no-carbon technology been built) and the “avoided energy cost” (The reduction in total energy cost of an electricity system caused by the introduction of a new plant).

This is an issue already mentioned above: as the RES are not predictable, if there is a need of a new 1 MW plant RES based, another generating capacity large enough to provide the electricity when RES are not available has to be taken into account.

This need, emerged after the introduction of RES, has already opened a debate in Italy as most of CCGTs are not economically profitable anymore and, therefore, the 25 billion of Euro financed by the banks in the last years to install the new plants are causing serious concern [30].

Table 9A. Net Benefits per Year per MW: Displacement of Coal Baseload Production					
Benefits per MW per Year	Wind	Solar	Hydro	Nuclear	Gas CC
Avoided Emissions (1)	\$106,697	\$69,502	\$168,934	\$405,574	\$416,534
Avoided Energy Cost (2)	\$74,412	\$50,938	\$141,991	\$289,565	\$296,836
Avoided Capacity Cost (3)	\$69,570	\$45,702	\$152,350	\$315,755	\$323,577
Costs per MW per Year:					
New Plant Emissions (1)	\$0	\$0	\$0	\$0	(\$137,796)
New Plant Energy Cost (2)	\$0	\$0	\$0	(\$72,403)	(\$250,737)
Capacity Cost Incurred (3)	(\$270,195)	(\$351,427)	(\$282,843)	(\$614,692)	(\$113,033)
Other Costs (4) (5)	(\$5,816)	(\$3,535)	\$0	(\$5,230)	\$0
Total Net Benefits	(\$25,333)	(\$188,820)	\$180,432	\$318,569	\$535,382
<i>Footnotes:</i>					
(1) Avoided and new plant emissions from Table 2A have been valued at \$50 per ton.					
(2) Avoided and new plant energy costs are from Table 4A.					
(3) Avoided and new plant capacity costs are from Tables 6A and 7.					
(4) Other costs for nuclear are from Table 8.					
(5) Wind and solar other costs are based on Ellerman and Marcantonini (May, 2013)					

Table 1. Net benefits per year per MW of new electrical capacity: displacement of coal base load production [29].

1.5 Harnessing RES

Despite RES are contributing, generally speaking, to reduce CO₂ emissions and fossil fuels dependency, as discussed in the previous chapters, many issues on how to maximize overall the benefits are still open. In particular, the typical problems associated to energy sources with low capacity factor: assuring constant power output and avoiding overload of distribution grid, have to be solved.

The scientific community and the stakeholders are prone to consider the development of a smart grid and energy storage a potential solution to both the problems. As for the integration of RES with ESS the reviews contained in [6], [31], [32] offer an overview of the potential technological solutions. Smart grids development is, indeed, the focus of many research and industrial projects all over the world [33], [34], [35], [36].

As for the case of Italy, some storage projects are under way. For example Terna, a leading electricity transmission grid operator in Italy, is involved in a series of storage project for a total of power of 35 MW and an energy of 232 MWh [37]. ENEL, a leading power company in Italy, according to the 2014-2016 Development Plan [38] is considering the installation of distributed storage facility up to a total of 100 MW.

1.5.1 The potential of micro-CHP systems

As above mentioned, the straightforward thermodynamic advantage of micro-CHP systems is the possibility to utilize the heat associated to the power production without the need of an expensive and energy dissipative heat distribution network. In this way, the fuel utilization factor can reach value as high as 90 %, depending on the technology used as prime mover and on the temperature level at which the heat is recovered.

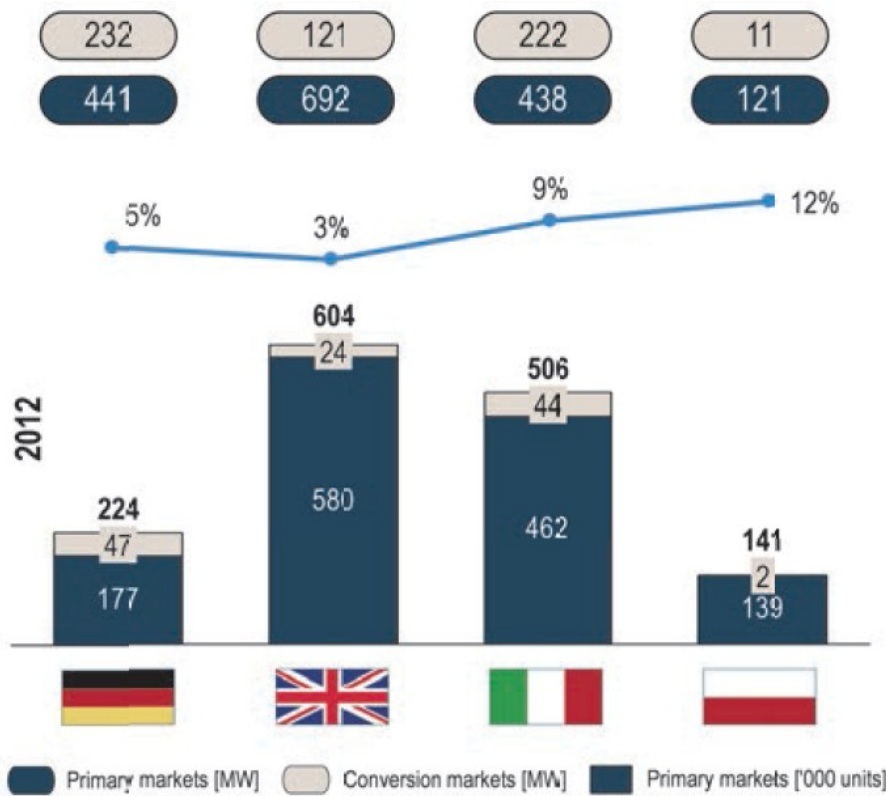


Figure 29. Addressable market for fuel cells in apartment buildings [39].

As shown in Figure 29, the addressable market in apartment buildings for micro-CHP systems such as fuel cells. could be more than 2 GWel. Despite the interesting potential market and the advantage in terms of primary energy utilization, micro-CHP is not today widely accepted and utilized. In Italy, there are many obstacles that hampers the market, a part from the technological maturity. One, is the complicated and variable regulative and legislative system. The second is that transmission grid operator, in these days, could not be favorable in fostering the introduction of a myriad and difficult to control power generators. Nevertheless, this seems not to be a technical problem anymore as, in few years, more than 500.000 new PV plants have been installed in Italy (Figure 30).

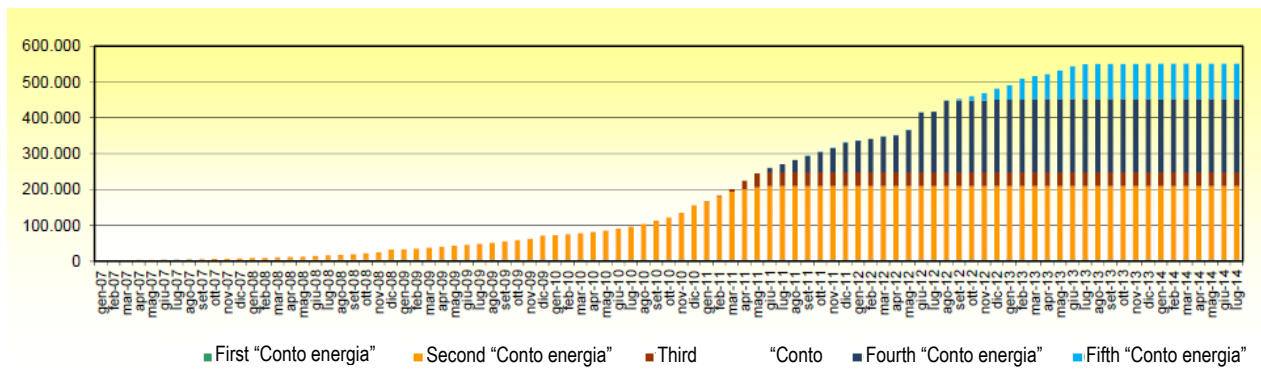


Figure 30. Number of new PV plants in Italy. Data at July 2014. The different colors indicate the different support schemes for PV (Conto Energia). Elaborated from [40].

If not properly supported, utilities could perceive DG as a loss of business and therefore not be enthusiastic about allowing final users to produce their own electricity.

To this respect, a much discussed research report: “Disruptive Challenges: Financial Implications and Strategic Responses to a Changing Retail Electric Business” was published in 2013 by the Edison Electric Institute [41]. Citing part of the summary:

“While the pace of disruption [introduction of DG, AN] cannot be predicted, the mere fact that we are seeing the beginning of customer disruption and that there is a large universe of companies pursuing this opportunity highlight the importance of proactive and timely planning to address these challenges early on so that uneconomic disruption does not proceed further. Ultimately, all stakeholders must embrace change in technology and business models in order to maintain a viable utility industry. “

A new technical motivation to introduce and support micro-CHP, that in this context is a non RES DG, could be the integration with RES DG.

Among the results of the integration there should be:

- availability of capacity in case of RES lack/failure;
- reduction of transmission grid overload;
- higher overall fuel efficiency;
- reduction in specific CO₂ emissions;
- reduction in electricity cost.

In the next chapter micro-CHP technologies will be discussed and the result of the integration analysed aiming to a peaceful coexistence or, at least, peaceful transition from “business as usual” to DG.



Figure 31. DG and business as usual transition...[2].

2 MICRO-COGENERATION: THE TECHNOLOGIES

2.1 Introduction

The potential of micro-cogeneration or micro-CHP for the exploitation of RES DG has been outlined in the previous chapter, here a review of the existing micro-CHP technologies are presented aiming at highlighting the characteristics that would enhance RES benefits.

Much has been written on micro-CHP and the detailed description of all the technologies options is beyond the aim of this chapter, however the cited references are useful sources of additional information.

2.2 Choice of the reference plant

As for the capacity of the plant, the focus has been concentrated on systems from 100 W to 10 kW.

This choice has been the results of an analysis of the average yearly electrical use of a typical Italian dwelling that ranges from 3000 to 4000 kWh [42] according to a typical layout as depicted in Figure 32. Assuming that the micro-CHP operates 24/7 with the possibility of thermal and electrical storage available, the continuous power output is in the range of 300-400 W. The upper limit of 10 kW refers to cases where a single power plant is connected to several users.

The fuel considered is natural gas as, in Europe, is one of the most widely used fuel for heating.

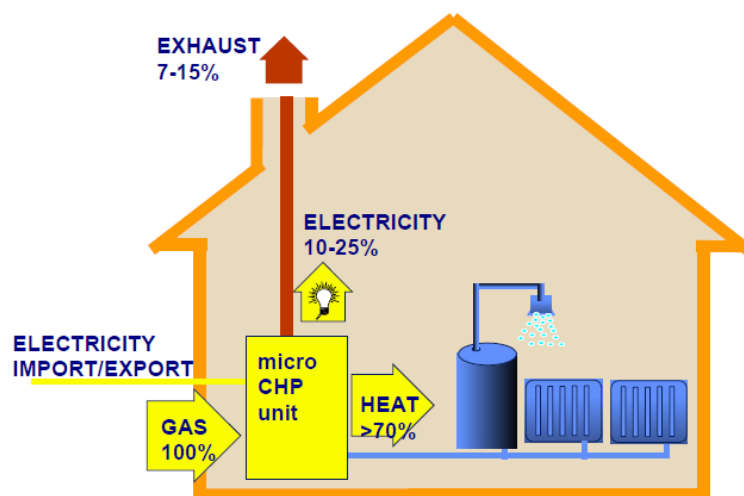


Figure 32. Micro CHP concept.

2.3 Technologies

The technology that are often cited, not taken into account the technology readiness level, as candidate for micro-CHP are:

- Reciprocating internal combustion engines
- Micro gas turbines
- Stirling engines
- Organic Rankine Cycles
- Fuel cells

Far from commercialization seems to be thermo-photovoltaic and thermoelectric generators together with many other solutions. An interesting review of micro-CHP technologies with data on efficiency and costs can be found in reference [21] and [43].

2.4 Reciprocating Internal Combustion Engines (ICE)

Reciprocating IC engines are based on the Otto cycle (spark ignition) or the Diesel cycle (compression ignition). Considering the utilization of natural gas for micro CHP engines, today only the Otto cycle is used. In the Otto engine, the mixture of air and fuel is compressed in each cylinder before ignition is caused by a spark.

In addition to the engine and generator, the micro-CHP system must include heat exchangers, switchboard (e.g. for grid parallel operation or islanding operation), engine lubrication system, acoustic insulation and catalytic converter for reducing emissions. Typical emissions for a Otto cycle without catalytic converter are: 0.6-2.6 g/kWh NO_x and 1.5-2.7 g/kWh CO [21].

Reciprocating internal combustion engines have mechanical efficiencies that range from 25– 30 %. In general, diesel engines are more efficient than spark ignition engines because of their higher compression ratios. However, the efficiency of large spark ignition engines approaches that of diesel engines of the same size. The overall efficiency in cogeneration mode reaches approximately 80–85% (LHV). The energy balance for a 1 kW system is shown in Figure 33.

Micro CHP engines used in cogeneration applications generally drive a synchronous generator at variable speed in order to maximize the efficiency at partial load operation.

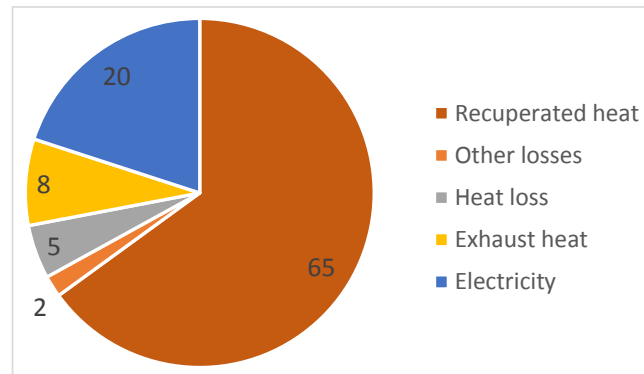


Figure 33. Typical energy balance for a 1 kW system. Fuel inlet 100%, reference to LHV [21].

The electrical efficiency remains fairly constant from full load to 75% load and, thereafter, it starts decreasing. The amount of heat generated from the jacket coolant water and exhaust gases increases as electrical efficiency of the engine decreases; i.e. the amount of useful heat derived from a cogeneration system increases as the efficiency of electric power delivered decreases.

The ICE technology is the most mature for cogeneration purposes as it can benefit from the experience and low production costs gained thanks to transportation applications. Generally, reciprocating internal combustion based cogeneration systems with power output lower than 500 kW cost between 1000 and 2000 €/kWe [21], with higher specific cost for smaller cogeneration systems.

In Table 1 the main specifications of two of the most popular on the market micro CHP are presented. The cost for the 1 kW plant is about 6000 € with an electrical efficiency of 20% (LHV) and total efficiency of 85%. More than 100.000 Ecowill units have been sold in Japan [44].

Characteristics	Ecowill (Honda)	Senertech (Dachs)
Electrical output [kWel]	1	5
Electrical efficiency (LHV) [%]	20%	26%
Heat recoverable [kWth]	3.25 kW	12.3
Total efficiency (Thermal+el.)[%]	85	89
Dimensions (WxDxH) [m]	0.38x0.58x0.88	0.72x1.1x1.0
Weight [kg]	81	520
Cost [€]	6000	13000
Catalytic converter	3 way (lambda sensor)	Oxidant

Table 2. Main specifications and cost for two micro CHP ICE. Fuel: natural gas [21].

2.5 Stirling engines

Stirling engine differs from internal combustion engine by the fact that the fuel combustion takes place externally to the working fluid and the cylinders. Pistons are driven by pressure changes due to heating and cooling of working fluid, which may be air or hydrogen. The Stirling engine normally drives a synchronous generator which is connected to the grid.

Stirling-operated facilities are relatively expensive and until now they are especially used in the smaller size categories. In order gain a good electrical efficiency, high temperatures are required (600-700°C). Presently, the electrical efficiency of Stirling engines can reach 30 %, and the overall efficiency of a Stirling engine cogeneration system is 65 – 85 %. Stirling engines also have good capability to operate under part-load conditions. Since the technology is still in the development phase, there is no statistical data for the reliability and availability of Stirling engines.

Capital costs of Stirling engine cogeneration systems have remained high. It is always difficult to have costs information for technology not completely mature but, according to [45], the 1 kW Whispergen model is sold in Europe for 10,000 €. The Baxi 1kW ECOGEN micro CHP is sold in UK at about € 10,000 as well.

Characteristics	SOLO Stirling 161	WhisperGen	STM power F260
Electrical output [kWel]	2-9	1.2	50
Electrical efficiency (LHV) [%]	24%	12%	30
Heat recoverable [kWth]	8-24	8	83
Total eff. (Thermal+el.) [%]	92 ⁽¹⁾	97 ⁽¹⁾	82 ⁽²⁾
Dimensions (WxDxH) [m]	1.28x0.7x0.98	0.5x0.6x0.85	2.57x0.86x1.33
Weight [kg]	450	138	1340
(1) Condensation (2) Hot water 55°C			

Table 3. Main specifications for three micro Stirling engine [21].

2.6 Micro gas turbine

As discussed in the previous Chapter, gas turbine is a well-established technology for power generation with typical efficiencies in Combined Cycle up to 60%.

However, as the size of turbines is reduced, it becomes increasingly difficult to achieve high conversion efficiencies, and micro-turbines, e.g. Capstone models C30 and C65, with power outputs of 30 kW_e and 65 kW_e, achieve only 25% and 29% electrical efficiencies respectively.

Most of the microturbines (MGT) fall outside the scope of this study in terms of their rated power. According to the available information, the C30 is the smallest microturbine available on the market.

In 2013, Micro Turbine Technology BV (MTT – Netherlands) has started the field tests of the ENERTWIN, a 3kWe (14.4kWt) micro-CHP package, with an electrical efficiency of 16% [46].

The heart of the microturbine is the compressor-turbine package, which is commonly mounted on a single shaft along with the electric generator. The microturbine also includes a heat exchanger, a recuperator and an inverter. The generator can often act also as a starter motor for the turbine.

Although the MGT efficiency is below that achievable from ICE, it is believed that the use of a single moving part should provide additional benefits in service life, reliability and cost.

From the experimental information available from plants in the range of 60-100 kW, the part load efficiency decreases sharply below 50% load (Figure 34).

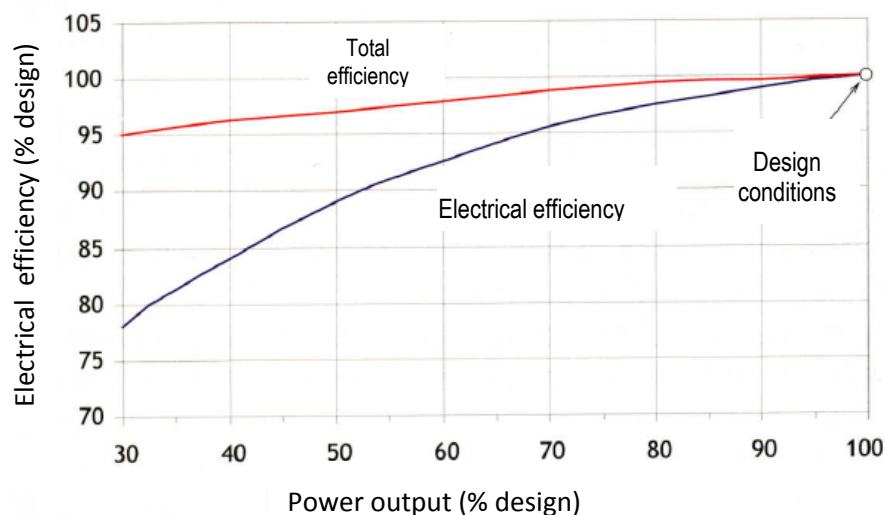


Figure 34. Part load efficiency of a micro GT [Elaborated from Capstone data [21]].

2.7 Organic Rankine Cycles

The Organic Rankine Cycle (ORC) works by pumping a working fluid in to a boiler where it is evaporated, passes through an expander and is finally re-condensed. As in the steam Rankine cycle, ORC is an external combustion engine. The working fluid that drives the expander is a low boiling point organic fluid such as R-134a, R245fa or hexamethyldisiloxane, which allows the system to run efficiently on low-temperature heat sources (even lower than 100 °C). Also investment costs of ORC are lower than those of steam boilers, because of the lower working pressure. The electrical efficiency of kWe size plants is in the range of 6-8%. ORC requires to dissipate all heat not converted in electricity and, as the efficiency is low, the quantity of heat is considerable and this can be a problem especially if air cooling is the only possible. In this case, if ambient temperature can be high, the exchanger unit can be bulky and electrical efficiency reduced.

Most ORC manufacturers concentrate on larger machines, with power outputs more than 500 kWe and efficiency up to 18-20%, but there are also machines in the kilowatt range being Energetix Genlec unit the only wall mounted system commercially available. The power output is 1 kWe and 7.2 kWt [47].

2.8 Fuel cells

2.8.1 Introduction

The description of this technology is more detailed as it will be shown, from a technical point of that fuel cells could be an interesting candidate to be integrated with RES DG and fuel cells will be the focus of the remaining chapters of this research.

2.8.2 Operating principle

Fuel Cells (FC) are electrochemical devices that convert directly the energy in the fuel in electricity. The fuel cells are similar to battery in terms of operating principle but, in the case of fuel cells, the fuel is stored outside the device, this not being the case of batteries, where the reactants are stored inside. Therefore, fuel cells generator runs as long as fuel is provided, as in ICE, and there is no need to replace or charge the device. Interesting books for operating principle and system applications are [48] and [7] specific for Proton Exchange Membrane fuel cells.

As in the batteries, fuel cells basic components are: two electrodes and one electrolyte as shown in **Figure 35**.

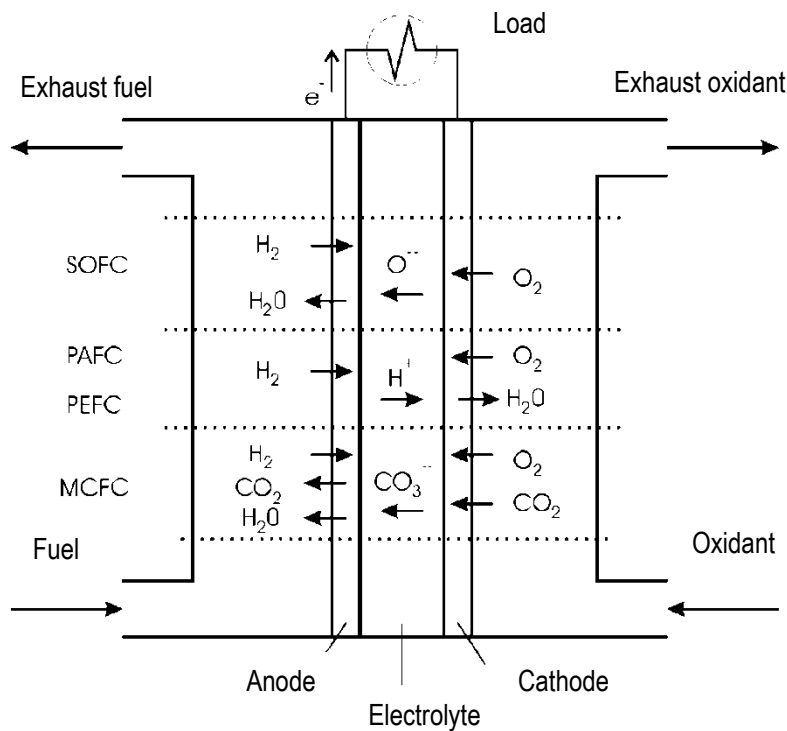


Figure 35. Schematic view of a fuel cell.

At the anode, the fuel, typically hydrogen or a hydrogen rich gas is oxidized, at the cathode pure oxygen or air oxygen is reduced. To produce higher power and voltage a number of single cells are connected in series through “bipolar plates” to form a “stack”, as shown in Figure 36. This architecture gives the possibility to easily build generators from few watts to MW.

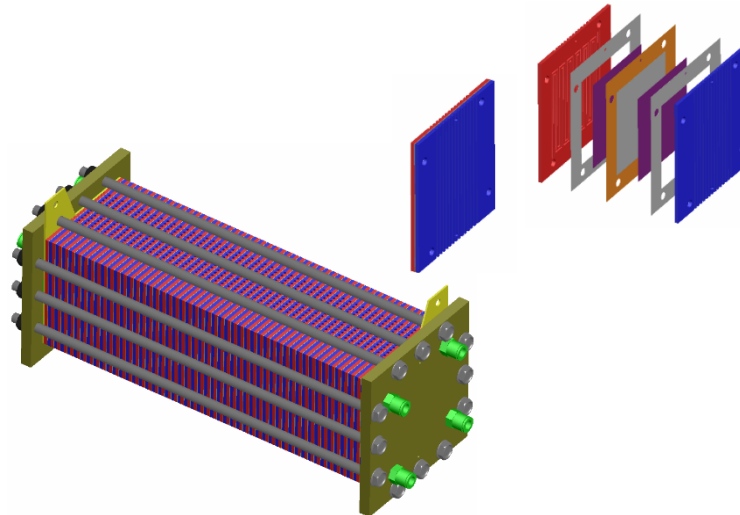


Figure 36. Schematic view of a fuel cell: from single cell to stack.

Fuel cell systems can be classified according to the type of electrolyte as presented in **Table 4**.

	PEMFC	AFC	HTPEMFC	PAFC	MCFC	SOFC
Electrolyte	Polymer Membrane	KOH	Pol. Memb./ Phosphoric Acid	Phosphoric Acid	Molten Carbonate	Solid Oxide
Temp. (°C)	70-80	80-100	120-180	200-220	600-650	800-1000
Corr.Den.	H	H	H	M	M	H
Reformer	External	External	External	External	Ext/Int	Ext/Int
Toll. CO ₂	Yes	No	Yes	Yes	Yes	Yes
Toll. CO	No	No	Yes	No	Yes	Yes
Typical Applications	Space. Transp. Portable	Space Transp. Portable	Transp. Micro CHP	Dist. Generation	Generaz. MW	Gen. Distrib.-MW
Typical system efficiency H ₂ (NG) LHV	35-50% (30-40%)	60% (NA)	30%-45% (25-40%)	47-50% (38-44%)	NA (50-55%)	NA (30-55%)

PEMFC: Proton Exchange Membrane Fuel Cell
AFC: Alkaline Fuel Cell

MCFC: Molten Carbonate Fuel Cell
SOFC: Solid Oxide Fuel Cell

HTPEMFC: High Temperature Proton Exchange Membrane Fuel Cell PAFC: Phosforic Acid Fuel Cell	DMFC: Direct Methanol Fuel Cell
--	---------------------------------

Table 4. Classification of fuel cells according to the electrolyte and main characteristics.

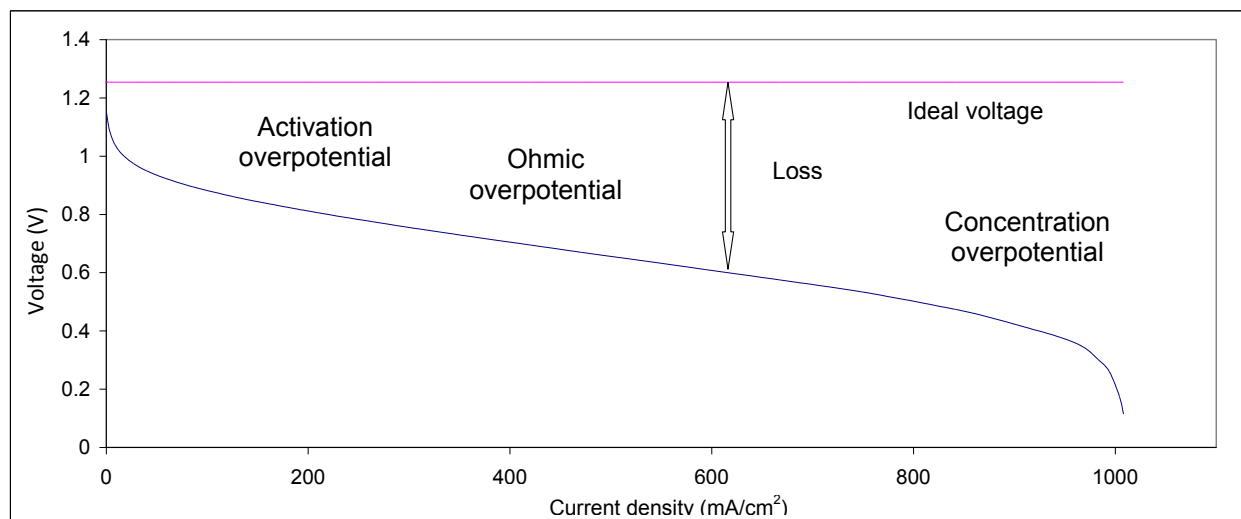


Figure 37. Typical polarization curve for a PEM fuel cells.

2.8.3 System integration and efficiency

Fuel cell based generators include not only the fuel cell stack but also:

- a fuel processor to allow operation with fuels other than hydrogen (e.g. natural gas, methanol);
- a power conditioner to regulate the output DC power of the cell and, if necessary, convert it AC with the requested frequency and voltage;
- an air management system to deliver air at the proper flow-rate, temperature, pressure and humidity to the cathode compartment;
- a thermal management system to heat up the stack during start up and remove heat from the stack during operation.
- a water management system to supply water for fuel processing and for reactant humidification.

A single cell with reactants at the proper pressure can reach electrical efficiencies as high as 80-90% depending on the current density. Taking into account all the necessary auxiliaries the efficiency of a typical PEM fuel cell generator fed with natural gas can be in the range of 30-45%, depending on size and load.

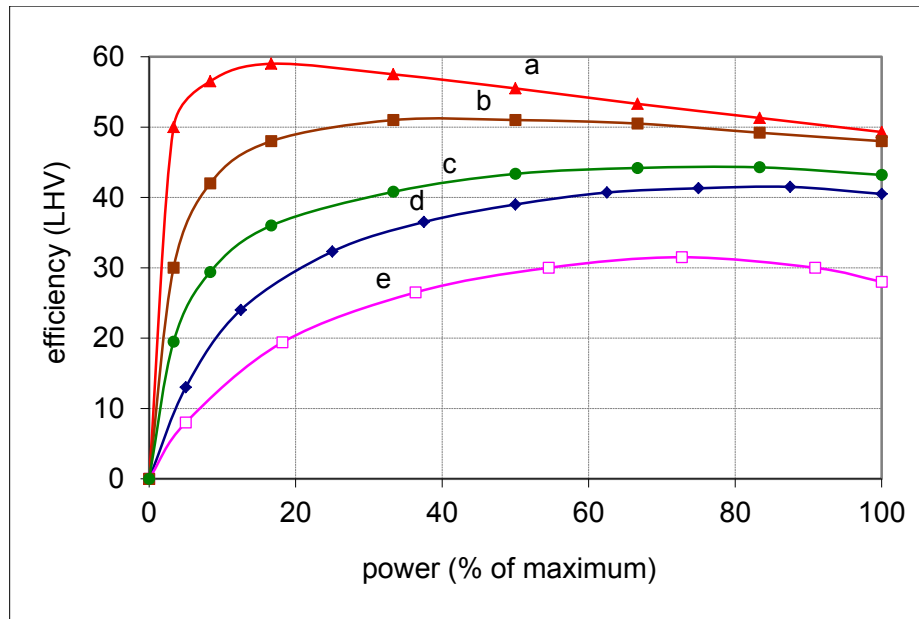


Figure 38. Typical efficiency curves for different types of engines with power output higher than 200 kW. a) Low pressure, low temperature fuel cell system. b) High pressure, high temperature fuel cell system. c) Fuel cell system with an on-board reformer. d) Compression-ignition engine (diesel). e) Spark-ignition engine. Elaborated from [7].

As presented in Figure 38, fuel cells engines fed with hydrocarbon and, therefore, including a fuel processor unit (curve c)) show efficiencies not far from those attainable with a diesel engines. Indeed, the emissions from a fuel cell fed with hydrogen are only water. If the fuel is a hydrocarbon processed by means of a reformer, the expected emission can easily controlled and lower than typical compression ignition or spark ignition engines.

The same figure shows, indeed, another interesting characteristic of fuel cells: the efficiency at part load can be higher than that at design load.

2.8.4 PEM fuel cells and micro-CHP

Considering the characteristics in Table 4 and the part load efficiency, Polymer Electrolyte Membrane (PEM) fuel cells appear to be a good candidate for micro-CHP applications. In PEM the most used electrolyte membrane is a perfluorinated polymer (normally Nafion®). These membranes are an excellent electrolyte because they comprise three key properties at the same time: (1) high proton conductivity; (2) efficient barrier to prevent mixing between fuel and the oxidant; and (2) chemically and mechanically stability. The drawback is that the proton conduction of these membranes depends strongly on the water content. Therefore, fuel cells where this type of membranes are used, maintain good performance as long as the operating temperature is below 75-80°C, otherwise the membrane dehydrates [49].

The low operating temperature infers some problems such as:

- intolerance to reactants impurities, mainly carbon monoxide (CO);
- slower electrochemical kinetics;
- complex heat and humidification management;
- complex heat recovery.

In the last years, research efforts have allowed the design of different polymer membranes capable of conserving high proton conductivity in anhydrous environments, maintaining high chemical and electrochemical stability at high temperature [50]. The major development can be grouped as follows [51], [52]:

1) utilization of modified PFSA membranes, by means of incorporating inorganic compound, such as SiO₂ and TiO₂;

2) utilization of sulfonated polyaromatic polymers and composite membranes, such as (S)PEEK, PI, PSF and SPSF;

3) water replacement. At high temperature, high proton conductivity can be achieved if water is replaced with a higher boiling point solvent for proton transport (e.g. phosphoric acid H₃PO₄ and imidazoles [HC₃H₃N₂, an alkaloid]). In this group, membranes based on PBI (polybenzimidazole), seem to assure heat resistance and good performances at $T \sim 125^{\circ}\text{--}200^{\circ}\text{C}$, tolerating high concentrations of CO (> 1%, up to 10%) [53], [54].

Considering i) the above mentioned advantages over conventional perfluorosulfonic acid based fuel cells and ii) considering as powering system the pre-existing methane gas distribution, the applications of fuel cells based on high temperature MEA is of great interest, especially in the residential microgeneration sector which is characterized by high potential diffusion. In this sector, HTPEM fuel cells may provide an extremely flexible power production system: the high temperature waste heat produced by the HTPEM fuel cells can be easily utilized for space heating and/or domestic hot water demands, and the heat-to-electric power production may be varied in a wide range through load and fuel utilization factor (and even temperature). As mentioned above, HTPEM fuel cells have an excellent behavior in modulating power output, as electrical efficiency increases with decreasing load factors. This allows to find an optimal trade-off point between efficiency and energy production, as well as between electrical and thermal power output, at part load. Respect to conventional PEM fuel cells based cogeneration systems, different studies [54], [55] demonstrated that a less complicated and more reliable system balance of plant can be used when HTPEM fuel cells are adopted, while system efficiency remains comparable. A summary of the main differences between LTPEM fuel cells and HTPEM fuel cells is shown in Table 5.

Considering the number of the potential installations, a system cost reduction, which is today a limiting factor, is expected.

Currently, the main concern regarding the employment of HTPEM fuel cells is the operational lifetime. In fact, for automotive applications, at least 5000 h lifetime is required, while for stationary power, 40000 h must be demonstrated. PEM fuel cells operational lifetime is associated both to membrane degradation, which is accelerated at high temperatures, and to chemical and morphological instability of the catalyst [56]. Relating to the catalyst, the main issue that occurs at high temperature are: i) corrosion of carbon support, ii) agglomeration of Pt particles, iii) Pt dissolution. As for the membrane problem of mechanical resistance and phosphoric acid loss during operation can occur. In Figure 39 is shown a cross section of an HTPEM MEA BASF Celtec 1000 before and after operation. It is possible to observe that in the used MEA the electrolyte shows a reduced thickness compared to the new one. On the long term the polymer mechanical stress can cause cross over problem impairing the cell performance.

The interest for the potential of HTPEM is confirmed by the supportive policies from the governments [43]. For instance, the U.S. Department of Energy's funding for fuel cells, hydrogen and related materials research totaled US\$ 244 million in the fiscal year of 2010, and in the

European Union a partnership between the European Commission and private companies had dedicated more than € 200 million to support research and demonstration activities. HTPEM technology it is still incipient in the overall market, however some companies are breaking through, mainly in Europe. Serenergy, is the only company which commercializes fuel cell stacks featuring HTPEM technology. At the moment they are able to manufacture and supply stacks with a nominal power of 32 kW operating at 140-170°C. In addition, other companies, such as Advent Technologies SA and Danish Power Systems, are able to supply membrane electrode assemblies (MEAs) design to operate at high temperatures.

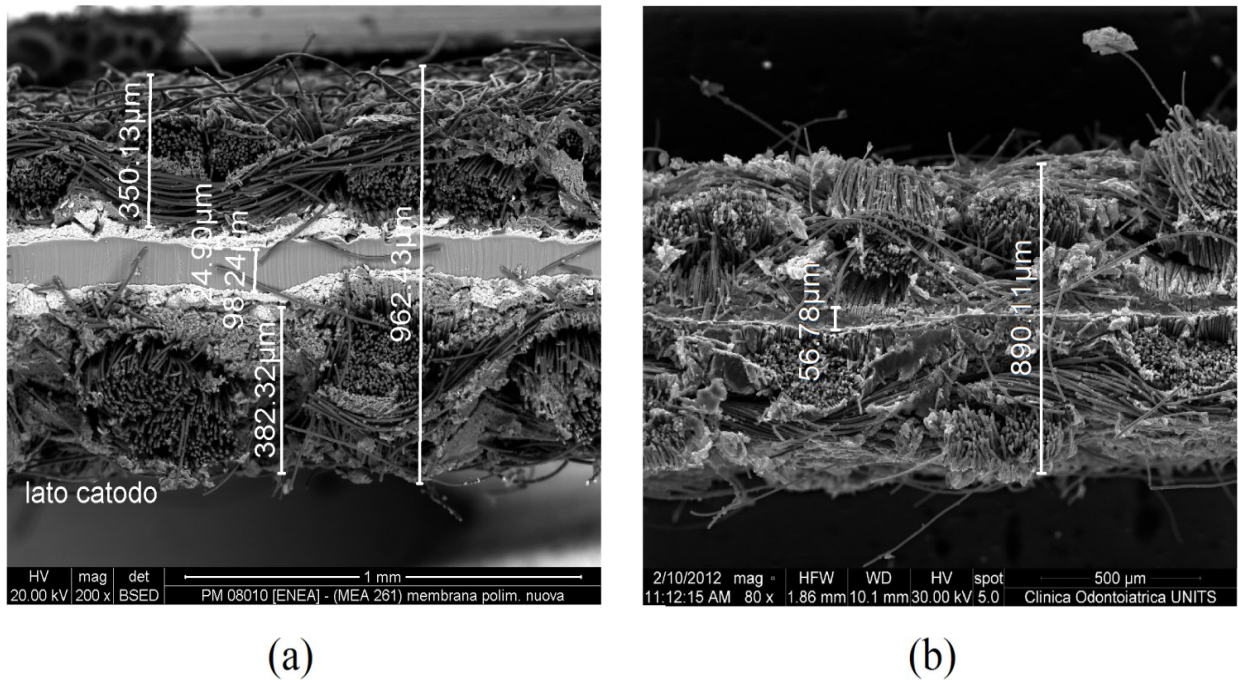


Figure 39. SEM image of a cross section of a HTPEM MEA before operation (a) and after operation (b).

LTPEM (T<100°C)	HTPEM (T>120°C)
Tolerance to fuel impurities: CO below 100ppm H ₂ S below 0.1 ppm CH ₃ OH below 1%	Tolerance to fuel impurities: CO up to 3% (~ 1%) H ₂ S up to 10 ppm CH ₃ OH up to 10%
Hydrogen or complex reformer required	Simplified system at reformat
Humidification required!	Independent of humidification
Membrane stability issue	High chemical stability of memb 20.000 hr [57]
Complex co- and tri-generation	Effective co- and tri-generation, direct use of heat possible

Table 5. Comparison between LTPEM and HTPEM

2.8.5 Costs and applications

Fuel cells remain an expensive technology, especially for the micro-CHP segment. The vast majority of non-portable fuel cells sold to consumers today are done so with the aid of a subsidy. The most famous example of financial support is the Ene-Farm scheme in Japan (Figure 40), where a government subsidy has facilitated the sale of more than 45,000 residential fuel cell units since the program began sales in 2009. The support scheme has contributed to the reduction of the retail price and, today, the Panasonic system (0.7 kW, 38% LHV efficiency) is sold at about € 15.000 and a lifetime of 10 year or 40.000 h is expected [58].

In Europe, Elcore has designed a system specifically for the German market. Unlike most fuel cell micro-CHP systems, the Elcore 2400 is not intended to be a full boiler replacement but rather an add-on. With an electrical output of 300 W and a thermal output of 600 W, the system is designed to meet the electrical base load of an average German home as well as the year-round hot water requirement, with some excess available for space heating. The unit price is € 9000 [59].

PAFC, even if not exactly suitable for micro CHP are, anyway, among the most commercialized type of fuel cells. In particular, the Pure cell model 400 and its predecessor model 200 have been sold in hundreds of units [60]. Another unit suitable for CHP with a power output of 100 kW is the Energy server produced by Bloom Energy. Bloom Energy Servers produce more than 130 MW for several major companies and non-profit organizations in the US [61]. Pure cell model 400 is sold at about 3000-5000 €/ kW and Bloom energy server at 7000 €/kW [43].

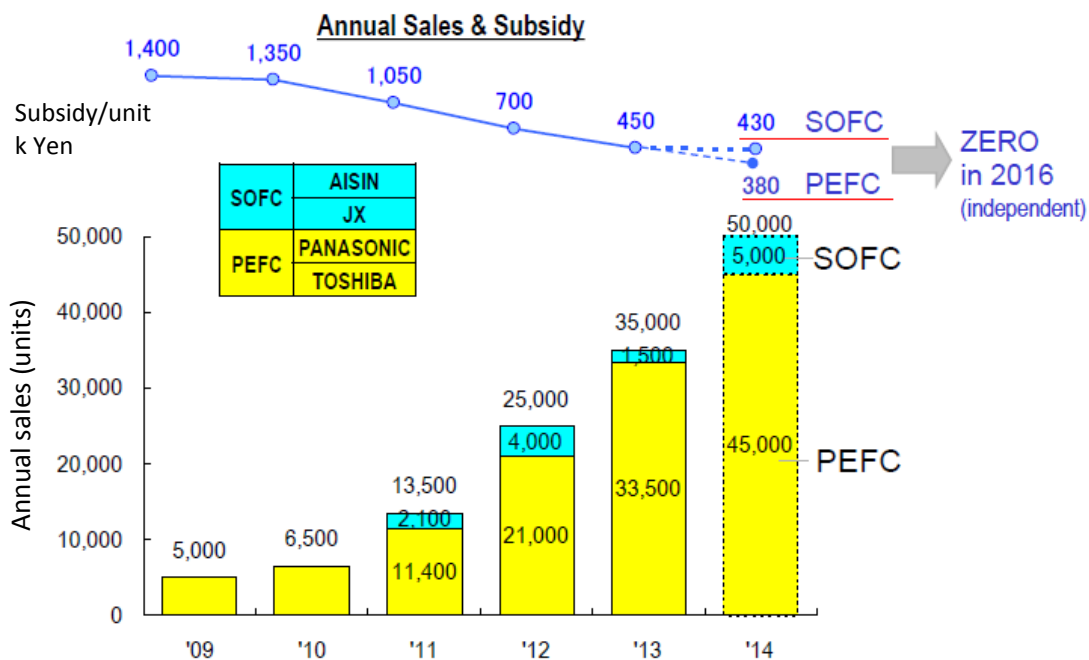


Figure 40. Japan FC sales and subsidy. Elaborated from [62].




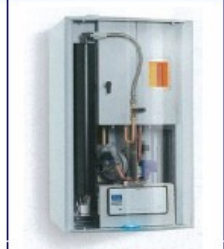






SOFC	Bosch +AISIN	CFCL	Hexis	Vaillant	SOFC Power
	 0.7W	 1.5kW	 1.0kW	 1.0kW	 2.5kW
PEFC	Baxi Innotech +TOSHIBA	Elcore	Viessmann +Panasonic	Dantherm Power	RBZ
	 ? ? W	 0.3kW	 0.75kW	 0.5-2kW	 5kW

Figure 41. Micro-CHP in Europe, some of the competitors in SOFC and PEM [63].

2.9 Micro-CHP: technologies comparison

In Chapter 1 it has been pointed out that the integration of micro-CHP with RES DG should aim to obtain the main following results:

- 1) availability of capacity in case of RES lack/failure;
- 2) reduction of transmission grid overload;
- 3) higher overall fuel efficiency;
- 4) reduction in specific CO₂ emissions;

On the basis of these points and additional considerations, the choice to study HTPEM micro-CHP, in the following Chapters, will be motivated.

In Table 6 a comparison of the presented technologies in the 1 kWe range that can be fuelled with natural gas and commercially available is presented.

Micro gas turbine are not considered as, in this power range, commercial available products have not been found.

	Availability of capacity/grid overload/lifetime/maintenance (1)	Efficiency/ emissions	Installation/dimensions/ technology
ICE	<p>Load response quite good.</p> <p>Not suitable to idle/low load as it can result in lifetime reduction.</p> <p>Overhaul expected every 6000-8000h. Many moving parts subjected to wear and high temperatures.</p> <p>Lifetime: NDA</p>	<p>Efficiency at design conditions abt. 25%.</p> <p>Decreasing at part load. Emission can be controlled better than automotive applications but it remains an ICE.</p>	<p>Require external exhaust.</p> <p>“Washing machine” size.</p> <p>Mature technology. More than 100.000 units sold.</p>
STIRLING	<p>Load response can be good.</p> <p>Not suitable to idle/low load as heat / electricity ratio high.</p> <p>Moving parts subjected to wear and moderate temperatures. No internal combustion.</p> <p>Lifetime: NDA</p>	<p>Efficiency at design conditions abt. 10%.</p> <p>Good at part load. Emission can be controlled as combustion is external and catalytic combustors with controlled temperature can be used.</p>	<p>Require external exhaust.</p> <p>“Washing machine” size.</p> <p>New market. Few units in operation.</p> <p>Direct integration with RES possible (solar thermal, biomass or other heat (T>300°C) sources)</p>
ORC	<p>Load response can be good.</p> <p>Not suitable to idle/low load as heat / electricity ratio high.</p> <p>Data are not available.</p> <p>As few moving parts are present and technology is similar to heat pumps, reduced maintenance and long lifetime expected.</p>	<p>Efficiency at design conditions abt. 10%.</p> <p>Good at part load. Emission can be controlled as combustion is external and catalytic combustors with controlled temperature can be used.</p>	<p>Require external exhaust.</p> <p>“Washing machine” size.</p> <p>New market. Few units in operation.</p> <p>Direct integration with RES possible (solar thermal, biomass or other low temperature (>120°C) sources)</p>
FC	<p>Load response very good but depending on fuel processor performance.</p> <p>Suitable to idle/low load.</p> <p>Few moving parts. No combustion in fuel cell. Catalytic combustion required in fuel processor. Lifetime of 40.000h expected</p>	<p>Efficiency at design conditions abt. 35%.</p> <p>Increasing efficiency at part load. Emission only from fuel processor. Emission can be controlled as combustion is external and catalytic combustors with controlled temperature can be used.</p>	<p>Require external exhaust.</p> <p>“Washing machine” size.</p> <p>Mature technology. More than 100.000 PEM units sold. SOFC: few units sold so far but sales increasing.</p>
(1) In all the systems load response can be excellent if storage system is available			

Table 6. Comparison of different micro CHP technologies in the range of 1kW.

From Table 6 it comes out that, in the considered power range, fuel cell systems seem to be the best candidate. The question that arises is: which is the most appropriate technology to use, PEM or SOFC? At the time the research project started (end of 2010) the prevailing technology was

PEM. But PEM showed some drawbacks (Table 5) and, as the progresses on PBI MEAs were quick with several emerging companies offering on the market different products, it was decided to focus on this technology.

High cost remains the main obstacle that hampers fuel cells commercialization. Indeed, a comparison can be made with PV cost. In few years PV module cost has dropped (Figure 42) since many supporting schemes have been introduced to promote the technology. If this will be the case for micro-CHP fuel cell systems, and the trend in technology improvements will be maintained, cost could benefit in a similar way.

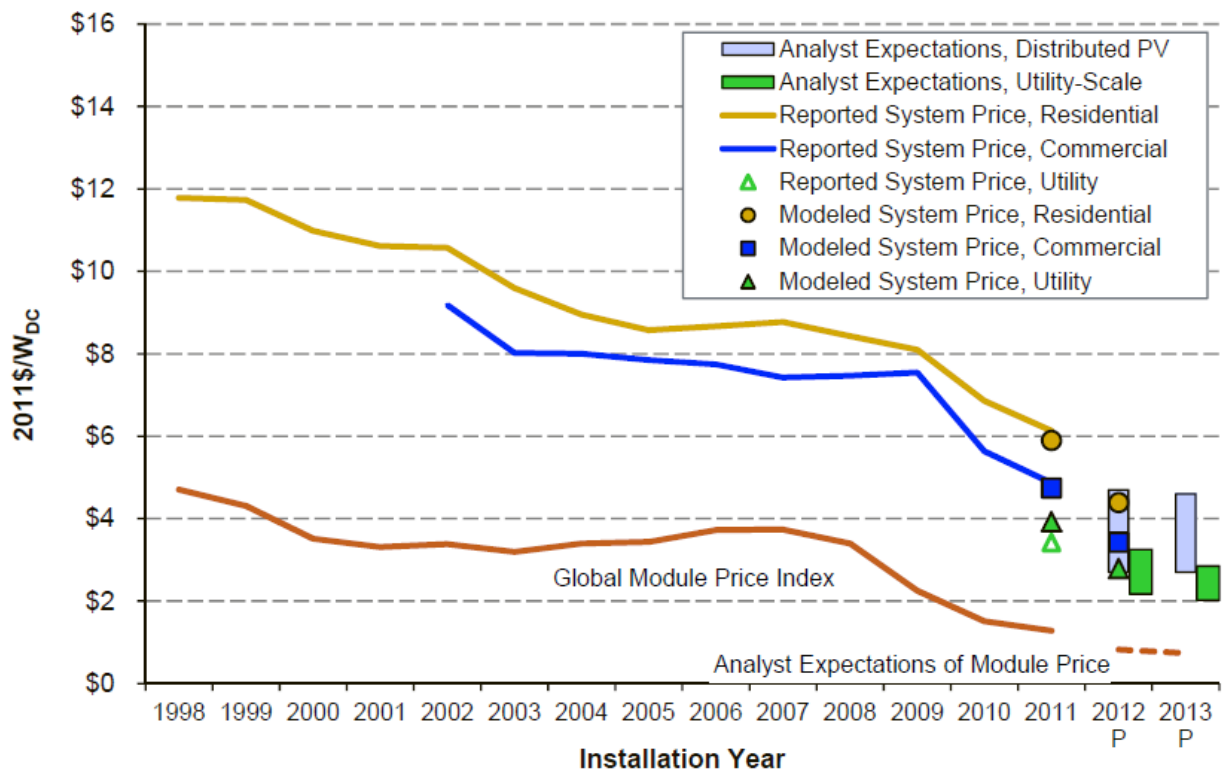


Figure 42. PV cost trend. In ten years the price of residential system has halved [64].

3 PAPERS AND REPORTS PRESENTED DURING THE RESEARCH

3.1 Introduction

In this paragraph the papers and report published during the PhD program and concerning the main research project are presented. The papers are grouped according to the tasks in which the research has been articulated:

Literature review and background

Test rig and automation system set up

Experimental characterization of single cells and stack

Experimental characterization of the fuel processor and complete system

Experimental degradation analysis

Simulation models development

List of the paper related to the main research activity:

- I. **R. Radu, N. Zuliani, R. Taccani, Design And Experimental Characterization Of A High Temperature Pem Fuel Cell Stack, Journal of Fuel cell Science and technology, 11/2011 vol. 8 pg 051007 1-5, ISSN 1550-624X.**
- II. Radu. R., Taccani R., Zuliani N. (2011). Utilizzo di un Reformer per l'Alimentazione di una Cella a Combustibile: Analisi del Sistema di Controllo. National Instrument - formato elettronico, pp.-- -, In: 18° NIDays forum tecnologico sulla progettazione grafica di sistemi. 23 febbraio 2011, Milano ,
- III. Zuliani N., Taccani R., Radu R. (2011). Effects of control strategies on the transient performance of a HTPEM fuel cell system fuelled with propane. ENEA, pp.261- 262, Vol. 1, In: 4th European Fuel Cell Conference and Exhibition. 14-16 dicembre 2011, Roma,
- IV. **R. Taccani, N. Zuliani, Effect of flow field design on performances of high temperature PEM fuel cells: Experimental analysis, International Journal of Hydrogen Energy, Volume 36, Issue 16, August 2011, Pages 10282-10287, ISSN: 0360-3199**
- V. Zuliani N., Taccani R., Radu R. (2011). Experimental and Theoretical Performance Analysis of an High Temperature PEM Fuel Cell fed With LPG Using a Compact Steam Reformer. ASME Digital Library, pp.-- -, In: ASME 2011 5th International Conference on Energy Sustainability . 7-10 Agosto 2011, Grand Hyat Washington DC – USA.
- VI. **Zuliani, N., Taccani, R., Microgeneration system based on HTPEM fuel cell fuelled with natural gas: Performance analysis, Applied Energy, 2012, Vol. 97 pp. 802-808.**
- VII. Valle F, Marmiroli B., Amenitsch H., Taccani R. (2012). Electron microscopy and small-angle X-ray scattering analysis of the catalyst layer degradation. Associazione

- Termotecnica Italiana - Sez. Friuli Venezia Giulia, Trieste: pp.1- 7, In: 67° Congresso nazionale ATI - Trieste 2012. Settembre 2012, Trieste.
- VIII. Zuliani N., Taccani R. (2012). Micro Combined Heat And Power System Based On Htpem Fuel Cell And Li-Ion Batteries: Performance Analysis. ATI Sezione FVG - Formato elettronico, pp.-- -, In: 67° Congresso Nazionale ATI. 11-14 Settembre 2012, Trieste.
- IX. N. Zuliani, R. Taccani (2013). Micro combined heat and power system based on htpem fuel cell and li-ion batteries: analysis of performance under different operating strategies . Università degli Studi del Sannio - Università degli Studi di Napoli, pp.-- -, In: Microgen III. Aprile 15-17, 2013, Napoli,
- X. N. Zuliani, F. Valle, R. Taccani (2013). Degrado accelerato di celle a combustibile polimeriche: sistema di acquisizione dati e controllo. National Instrument , pp.0- 1, In: NI LabVIEW Days 2013. settembre 2013, Milano,
- XI. **Zuliani N., Taccani R., Energy simulation model and parametric analysis of a micro cogeneration system based on a htpem fuel cell and battery storage, Proceeding of ICAE2013, International Conference on Applied Energy, Pretoria 2013.**
- XII. F. Valle, N. Zuliani, B. Marmioli, H. Amenitsch, R. Taccani (2013). Experimental analysis of catalyst degradation in High Temperature PEM Fuel Cells subjected to accelerated ageing tests. pp.1- 9, In: 5th International Conference Fundamentals & Development of Fuel Cells. 16-18 April 2013, Conference Center Karlsruhe, Germany.
- XIII. R. Radu, R. Taccani (2013). Monitoraggio e controllo di un sistema micro-cogenerativo con celle a combustibile. National Instruments Italy, pp.1- 6, In: NI Days 2013. 27/02/2013, Milano.
- XIV. **R. Radu, R. Taccani, M. Scagliotti, C. Valli (2013). HT PEM fuel cell system fed with biogas: experimental characterizations. ECOS 2013, pp.1- 9, In: 26th International Conference on Efficiency, Cost, Optimization, Simulation and Environmental Impact of Energy Systems (ECOS). July 16-19, 2013, Guilin, Guangxi, China.**
- XV. N. Zuliani, F. Valle, R. Taccani Performance degradation study on polybenzimidazole fuel cells subjected to different ageing tests, European Fuel Cell Conference, Roma 2013.
- XVI. **F. Valle, N. Zuliani, B. Marmioli, H. Amenitsch, R. Taccani (2014), SAXS Analysis of Catalyst Degradation in High Temperature PEM Fuel Cells Subjected to Accelerated Ageing Tests, Fuel cells, Wiley-VHC.**

In bold letters the papers that have been attached to the thesis. Some of the activity carried out in 2011 has started before the official initial date of the PhD course.

3.2 Literature review and background

A literature review and background on the DG are presented in Ch. 1 a Ch. 2. Specific topic oriented literature review are presented in the attached papers.

3.3 Simulation models development

In order to design the system a process simulation model of a 1 kWe HTPEM based micro-CHP has been implemented [VI]. The model encompasses two subsystem: the fuel cell and the reformer.

The voltage of the cell is obtained on the basis of a semi-empirical model [65] and expressed with the following equation:

$$U_{cell} = U_0 - \frac{RT}{4\alpha_c} \ln \left(\frac{i}{i_0} \right) - i R_{ohmic} - \frac{RT}{\lambda_{cat}} \ln \left(\frac{i}{i_0} \right) + U_{CO}$$

Referring to equation (1), U_{cell} is the cell voltage, U_0 is the open circuit voltage. The second term represents the Tafel equation and includes the charge transfer coefficient α_c , the current density i and the exchange current densities i_0 . The third term is related to the ohmic loss. In the fourth term the resistance associated with the concentration losses is related to the cathode stoichiometry λ_{cat} . The variables i_0 , R_{ohmic} , α_c and R_{conc} , are made temperature dependant through suitable regressions. The last term represents the anode overpotential due to the CO poisoning effect on the anode catalyst layer. The fuel cell model is zero-dimensional, therefore no spatial variation of its physical properties is considered. For the stack, the number of cells considered is 100 in order to achieve an electric power of 1 kW at 0.5 V single cell voltage. The active area is 50 cm² and the stack is air cooled. The stack operating temperature has been assumed equal to 160°C. The stack energy balance is used to evaluate the stack thermal power output. It takes into account for heat losses to surroundings and heat losses due to the reactants cooling effect. The fuel cell model is implemented in Fortran and then integrated in the commercial SW for industrial process simulation, Aspen Plus®, that has been used to model the fuel processor. The model has been used, for example, to analyse the system performance at different loads (Figure 43).

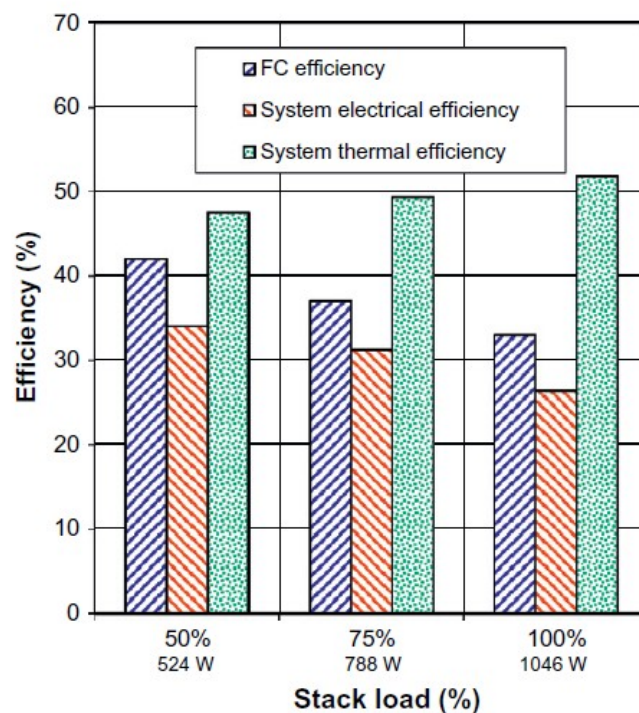


Figure 43. Fuel cell and system electrical and thermal efficiencies as function of stack load [VIII].

The model has been then used to assess the potential of the micro CHP in combination with distributed electrical storage [VIII, XI]. The considered plant is composed of a 1 kW_{el} fuel cell system, which encompasses a fuel processor and a HPEM fuel cell stack, and a 3 kWh lithium-ion battery pack. A PV array composed of 7 modules of 300 Wp is included. An auxiliary boiler is used when heat from the fuel cell system is not enough for providing the heating demand. Fuel cell system, battery pack and grid are electrically connected by means of a power conditioning system. Figure 44 shows the electrical system schematic layout.

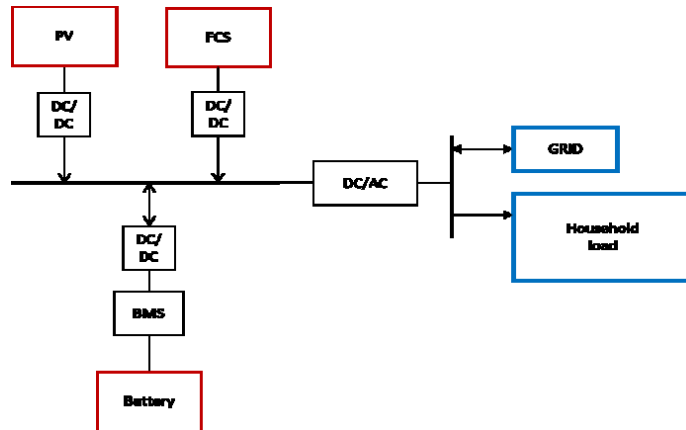


Figure 44. System lay-out [XI].

On the basis of a typical electrical and load profile for an Italian dwelling (Figure 45), it has been possible, for example, to evaluate the PES (Primary Energy Saving index) achievable with different plant configurations (Figure 46).

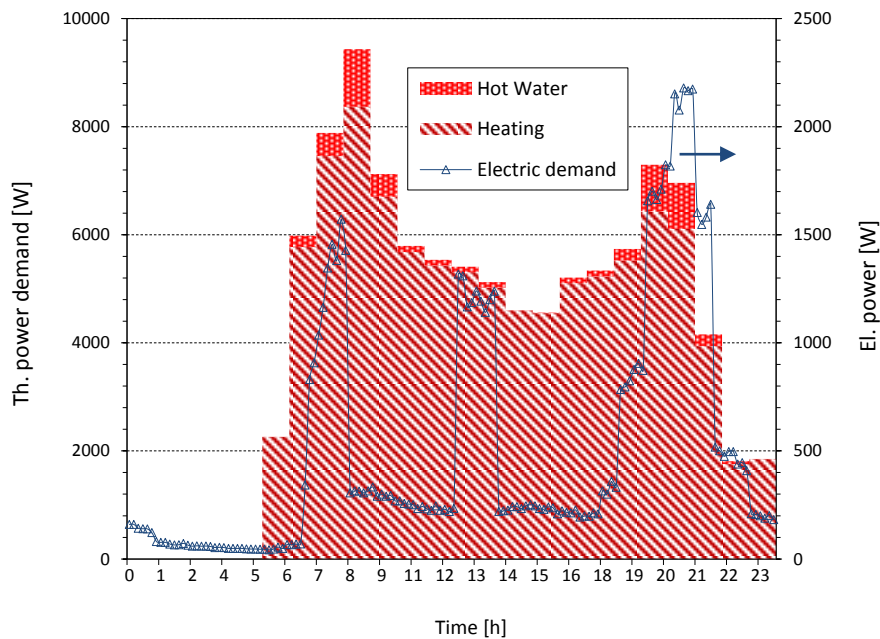


Figure 45. Electric and thermal power load curves assumed for the January typical day [XI].

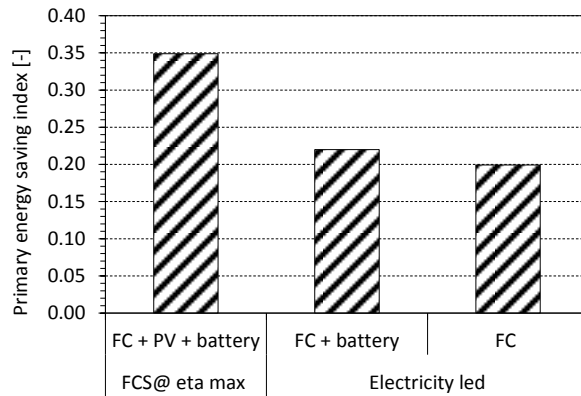


Figure 46. Primary energy saving index for the three considered system configuration [XI].

3.4 Test rig and automation system set up

In order to characterize the fuel cells both as single units and stacks, a test rig with the necessary equipment to measure the operating variables have been implemented. In a following phase, a test rig to analyze the performance of the fuel processor and the complete system has been developed. The description of the systems is presented in the technical report [II, XIII].

The SW used for the data acquisition and for the development of the Graphic User Interfaces is Labview. The hardware is based on Compact RIO (National Instruments) modules.

An example of the interface used for the data acquisition and control of the fuel cell plus reformer aggregate is shown in Figure 47.

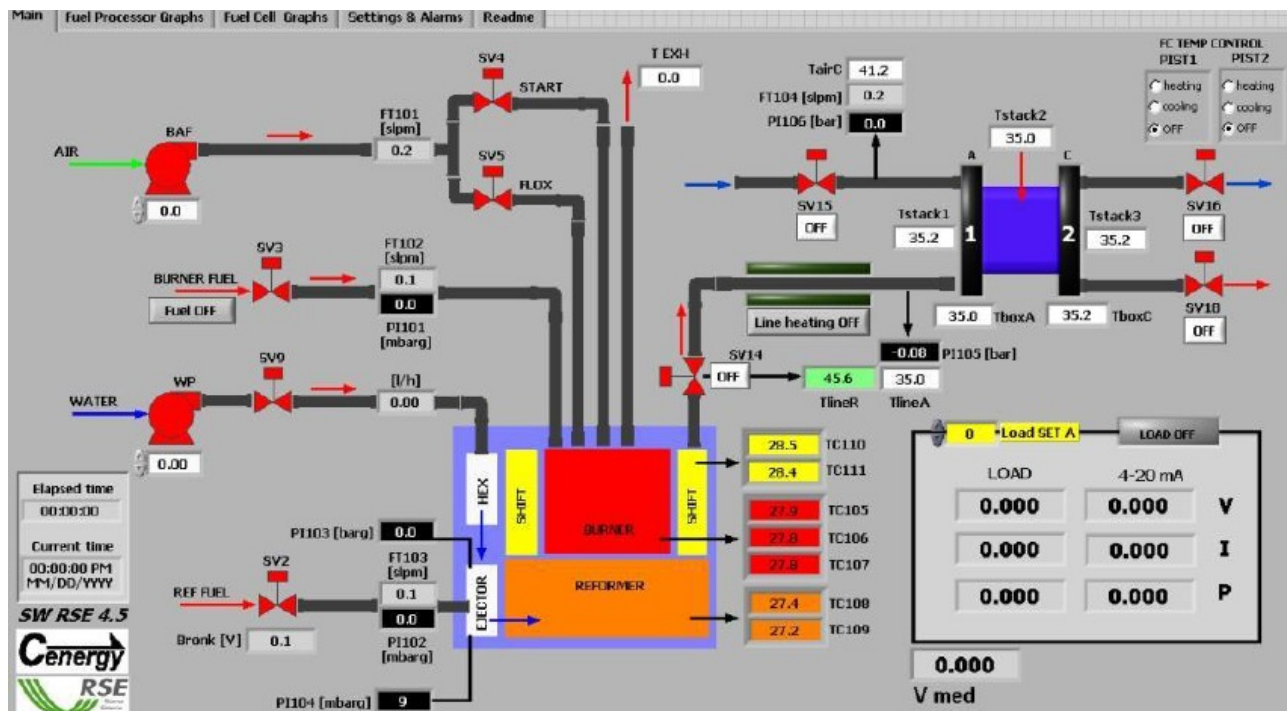


Figure 47. Graphic interface of the data acquisition and control system of the fuel cell based micro-CHP [XIII].

3.5 Experimental characterization of single cells and stack

Several single cells and different bipolar plates' configurations have been tested in order to identify the right combination of material and components design to achieve the best performance. In [IV] a study on how the geometry of the flow distribution channels in the bipolar plates affect the cell performance is carried out. Three different channel geometries have been considered: a) 5 step serpentine pattern, b) 4 step serpentine pattern c) parallel channels pattern.

Some of the results are shown in Figure 48: in the considered operating conditions the geometry that allows reaching higher performance in terms of polarization curve is the five and four step serpentine. The lower performance of parallel channels can be the consequence of the formation of reactants preferential paths that reduce oxygen partial pressure, affecting cell performance. This behavior is confirmed by fluid dynamics simulation models and experimental data available in literature [66],[67].

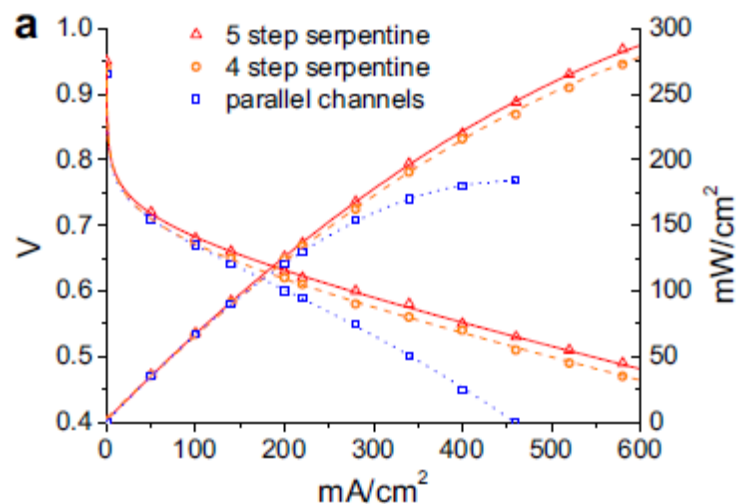


Figure 48. Polarization and power density curves measured with the same operating conditions but using different bipolar plates [IV].

A stack characterization is presented in [I]. The stack has three cells fed in parallel. Each cell contains a commercial PBI BASF Fuel Cell Celtec P-1000 MEA, two bipolar plates and the gaskets that seal the active area and the reactant manifolds. The tests have been carried out with hydrogen and syngas with different compositions (Table 7).

Mixture	Composition		
	CO %	CO ₂ %	H ₂ %
M #1	0.5	30.0	69.5
M #2	1.0	29.0	70.0
M #3	1.5	28.4	70.1
M #4	2.0	28.0	70.0

Table 7. Composition of the gas mixtures used in the presented experimental data [I].

With pure hydrogen at 180 °C, as shown in Figure 49, the stack reaches a maximum power output of 64 W at 1.2 V. Keeping the same level of stack voltage, at 160 °C, the stack output decreases to

60 W. At 1.8 V, the power outputs for 160 °C and 180 °C are 30 W and 32 W, respectively. The differences between adjacent performance curves slightly decrease as the stack temperature increases. For example, considering a stack current of 31 A, from 120 °C to 140 °C the stack voltage increases by 120 mV, while the differences between 140 °C and 160 °C, and 160 °C and 180 °C, are 90 and 30 mV, respectively.

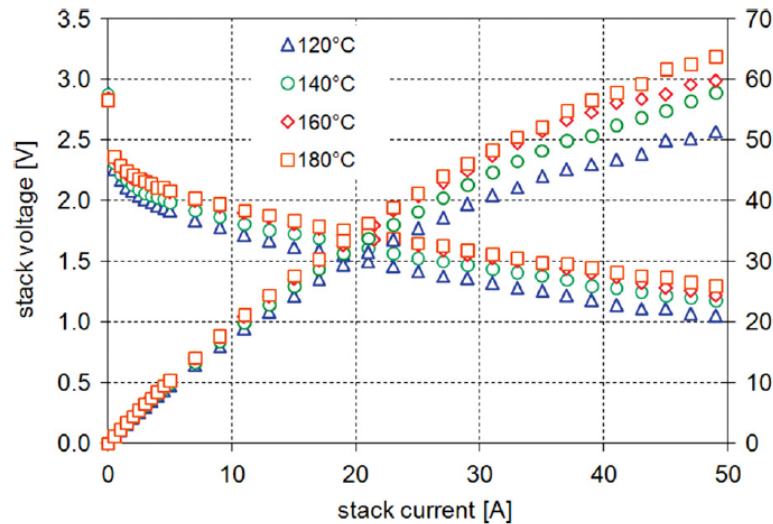


Figure 49. Stack performance with pure hydrogen, at different operating temperatures. Anode stoichiometry 1.5, cathode stoichiometry 3.0 [I].

The effect of CO in the syngas is important as it determines the syngas purity level to be obtained with the reformer. The influences of both temperature and CO concentration on stack operation are illustrated in Figure 50, which shows the effects of the latter operating variable on stack current at a cell voltage of 0.6 V. The first group of columns is related to the pure hydrogen data, while the other four groups are for the simulated reformates. The presented data emphasize that a higher operating temperature increases stack performance and diminishes the influence of CO concentration. For 180 °C, the increase of CO concentration from 0.5 to 2% decreases the stack current by 7.5% (from 14.6 to 13.5 A), while for 120 °C, the current decreases by 54.3% (from 4.6 to 2.1 A). Although the comparison between the data regarding the simulated reformates shows only the influence of CO concentration, comparison with the pure hydrogen data also contains the effect of hydrogen partial pressure. In this case, the significant performance losses are related to the CO poisoning effect, but also to the decrease in hydrogen partial pressure from 1 to 0.7.

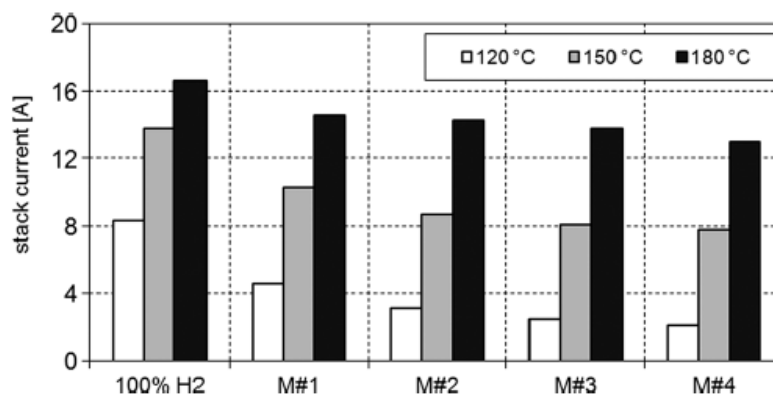


Figure 50. Influence of CO concentration and operating temperature on the stack current at cell voltage of 0.6 V [I].

3.6 Experimental characterization of the fuel processor and complete system

In order to use natural gas as fuel for the stack a steam reforming reactor (fuel processor) has been used. An series of tests have been carried out in order to measure the efficiency and the effect of fuel composition and operating variable on syngas composition and cell/stack performance [III,VI,VI,XIV]. The micro-CHP plant schematic is shown in [V].

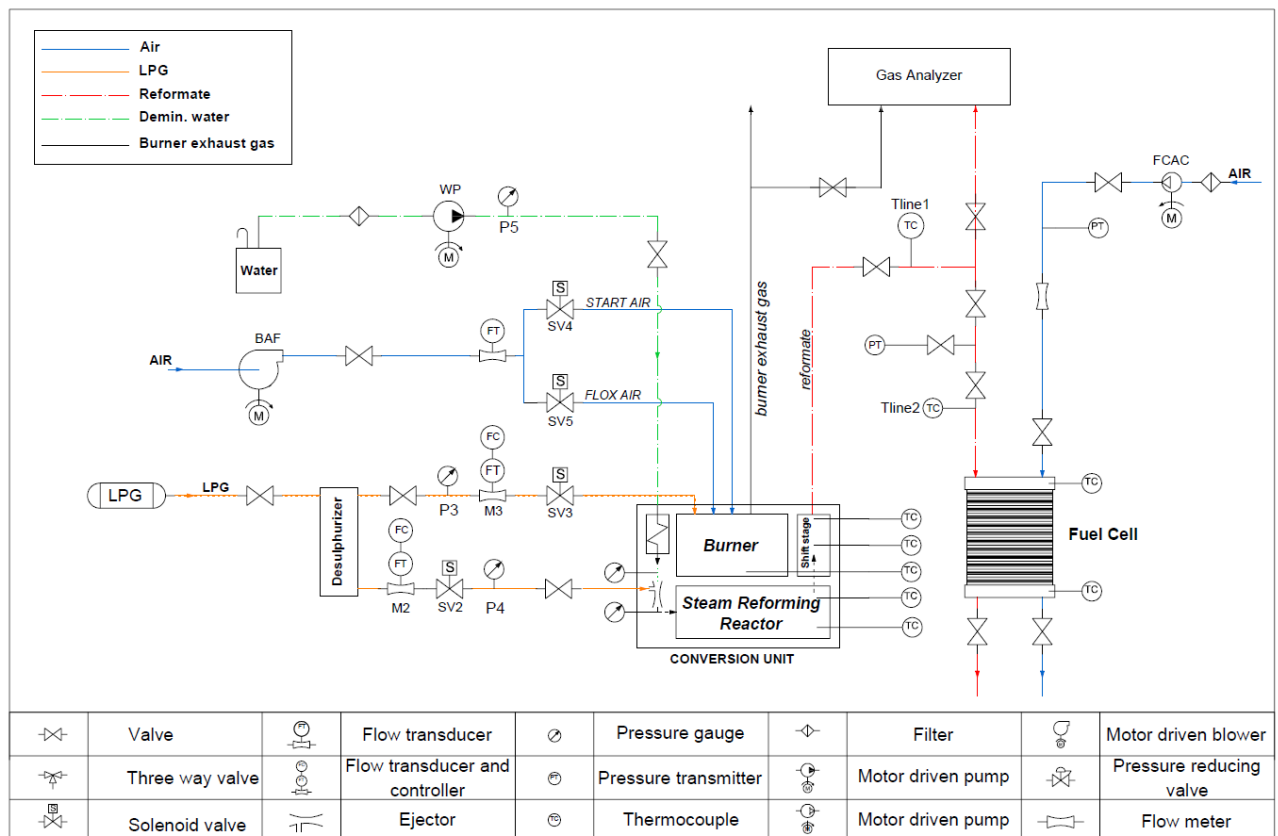


Figure 51. Simplified schematic of the considered plant [V].

The system encompasses two main components: the fuel processor and the stack.

✓ Fuel processor

The fuel processor is composed of a burner, a steam reforming reactor, a single CO purification stage (water gas shift reactor) and heat exchangers. The burner unit consists of an integrated start burner, which operates as a classical diffusion burner and is used to heat-up the combustion chamber above the self-ignition temperature of the gas mixture (about 800°C). At this temperature the burner can be switched to a flameless combustion using a catalytic bed. Therefore fuels with different heating values, such as fuel cell anode off gas, can be used and local temperature peaks are avoided also, leading to low NO_x-emissions. The reforming reactor is based on a Nickel catalyst and consists of a annular reactor heated centrally by the burner. The gas leaving the reformer enters a single stage water gas shift reactor (WGSR) to reduce CO. The WGSR is based on a Cu-ZnO catalyst and it is cooled/tempered by means of evaporating process water. Integrated heat exchangers are meant for LPG and process water streams heating up using the exhaust gas from the burner and the product hydrogen rich gas from the reforming reactor. The

reformer fuel is supplied by means of a steam jet pump. Driving force is the overheated steam at an adjustable pressure level supplied by the water pump. In the nozzle the LPG is mixed with the steam. Other components of the system are: an air blower which supplies air to the burner, a water pump that supplies demineralized water to the reformer, valves and mass flow transducer and controller to monitor streams flow rates. At design conditions syngas flow rate is expected to be $2.0 \text{ Nm}^3/\text{h}$ and the composition to be (vol. dry basis): hydrogen 75%-79%, CO_2 20%-23%, CH_4 <1%, CO <1%.

✓ *Fuel cell stack*

The tests have been carried out on a set of single cells and stack but all of them using commercial PBI BASF Fuel Cell Celtec P-1000 MEA. The MEA has an active area of 50 cm^2 and an average thickness of $860 \mu\text{m}$. The membrane thickness is about $60 \mu\text{m}$ and has a phosphoric acid content of more than 95 wt% in a PBI matrix. The platinum catalyst load is 0.75 mg/cm^2 on the cathode and 1 mg/cm^2 on the anode.

The experimental measurements have been carried out both in laboratory conditions [[III,VI,VI] and during a field test [XIV]. The latter has been carried out using the gas from a digestion plant near Padova (Italy). A selection of the main results obtained during the tests is hereafter presented.

Analysis of Reformer Start Up Transient

While fuel cells operated with hydrogen respond very quickly to load variation this is not the case for hydrocarbon fuelled system using a reformer. Indeed, start up transient is crucial for a wider fuel cells market penetration. To this respect, modern internal combustion engines are able to reach full power in few seconds after start up. This can be achieved as the thermal inertia of internal combustion engine is lower when compared with a reformer unit. For the proper operation of the reformer two critical temperatures have to be reached: the reformer reaction takes place at approx. 650°C and a good efficiency in the shift reactor is obtained at $200\text{-}250^\circ\text{C}$. An example of the transient operation of the fuel processor when using two different fuels, LPG and biogas, is shown in Figure 52 and Figure 53. It is possible to observe that when LPG is used, the proper temperature for shift reaction operation (180°C) is reached in about 70 min. When biogas is used and the LHV is lower, it takes more than 90 min to reach the same temperature.

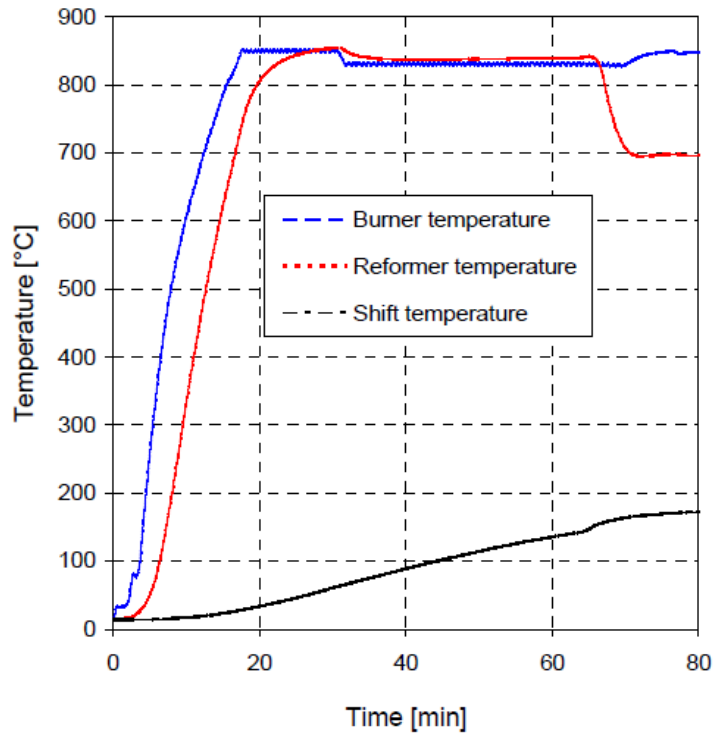


Figure 52. Fuel processor startup. Reactors temperature profile over time. Fuel LPG [V].

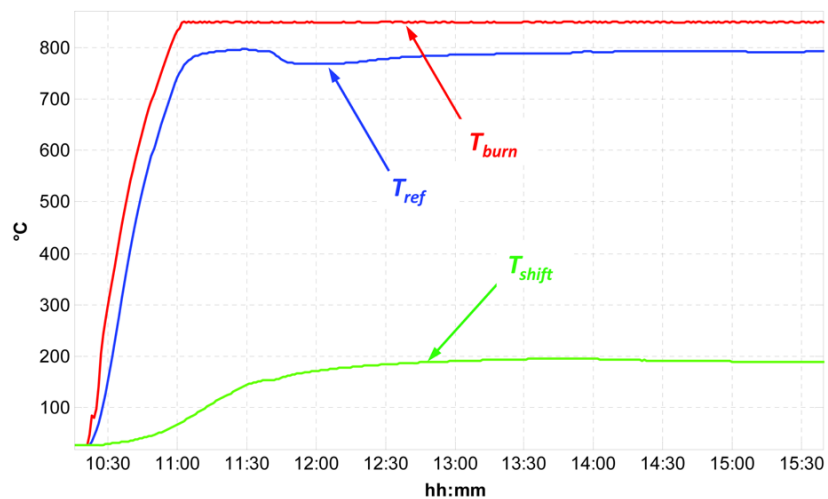


Figure 53. Fuel processor startup. Reactors temperature profile over time. Fuel biogas [XIV].

Overall system performance

Figure 54 presents the comparison between the cell performances obtained with biogas reformat at the beginning of the field tests and the data obtained with hydrogen and simulated reformat (56% H_2 , 0.5% CO , 43.5 % CO_2). All the presented data refer to an operating temperature of 160 °C. The biogas reformat composition was, on dry basis, 70% H_2 , 0.2% CO , the rest CO_2 .

Figure 55 presents the performance curves obtained with the 22 cell stack fuelled with biogas reformate, with a hydrogen content of 61.7 % and 0.1 % of carbon monoxide. The stack generated a maximum power of 133.8 W @ 11.27 V (512 mV of cell average voltage).

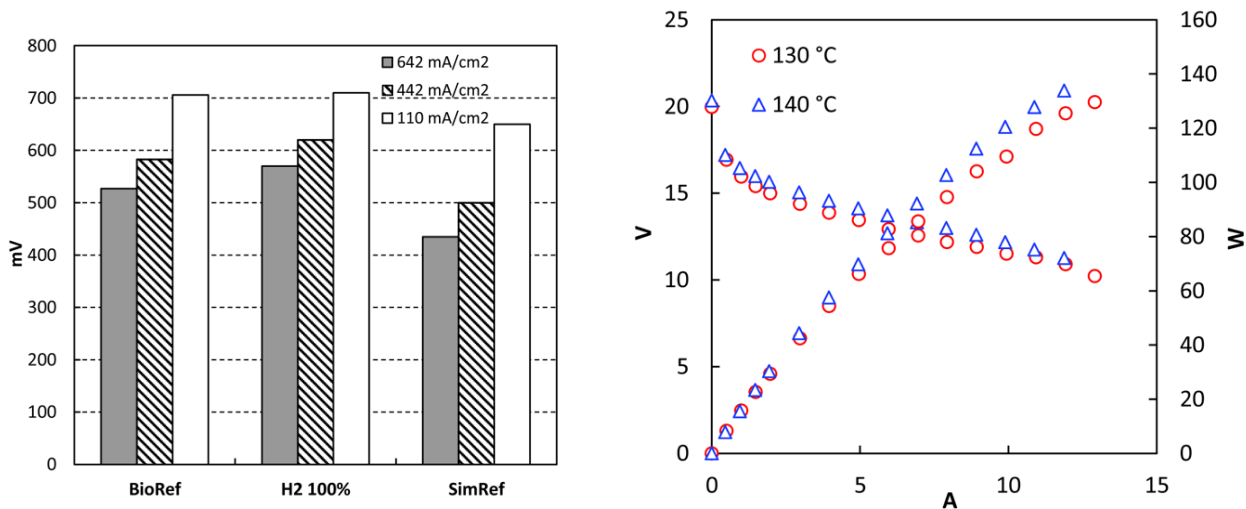


Figure 54. Single cell performance comparison (BioRef = biogas reformate, SimRef = synthetic reformate). Operating temperature: 160 °C [XIV].

Figure 55. Stack (22 cells) performance with biogas reformate at different operating temperatures [XIV].

In Figure 56 the stack polarization curve is presented together with the single cell curve. To preserve the integrity of the stack, it was decided to limit the operating temperature at 140°C, therefore, it is difficult to assess the performance difference between the stack and single cell, where the data were measured at 160°C.

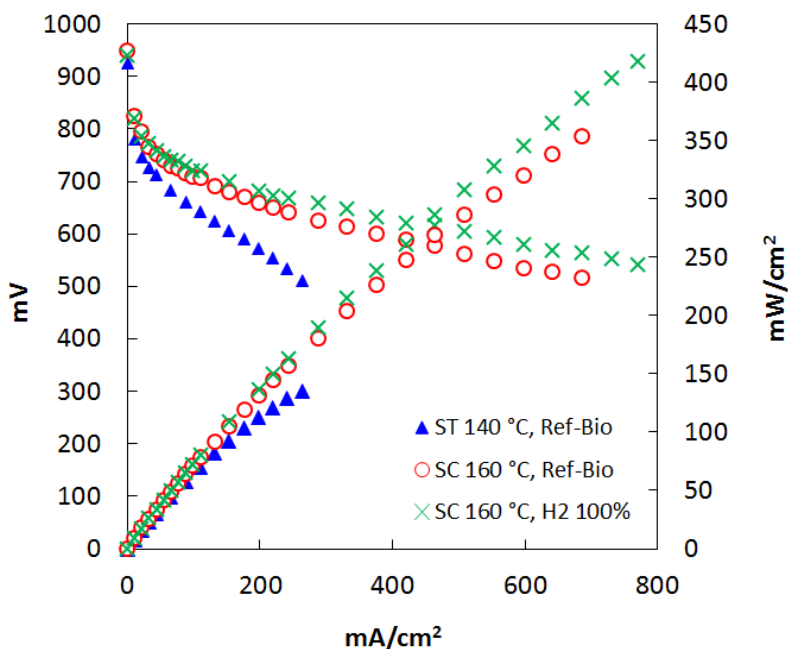


Figure 56. Comparison between the stack average cell and single cell performance. Ref-Bio is reformate biogas [XIV].

On the considered operating range, the stack reached a maximum output of 321 W @ 11.1 V, when fed with pure hydrogen. With the simulated reformate, at the same voltage, the power

output decreases to about 250 W. The stack performance was affected also by a non uniform temperature distribution as shown in Figure 57, where a thermo image of the stack is shown. A temperature difference as high as 25 °C has been measured from stack center to stack end plates.

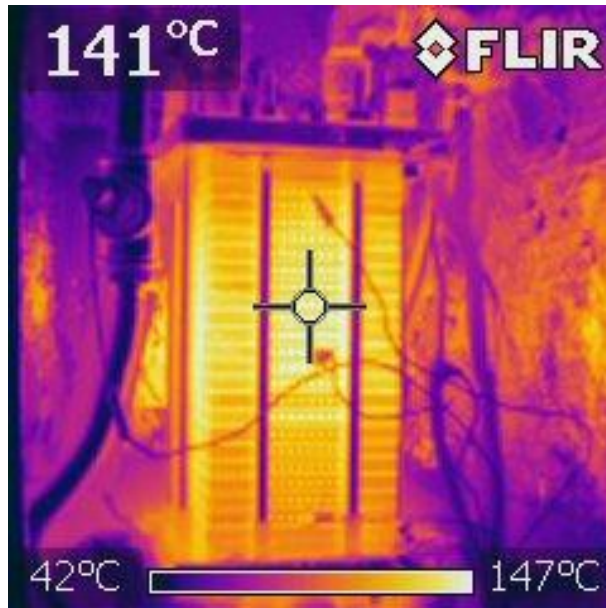


Figure 57. Thermo image of the stack. A temperature difference as high as 25 °C has been measured from stack center to stack end plates.

The non-uniform temperature on the stack, reflected on the single cell voltage dispersion as shown in Figure 58, where the voltage of the single cells in the stack is shown at different currents. The stack temperature at cell number 12 was 140°C. In the graph, it is possible to note that the lower voltage at the stack ends is probably attributable to the lower temperature (see Figure 57). Always in Figure 58 it is possible to observe that other cell voltages are lower, even if the cell are in the center of the stack, where the temperature is supposed to be higher. The stack operation has been affected by the poor performance of some cell during all the tests. For example cell number 6 has always shown a lower voltage independently from the temperature. This is probably due to some water condensation problems inside the cell during reformer start-up and shut-down transients.

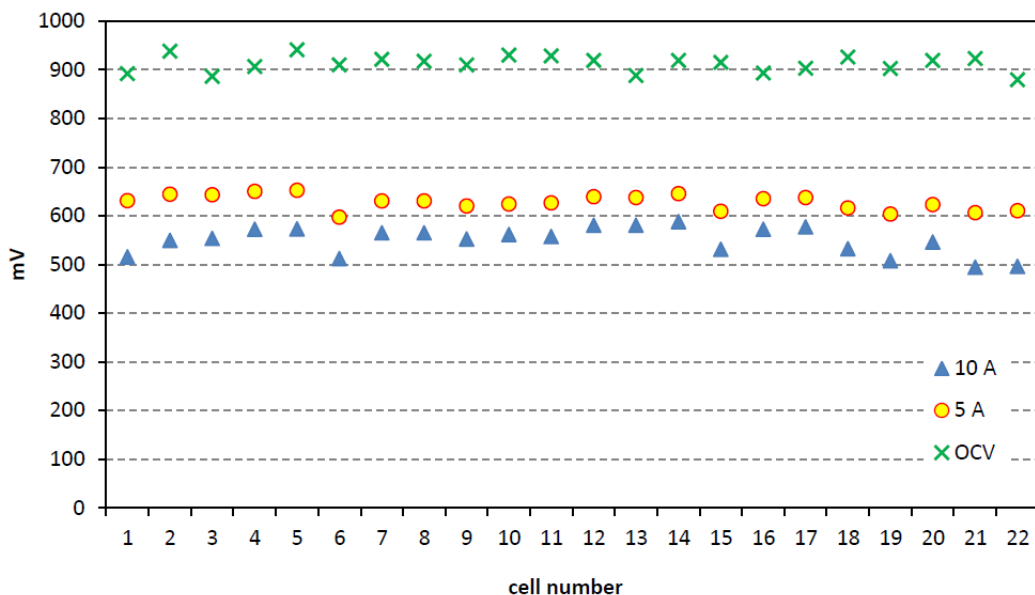


Figure 58. Typical stack voltage distribution at different currents, T=140°C.

The fuel processor and stack performance was completed by the Gas Chromatography (GC) analysis. The GC was also applied for the anode-off gas composition.

As shown in Figure 59, on volumetric dry basis, the biogas composition was: 61.7% methane and 36.9% carbon dioxide. The reformat composition was: 62% H₂, 0.1% CO, 29.6% CO₂, 7.9% CH₄ (vol. dry). The high concentration of CH₄ was a problem during all the tests. Several operating conditions were tested but it was not possible to reduce the concentration below this level.

In the anode exhaust, an oxygen concentration of 2.7% was found, pointing out a cross-over problem.

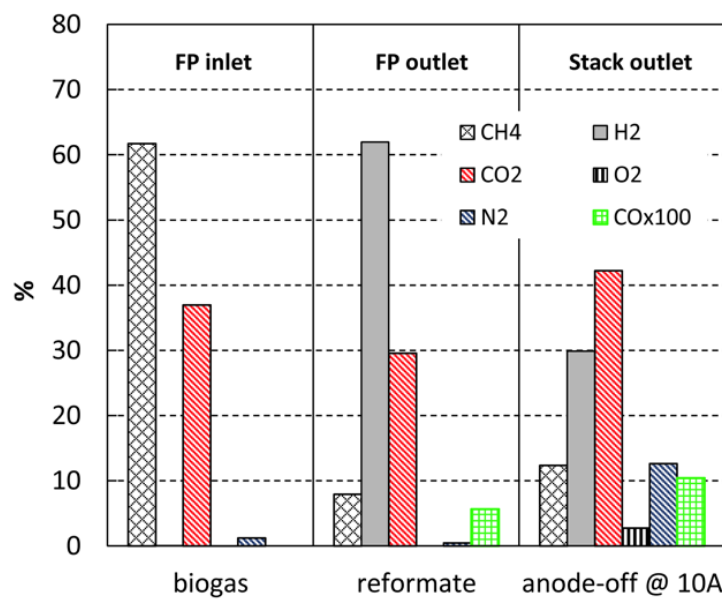


Figure 59. Biogas, reformat and anode-off gas volumetric composition (vol. dry)

The experimental research was aimed also, to the evaluation of the efficiencies of the overall system and its main components, with and without the anode-off gas recirculation. The efficiency calculations were done based on the layout presented Figure 60.

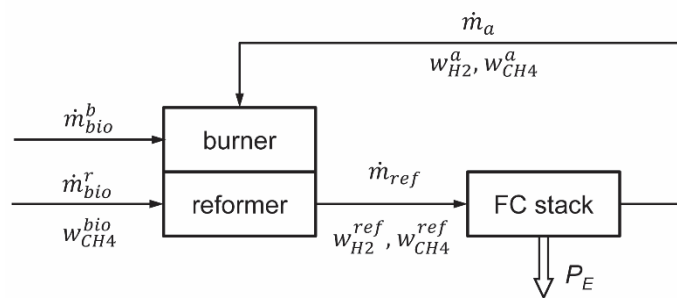


Figure 60. Schematic representation of the fuel flows.

The system electrical efficiency η_{SYS} was calculated according to Eq.1, as the ratio between the stack electric power (P_E) and the biogas power input. The last term was expressed as the product between the methane mass fraction in the biogas ($w_{CH_4}^{bio}$), the sum of the biogas flow rates for the burner and reformer (m_{bio}^b and m_{bio}^r) and the lower heating value of the methane, LHV_{CH_4} . The power for the auxiliaries was not taken into account as the system is not optimized yet.

$$\eta_{SYS} = \frac{P_E}{w_{CH_4}^{bio} \cdot m_{bio}^b + m_{bio}^r \cdot LHV_{CH_4}} \quad (1)$$

The stack electrical efficiency, η_{FC} , was calculated, according to Eq.2, considering the hydrogen mass fraction in the reformat $w_{H_2}^{ref}$, the reformat mass flow rate, m_{ref} , and the hydrogen lower heating value, LHV_{H_2} .

$$\eta_{FC} = \frac{P_E}{w_{H_2}^{ref} \cdot m_{ref} \cdot LHV_{H_2}} \quad (2)$$

The fuel processor efficiency η_{FP} (Eq.3) was calculated as the ratio between the reformer power output and the sum of biogas and anode-off gas power inputs. The reformer output was expressed as the product between the hydrogen mass fraction $w_{H_2}^{ref}$, the reformat mass flow rate m_{ref} and the hydrogen LHV, LHV_{H_2} . The anode-off gas contribution was expressed as a function of the methane, hydrogen and CO mass fractions in the biogas and anode-off gas ($w_{CH_4}^{bio}, w_{CH_4}^a, w_{H_2}^a, w_{CO}^a$), their lower heating values (LHV_{CH_4} and LHV_{H_2}) and the anode-off gas mass flow rate (m_a).

$$\eta_{FP} = \frac{w_{H_2}^{ref} \cdot m_{ref} \cdot LHV_{H_2}}{w_{CH_4}^{bio} \cdot (m_{bio}^b + m_{bio}^r) \cdot LHV_{CH_4} + w_{H_2}^a \cdot LHV_{H_2} + w_{CH_4}^a \cdot LHV_{CH_4} + w_{CO}^a \cdot LHV_{CO} \cdot m_a} \quad (3)$$

The system efficiency values, for the operating point of 10A, together with stack efficiencies are presented in Table 8.

A maximum system efficiency of 13.9 % was obtained with the anode-off recirculation. The HTPEM stack efficiency fed with reformat was not affected by the anode-off gas recirculation and was equal to 23.2 %. The measured value was lower than those obtained during the laboratory tests: 31.9% with hydrogen and 28.5% with simulated reformat. The maximum value of the fuel processor efficiency (60%) was reached with the anode-off gas recirculation.

Overall, the system fuelled with biogas, operated with relatively low efficiency values, if compared to the 38% of the Panasonic 1kW LT-PEM system [58].

The reduction of the stack efficiency when operated with the biogas reformat, can be related to the fuel composition and the lower operating temperature (140 °C). Moreover, as mentioned above, the stack temperature was not uniform causing low performance in some cells.

The reformer efficiency was lower than expected, probably because the catalyst was partially deactivated as an high CH₄ content was always found in the reformat. Assuming that the stack efficiency can be reasonably raised to 30% and reformer efficiency to 65%, the system efficiency could be 19.5%. Indeed, this is a value that should be further reduced as, in this analysis, BOP components power consumption, has not been taken into account. The reason is that the BOP component used are not optimized for low power consumption and the stack tested was reduced in power, as the original stack was damaged by water flooding. Nevertheless, as the cell operating temperature in HT-PEM is higher, it is expected that the thermal power recoverable is higher as well compared to LT-PEM and, therefore, total efficiency could be as high as in LT-PEM systems.

Table 8. System and stack efficiency values

	Field tests		Stack laboratory tests	
	Biogas with anode-off rec.	Biogas w/o anode-off rec.	H ₂ 100%	SimRef
Stack electrical efficiency η_{FC} [%]	23.2 (*)	23.2 (*)	31.9 (**)	28.5 (**)
Fuel processor efficiency η_{FP} [%]	60.0	47.7	-	-
System efficiency η_{SYS} [%]	13.9	11.1	-	-

(*) stack temperature 140°C, (**) stack temperature 160°C,

3.7 Experimental degradation analysis

One of the key issues still open that hamper fuel cells utilization is performance degradation over time. The field tests have pointed out that one of the major problems is the presence of liquid water in the fuel cell. This condition is prone to happen if pipe insulation is poor or during transient conditions. Another issue is the possible presence of oxygen (air) in the shift reactor as it could results in catalyst degradation. This event has to be prevented including in the anode circuit the necessary valves that have to be closed even in the event of power loss. As for the MEA degradation, the single cell was operated with biogas for a total time of 821 h, at 160 °C. The first 170 hours the current was set at 10 A, while for the rest of the test period the current was set to 5 A. On the basis of the data at 5 A, the performance loss rate of the cell was 60 μ V/h. The stack was in service for a total 417 hours, with current loads from 2.5 up to 10 A. Due to the necessity to test several thermal management options, the stack was operated more than 50% of the test time with low current. During the operation, the stack experienced several shut-downs, due to failures in the safety system set-up. Based on the operation at 5 A, the average cell voltage degradation was about 66 μ V/h [XIV].

At lab level, in order to analyze the effect of load cycles and start and stop cycles a specific test set has been carried out [XV]. Three different ageing procedures have been considered and applied on three HTPeM Membrane Electrode Assemblies (MEAs) operated with hydrogen and air. The MEAs have been labeled as MEA (a), MEA (b) and MEA (c). MEA (a) has been subjected to 100,000

triangular sweep cycles between 0.01 A/cm^2 and 0.5 A/cm^2 . MEA (b) has been subjected to 100,000 triangular sweep cycle between Open Circuit Voltage (OCV) and 0.5 A/cm^2 . During load cycling, MEA temperatures were kept constant at $160 \text{ }^\circ\text{C}$. MEA (c) has been subjected to 650 start/stop cycles. Start/stop procedures consist of temperature cycles from $40 \text{ }^\circ\text{C}$ to $160 \text{ }^\circ\text{C}$. A 10 A load is imposed from $120 \text{ }^\circ\text{C}$ to $160 \text{ }^\circ\text{C}$. For MEA a) and MEA b) a degradation rate of $40 \text{ } \mu\text{V/h}$ has been found. For MEA c), subjected to start and stop cycles, the performance loss is about $12 \text{ } \mu\text{V/cycle}$ for the first 450 cycles. Between 450 and 650 start/stop cycles degradation rate increases to 0.27 mV/cycle .

To have a better insight of the catalyst degradation, in the framework of a research project in collaboration with the University of Graz, a tentative procedure to characterize the nano-morphology of the catalyst platinum particles using SAXS (Small Angle X ray Scattering) has been developed. This part of the research is presented [VII, XII, XVI] and is still in progress. The MEAs subjected to the accelerated degradation test mentioned above have been analyzed with SAXS at the end of the cycles and the particle size distribution has been assessed and compared to a new (non used) MEA. In Figure 61 the SAXS scattering intensity curves of MEA_ref, MEA_a) and MEA_b) are presented.

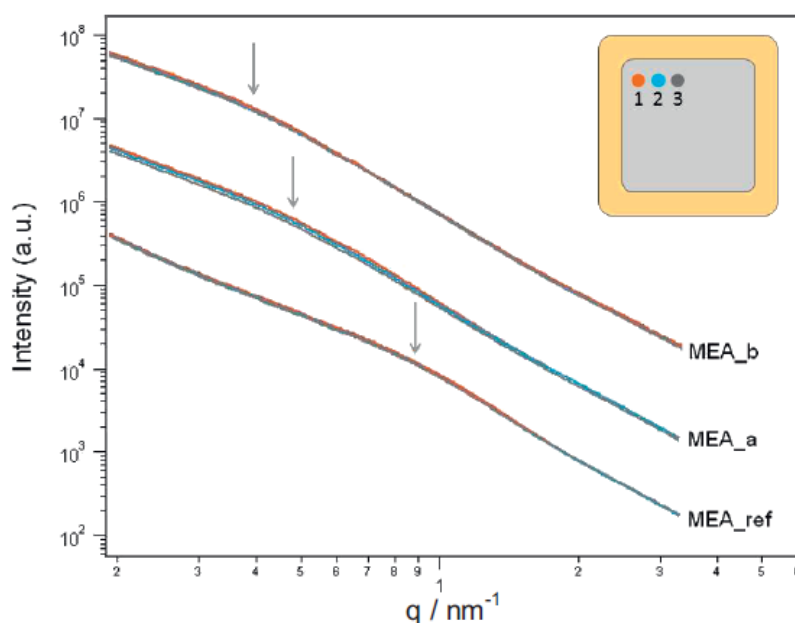


Figure 61. SAXS scattering intensity curves of MEA_ref, MEA_a) and MEA_b). For each sample, three different areas on the MEA surface have been analyzed (1, 2, 3), as shown in the top right inset of the graph where they have been indicated by colored spots. The intensities of the three sets of samples have been scaled by a factor of 10 to each other in order to resolve better the differences. The arrows indicate the scattering of the Pt particles [XVI].

The fitting of the intensity scattering curves allowed the determination of the volume size distribution of the particles, as shown in Figure 7. Three different areas for each sample, as shown in Figure 6, have been examined. The mean radius of the particles R and the root mean square deviation of the radius sR have been used to quantify the distributions. The mean radius of the Pt NPs in the reference sample MEA_ref is 2.61 nm , while it is 4.54 nm for MEA_a, with 74% increase, and 5.28 nm for MEA_b, with 102% increase. The error of the mean radii calculated for the three single measurements for each set is lower than 0.2 nm . The size distribution width of MEA_ref is smaller than the other two. The larger catalyst NPs polydispersity in the operated samples could

be due to the Ostwald ripening process. Another cause could be a different catalyst growth dynamics in anode and cathode, since both the catalyst composition and the electrochemical environment are different. The position of the distribution maximum is similar in the cycled samples, but the size distribution width of MEA_b is larger. The polydispersity of the mean radius is thus larger for the sample subjected to OCV at each cycle (MEA_b). OCV operation, as expected, seems thus to have an influence on the evolution of the catalyst; in particular it seems to affect both the polydispersity of the catalyst particles size and their mean growth.

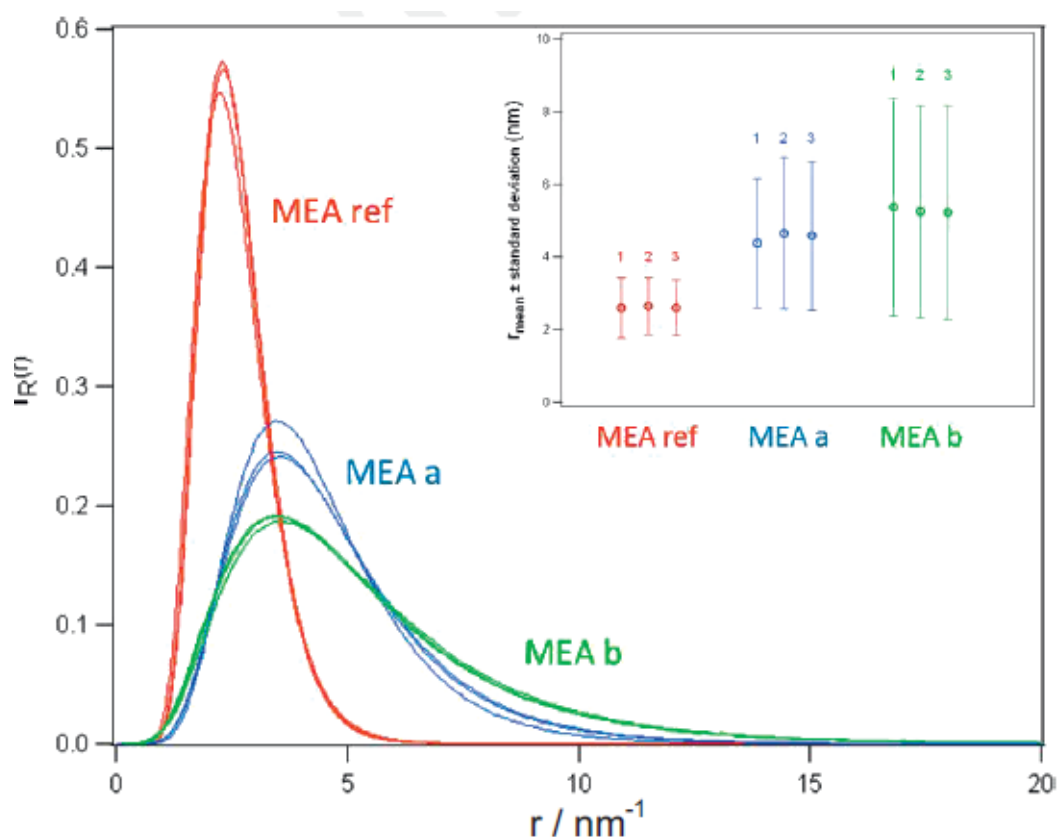


Figure 62. Volume size distributions of MEA_ref, MEA_a, and MEA_b. On the inset, the mean radii with the standard deviations of the distribution are shown. For each sample, three different areas have been analyzed (1, 2, 3) in reference to the inset of Figure 61 [XVI].

4 CONCLUSIONS

A transition from a heavily centralized power grid to one with rooftop solar panels, natural gas generators at homes and businesses, plug-in electric vehicles, and technologies to reduce electricity use is clearly underway. From one side, the benefits of RES are evident in terms of CO₂ emissions reduction but, from another side, there are many, in some cases hidden, drawbacks. This research has aimed to analyze these benefits and through the analysis of the latest available data, point out some of the problems with the target to identify possible remedies and improvement in RES exploitation. In particular, the utilization of micro-cogeneration system has been considered, being the research question of this thesis:

“Can fuel cell based micro-cogeneration systems be a technical viable option? To which extent these systems can contribute to reduce energy consumption and facilitate the exploitation of RES?”

The activities on which the research have been articulated have been:

Literature review and background

Simulation models development

Test rig and automation system set up

Experimental characterization of single cells and stack

Experimental characterization of the fuel processor and complete system

Experimental degradation analysis

In the following the main outputs of the single activities will be presented.

Literature review and background

The literature review pointed out that, to what concern effects of renewable energy sources distributed generation in terms of electricity costs and environmental effects, there are no conclusive studies. The problem is complex and the daily changing scenario is affected more from incentive schemes, policy measures and market choices than technological hurdles.

Indeed, benefits of RES DG were evident when considering the specific CO₂ emission in countries where RES support schemes have been applied but, on the other hand, fossil fuel CO₂ specific emissions, in some cases, showed a surge [28].

As for the technical measures that can be adopted to better exploit RES the crucial issues is to introduce systems able to balance the electrical production.

The best candidates seem to be flexible distributed generators co-generators. This last option of combined production of heat and electricity and, ideally, cold production as well, allows to introduce two additional benefits: *i)* a higher first law efficiency, *ii)* if heat storage with integrated electrical heating is available, there is the possibility to store energy in case of RES exceeding demand. This possibility can be enhanced if heat pumps and cold storage is available. The quantity of energy stored is limited but the specific cost per kWh lower than electrochemical systems.

Coming to the size of the plants several point of views can be found. In this work it has been chosen to focus on the plant that allow satisfy the average electrical consumption of a single dwelling. This choice has been driven by the search of maximum flexibility and maximum fuel efficiency. On this basis the plant size results to be 300-1000 W.

The next point is which the best fuel for this type of plant. Considering the existing infrastructure, the cost and the emissions it results to be natural gas.

Next step is to choose the type of engine. Considering the size, the efficiency and the technological maturity fuel cells seem to be the best choice. At the time of writing High Temperature Fuel Cells was the most promising technology as able to operate at temperature up to 180°C and to withstand high CO concentration reformat gas.

Simulation models development

The theoretical analysis allowed examining which is the potential of fuel cell based micro-CHP in terms fuel efficiency and energy saving. Several fuel cell simulation models are available in literature but it was decided to focus on a semi empirical zero-dimensional one as the main objective was to study the performance of the system more than that of specific components. For a 1 kWe system electrical part load efficiency can be as high as 30%, even if PES depends very much on system configuration and operating strategies. The analysis has been extended to system where electrical and thermal storage is included. Different load profiles typical for a single domestic dwelling have been considered. The analysis show that the PES and system costs are affected by the load profile and higher PES and lower system costs can be obtained if load management is introduced to leveled the electrical consumption. Today, on the shelf switches to control domestic loads priority are available at low price and therefore this could ease the introduction of such generation systems.

Test rig and automation system set up

This has been a very challenging and interesting part of the activity because it contributed to understand the importance and complexity of the control system required to optimize the performance and protect the system from potentially detrimental operating conditions. Two main system have been developed: one for the lab tests and one for the control of the on-field generator. In both cases the automation was based on National Instrument HW and SW. As for the lab system particular care has to be put on cell/stack temperature control in order to acquire significant polarization curves. The development of the on-field automation system was much more complex as it encompassed the control of the: fuel processor, stack, heat management and safety procedures. The system could be controlled remotely.

From practical point of view, in the perspective of a domestic indoor installation, it has to be stressed that the reformer is a highly toxic and explosive gas generator. Protection against CO accidental leakage has to be implemented.

Experimental characterization of single cells and stack

The characterization of different cells and configuration allowed gathering the necessary information to develop the complete micro-CHP system. In most cases the MEA specifications given by the producers have been obtained. The effect of cell temperature and CO concentration in the fuel assessed. The test showed that the MEA can withstand high CO concentration without compromising performance. Considering a short stack of three cells, at 180°C and 0.6V the current with pure hydrogen is 17 A and with 2% of CO is 13.5 A (-20%). Experimental data show that a higher operating temperature increases cell performance and diminishes the influence of CO concentration. Always in the case of 180 °C, the increase of CO concentration from 0.5 to 2% decreases the stack current by 7.5% (from 14.6 to 13.5 A), while for 120 °C, the current decreases by 54.3% (from 4.6 to 2.1 A). Considering that a typical fuel reformer with a single shift converter can achieve CO concentration of 0.5%, it emerges that the considered MEA can be used without introducing additional CO purification stages. As for the bipolar plates material, the choice of composite seem to be a viable solution, in the short term, both from the point of view of life-span, performance and cost. Even if not studied in this research, on a longer term, metallic plates could be an option to reduce costs and improve durability.

Experimental characterization of the fuel processor and complete system

This has been the richest and interesting activity during the project in terms of knowledge and lesson learned. Implementing a system out of the lab in an industrial context has given the possibility to assess the validity of the solutions coming out from the theoretical study. First of all, the possibility to operate the reformer with biogas coming from the digestion plant was assessed: the reformer showed good performance in all the operating conditions: the biogas low calorific value did not impair the operation of the catalytic reformer. The heat necessary for the reforming reaction was available even if the necessary reactor temperature was reached in a longer time compared to LPG. The biofilter showed the necessary removal capacity to reduce H₂S concentration down to few ppm even if at inlet the biogas contained up to 500 ppm of H₂S. Therefore, considering that there was an additional filter, the biogas sulfur did not compromise at all the catalyst in the reformer and in the MEAs. The hydrogen concentration at the fuel processor outlet was higher than 60% and CO lower than 1%. In this condition the performance of the cell obtained in lab tests was confirmed. Many have been the problems to be solved on the spot. Most of the “unexpected” problems come out from water condensing in the pipes. This could seem a trivial problem, considering the complexity of the system but it is, indeed, crucial, as liquid water can permanently damage the MEAs and causing detrimental backpressure in component system that can affect system operation.

It was impossible to assess the real electrical efficiency of the system for two reasons: the full size stack was damaged during start up due to liquid water and the experimental activity was based on a reduced size stack (300 W with H₂), the second reason was the that the automation system was not optimized for “low consumption” and therefore its power consumption has not been taken into account. On this hypothesis, the measured system electrical efficiency was 14%. It is expected that this value can be improved up to 20% rising the temperature of the stack and with a new reformer.

Actually, low power consumption balance of plant components begins to be affordable only today as, in the past, this was not a priority in most of the applications.

Experimental degradation analysis

This part of the research, still in progress, offers many interesting options of development. The measured level of degradation during the field tests with biogas were satisfactory (60 $\mu\text{V}/\text{h}$ for the single cell), even if longer test period should be considered. For this reason accelerated test procedures have been implemented at lab level. In this case, after 100,000 load cycles, an average degradation rate of 40 $\mu\text{V}/\text{h}$ has been found. This value is coherent with the one measured in the field tests as, in the latter case, start and stop cycles were included. Indeed, all these values require further investigations and experimental confirmation. The challenge is to analyze in details the MEA degradation using nanomorphology characterization techniques together with traditional diagnostic techniques such as electrochemical impedance spectroscopy and cyclic voltammetry. As for nano morphological characterization, a tentative procedure to using Small angle X ray scattering (SAXS) as been implemented and first results are today in a phase of confirmation using standard techniques such as transmission electron microscopy (TEM). The new approach opens the possibility to fast scan, ex-situ, large portions of the MEA, in order to assess the morphology of the catalyst. This techniques, could facilitate the development of degradation models in order to correlate the loss of performance to the operative profile and, eventually, identify possible detrimental operating conditions in order to extend cell life.

Coming back specifically to the research question, what achieved can be summarized in the following points:

- It has been proven that fuel cell based micro-CHP is a technically viable option. In particular, the high temperature MEA used can handle low quality reformat allowing simplification and cost reduction of the fuel reformer when fuels different than hydrogen are used. The system has operated “unmanned” for more than 1000 h in a harsh environment fuelled with biogas.
- Cell performance degradation is still an issue. Despite the MEA maker has proven a lifetime at constant load of more than 20.000 h, in real conditions and, in particular, when subjected to start and stop cycles, the MEA shows a degradation that is in the range of several tens of $\mu\text{V}/\text{h}$.
- Overall the stack is very sensitive to liquid water that, in theory should not be present, but in practice, especially during transients, is often inevitable.
- During the research, a tentative procedure to using Small angle X ray scattering to fast scan large portion of the MEA and provide information on some of the degradation phenomena has been implemented.
- The analysis of RES deployment, with particular reference to EU, shows that micro-DG could help RES exploitation and mitigate some of RES drawbacks. In electrical networks with a substantial amount of RES, smart fast-reacting natural gas micro-DGs offer the possibility to keep the system balanced.
- The simulation models have demonstrated that micro-CHPs, in particular when coupled with storage capability, allow to reach PES from 0.20 to 0.30, depending on system configuration and load profile.

To whom is writing it is clear that, on the market, some international companies are offering micro-CHP system with a similar output and have achieved a much higher level of system integration.

Indeed, it is believed that the contribution of this research, from the experimental point of view, is to have published and made available all the data and phases of the design, development and testing process of the system. While, the prospect of using nanomorphology characterization techniques to better exploit and tune standard techniques, remains a very promising path to follow and field of potential very interesting development both in terms of basic research and from the technological application standpoint.

Future work

Analyzing *a posteriori* the activity carried out, some of the points that remain to be further investigated or deserve additional improvement are:

- The field experiments, even if they lasted, overall, for more than a thousand hours, could be extended. Indeed, the termination of the experiment was not caused by technical problems but by limited resources.
- The tests should be completed using natural gas as well and not only biogas.
- The calculation of the efficiency of the system should take into account for BOP components as well. In this case, a stack with a higher power output and optimized BOP components should be considered.
- The degradation analysis data remains to be confirmed with additional tests.

Bottom line

It seems that renewable and distributed generation are here to stay. Their production is expected to double every ten years, on conservative estimates. Grid operators are going to recognize that this supply must be treated as any other supply source and be fully integrated into their transmission and distribution network operations systems. Rather than apply existing solutions to a new problem, utilities should look for innovative and cost-effective solutions that are designed to solve or mitigate the problem. Micro-CHP with integrated storage can be a solution.

As for fuel cells, it has been demonstrated that, from the technical point of view, the system is feasible but it is not only expensive: it is complex, including many components and reactors. Therefore, it is difficult to forecast a rapid reduction in production cost. At the same time, there are involved highly flammable and toxic gases and indoor installation is to be considered with extremely care. Nevertheless, other technologies have witnessed rapid cost changes: in recent year the subsidies on PV has caused a drop in prices. Complexity and challenges have always thrilled human being. Many are the cases of technological barriers surprisingly and easily overcome in few years. Today, hybrid cars are an example: few years ago it was difficult (for some impossible) to think that the market will have offered hybrid city car at a price slightly higher than conventional.

The question probably is: “do we really want to consume less? Are we motivate enough and ready to renounce to something?”

Or, what we want, it is more simply (and more human) consume more for less and, if possible, not harming our planet. This is probably what utilities want as well...

ACKNOWLEDGMENTS

First of all I would like to thank my supervisor, Prof. Marta Boaro for her advice, support and trust during the research work. Then, I would like to thank the director of the PhD program, Prof. Alfredo Soldati. With his knowledge of the richness and of the anomalies of the Italian research systems, he has always directed me to achieve the best from this experience. I have to thank, then, Kristin for supporting me throughout this effort.

As for the everyday work, I feel really lucky to have the possibility to thank many people. Among these I would like to thank, in particular, Robert, Fabio, Nicola, Diego and Piero.

REFERENCES

- [1] Craig Winneker, Ed., *Global Market Outlook for Photovoltaic 2013-2020*. EPIA, 2013.
- [2] "Europe's electricity providers face an existential threat," *The Economist*.
- [3] "Global carbon markets' value dropped 38% in 2013," *The Guardian*.
- [4] X. P. Chen, Y. D. Wang, H. D. Yu, D. W. Wu, Y. Li, and a. P. Roskilly, "A domestic CHP system with hybrid electrical energy storage," *Energy Build.*, vol. 55, pp. 361–368, Dec. 2012.
- [5] E. Pohl and D. Diarra, "A method to determine primary energy savings of CHP plants considering plant-side and demand-side characteristics," *Appl. Energy*, vol. 113, pp. 287–293, Jan. 2014.
- [6] T. Kousksou, P. Bruel, a. Jamil, T. El Rhafiki, and Y. Zeraouli, "Energy storage: Applications and challenges," *Sol. Energy Mater. Sol. Cells*, vol. 120, pp. 59–80, Jan. 2014.
- [7] F. Barbir, "PEM Fuel Cells." Academic Press, 2012.
- [8] OECD IEA, *Key World Energy Statistics*. Paris: OECD IEA, 2013.
- [9] M. Leahy, J. L. Barden, B. T. Murphy, N. Slater-thompson, and D. Peterson, "International Energy Outlook 2013," 2013.
- [10] *Tracking Clean Energy Progress 2013 Tracking Clean Energy Progress 2013*. Paris: OECD/IEA, 2013.
- [11] M. Moran, H. Shapiro, D. Boettner, and M. Bailey, *Fundamentals of engineering thermodynamics*, 8th ed. Wiley, 2014.
- [12] I. WEO, *World Energy Outlook 2012*. Parigi: IEA, 2012.
- [13] a. Picciariello, J. Reneses, P. Frias, and L. Söder, "Distributed generation and distribution pricing: Why do we need new tariff design methodologies?," *Electr. Power Syst. Res.*, vol. 119, pp. 370–376, Feb. 2015.
- [14] P. Paliwal, N. P. Patidar, and R. K. Nema, "Planning of grid integrated distributed generators: A review of technology, objectives and techniques," *Renew. Sustain. Energy Rev.*, vol. 40, pp. 557–570, Dec. 2014.
- [15] T. Ackermann, G. Andersson, and L. Söder, "Distributed generation: a definition," *Electr. Power Syst. Res.*, vol. 57, no. 3, pp. 195–204, Apr. 2001.

- [16] “Distributed Generation in Liberalised Electricity Markets.” OECD Publishing, 26-Jun-2002.
- [17] S. Ropenus, H. K. Jacobsen, and S. T. Schröder, “Network regulation and support schemes – How policy interactions affect the integration of distributed generation,” *Renew. Energy*, vol. 36, no. 7, pp. 1949–1956, Jul. 2011.
- [18] “Share of renewable energy in gross final energy consumption,” *European Environmental Agency*, 2014. .
- [19] G. Corbetta and T. Miloradovic, *Wind in power–2013 European statistics*, no. February. European Wind Energy Association (EWEA), 2014, pp. 1–12.
- [20] “www.entsoe.eu,” 2014. .
- [21] P. S. Ennio Macchi, Stefano Campanari, “La microgenerazione a gas naturale.” Milano, 2005.
- [22] Delta Energy & Environment, “Micro-CHP Market Statistics & 2020 Forecast,” Edinburgh, 2013.
- [23] *Combined Heat and Power*. OECD/IEA, 2008.
- [24] “Per due ore soltanto rinnovabili, domenica l’Italia è stata più verde,” *La Repubblica*, Roma.
- [25] J. Mayer, “Electricity Production and Spot-Prices in Germany 2014,” 2014.
- [26] “Produzione oraria per fonte in Italia nel mese di luglio 2013,” 2013. [Online]. Available: <http://dataenergia.altervista.org>.
- [27] L. Maugeri, “The Shale Oil Boom: A U.S. Phenomenon,” no. June. Discussion Paper 2013-05, Belfer Center for Science and International Affairs, Harvard Kennedy School, 2013.
- [28] “Fattori di emissione per la produzione ed il consumo di energia elettrica in Italia.” Istituto superiore per la protezione e la ricerca ambientale (ISPRA), Italy, 2013.
- [29] C. R. Frank, “THE NET BENEFITS OF LOW AND NO-CARBON ELECTRICITY,” *Glob. Econ. Dev.*, no. May, 2014.
- [30] G. Meneghello, “Il soccorso ai cicli combinati e a quei 25 miliardi di investimenti,” 2012. [Online]. Available: qualenergia.it.
- [31] O. M. Toledo, D. Oliveira Filho, and A. S. A. C. Diniz, “Distributed photovoltaic generation and energy storage systems: A review,” *Renew. Sustain. Energy Rev.*, vol. 14, no. 1, pp. 506–511, Jan. 2010.
- [32] A. Rabiee, H. Khorramdel, and J. Aghaei, “RETRACTED: A review of energy storage systems in microgrids with wind turbines,” *Renew. Sustain. Energy Rev.*, vol. 18, pp. 316–326, Feb. 2013.

- [33] L. Gelazanskas and K. A. A. Gamage, "Demand side management in smart grid : A review and proposals for future direction," *Sustain. Cities Soc.*, vol. 11, pp. 22–30, 2014.
- [34] S. Luthra, S. Kumar, R. Kharb, M. F. Ansari, and S. L. Shimmi, "Adoption of smart grid technologies: An analysis of interactions among barriers," *Renew. Sustain. Energy Rev.*, vol. 33, pp. 554–565, May 2014.
- [35] M. a. Brown, "Enhancing efficiency and renewables with smart grid technologies and policies," *Futures*, vol. 58, pp. 21–33, Apr. 2014.
- [36] S. Ruiz-Romero, A. Colmenar-Santos, F. Mur-Pérez, and Á. López-Rey, "Integration of distributed generation in the power distribution network: The need for smart grid control systems, communication and equipment for a smart city — Use cases," *Renew. Sustain. Energy Rev.*, vol. 38, pp. 223–234, Oct. 2014.
- [37] A. P. L. E. E. IL GAS, "Delibera dell'AEEG 66/2013/R/EEL," vol. 2012. pp. 1–9, 2013.
- [38] "Piano di Sviluppo annuale e pluriennale delle Infrastrutture di Enel Distribuzione S.p.A. 2014 – 2016," 2014.
- [39] H. Ammermann, "Advancing Europe's energy systems: stationary fuel cells in distributed generation," Luxemburg, 2015.
- [40] "Numerosità Potenza Cumulata (kW) Grafici della numerosità e della potenza totale degli impianti mensilmente entrati in esercizio con il Conto Energia . Potenza Mensile (kW)." GSE, 2014.
- [41] F. Implications and E. Business, "Disruptive Challenges: Financial Implications and Strategic Responses to a Changing Retail Electric Business," 2013.
- [42] A. D. Franco Di Andrea, "Misure dei Consumi di ENergia in 110 abitazioni Italiane apparecchi di illuminazione (Progetto MICENE)," 2004.
- [43] K. Klobut, J. Ikaheimo, and J. Ihonen, "Micro-CHP technologies for distributed generation," 2010.
- [44] H. Tanaka, A. Suzuki, and K. Yamamoto, "NEW ECOWILL-A NEW GENERATION GAS ENGINE MICRO-CHP," in *International Gas Union Research Conference 2011*, 2011.
- [45] [Http://www.microchap.info](http://www.microchap.info), "Micro CHP specs comparison." 2014.
- [46] K. Kusterer, "PERFORMANCE OPTIMIZATION OF A 3KW MICROTURBINE FOR CHP APPLICATIONS," in *ASME Turbo Expo 2012*, 2012, pp. 1–10.
- [47] [Http://www.flowenergy.uk.com](http://www.flowenergy.uk.com), "2014 Flow energy ORC specs," 2014. .
- [48] M. Mench, *Fuel Cell Engines*. John Wiley & Sons, 2008.

- [49] C. Ma, L. Zhang, S. Mukerjee, D. Ofer, and B. Nair, "An investigation of proton conduction in select PEM's and reaction layer interfaces-designed for elevated temperature operation," *J. Memb. Sci.*, vol. 219, no. 1–2, pp. 123–136, Jul. 2003.
- [50] R. W. Kopitzke, C. a. Linkous, and G. L. Nelson, "Thermal stability of high temperature polymers and their sulfonated derivatives under inert and saturated vapor conditions," *Polym. Degrad. Stab.*, vol. 67, no. 2, pp. 335–344, Feb. 2000.
- [51] Z. Liu, Y.-M. Tsou, G. Calundann, and E. De Castro, "New process for high temperature polybenzimidazole membrane production and its impact on the membrane and the membrane electrode assembly," *J. Power Sources*, vol. 196, no. 3, pp. 1055–1060, Feb. 2011.
- [52] Q. Li, J. O. Jensen, R. F. Savinell, and N. J. Bjerrum, "High temperature proton exchange membranes based on polybenzimidazoles for fuel cells," *Prog. Polym. Sci.*, vol. 34, no. 5, pp. 449–477, May 2009.
- [53] S. J. Andreasen, J. R. Vang, and S. K. Kær, "High temperature PEM fuel cell performance characterisation with CO and CO₂ using electrochemical impedance spectroscopy," *Int. J. Hydrogen Energy*, vol. 36, no. 16, pp. 9815–9830, Aug. 2011.
- [54] a Korsgaard, M. Nielsen, and S. Kar, "Part one: A novel model of HTPEM-based micro-combined heat and power fuel cell system," *Int. J. Hydrogen Energy*, vol. 33, no. 7, pp. 1909–1920, Apr. 2008.
- [55] C. Pan, R. He, Q. Li, J. O. Jensen, N. J. Bjerrum, H. A. Hjulmand, and A. B. Jensen, "Integration of high temperature PEM fuel cells with a methanol reformer," *J. Power Sources*, vol. 145, no. 2, pp. 392–398, Aug. 2005.
- [56] Q. F. Li, H. C. Rudbeck, a. Chromik, J. O. Jensen, C. Pan, T. Steenberg, M. Calverley, N. J. Bjerrum, and J. Kerres, "Properties, degradation and high temperature fuel cell test of different types of PBI and PBI blend membranes," *J. Memb. Sci.*, vol. 347, no. 1–2, pp. 260–270, Feb. 2010.
- [57] "Celtec 1000 Technical specifications," 2010.
- [58] Panasonic, "Panasonic domestic fuel cell CHP specifications." 2008.
- [59] J. Wing, "Handling the Cost of Residential Fuel Cells," *Fuel Cell Today*, no. August, 2013.
- [60] S. V Kanuri, "UTC Power and the PureCell Model 400 fuel cell power plant finding wide application," *Fuel Cells Bull.*, vol. 2012, no. 2, pp. 12–15, Feb. 2012.
- [61] "Connecticut shopping mall is first powered by Bloom Energy," *Fuel Cells Bull.*, vol. 2014, no. 11, p. 7, Nov. 2014.
- [62] "Fuel cell CHP passes the point of no return," *Cogeneration & on site power production (on line edition)*, no. March 25, 2014.

- [63] O. Nishimura, "AISIN SOFC in Japanese Market and Entry into European Market," in *Fuel cell expertise network webinar June 26 2014*, 2014, pp. 1–19.
- [64] D. Feldman, G. Barbose, R. Wiser, N. Darghouth, and A. Goodrich, "Photovoltaic (PV) Pricing Trends : Historical , Recent , and Near-Term Projections Photovoltaic (PV) Pricing Trends : Historical , Recent , and Near-Term Projections," 2012.
- [65] Korsgaard R. A. and et al., "Modeling of CO Influence in PBI Electrolyte PEM Fuels Cells," in *4th International Conference on Fuel Cell Science - IRVINE CA*, 2006.
- [66] R. R. G. Kumar Atul, "Effect of gas flow-field design in the bipolar/end plates on the steady and transient state performance of polymer electrolyte membrane fuel cells," *J Power Sources*, vol. 155, no. 264–271.
- [67] Diego Ubeda et al., "Three dimensional model of a 50 cm² PBI-Based PEM fuel cell," in *Proceedings of European Fuel Cell Technology & Applicationse "Piero lunghi conference"*, Rome, 2009.

List of the paper related to the PhD research activity

- I. **R. Radu, N. Zuliani, R. Taccani, Design And Experimental Characterization Of A High Temperature Pem Fuel Cell Stack, Journal of Fuel cell Science and technology, 11/2011 vol. 8 pg 051007 1-5, ISSN 1550-624X.**
- II. Radu. R., Taccani R., Zuliani N. (2011). Utilizzo di un Reformer per l'Alimentazione di una Cella a Combustibile: Analisi del Sistema di Controllo. National Instrument - formato elettronico, pp.-- -, In: 18° NIDays forum tecnologico sulla progettazione grafica di sistemi. 23 febbraio 2011, Milano ,
- III. Zuliani N., Taccani R., Radu R. (2011). Effects of control strategies on the transient performance of a HTPEM fuel cell system fuelled with propane. ENEA, pp.261- 262, Vol. 1, In: 4th European Fuel Cell Conference and Exhibition. 14-16 dicembre 2011, Roma,
- IV. **R. Taccani, N. Zuliani, Effect of flow field design on performances of high temperature PEM fuel cells: Experimental analysis, International Journal of Hydrogen Energy, Volume 36, Issue 16, August 2011, Pages 10282-10287, ISSN: 0360-3199**
- V. Zuliani N., Taccani R., Radu R. (2011). Experimental and Theoretical Performance Analysis of an High Temperature PEM Fuel Cell fed With LPG Using a Compact Steam Reformer. ASME Digital Library, pp.-- -, In: ASME 2011 5th International Conference on Energy Sustainability . 7-10 Agosto 2011, Grand Hyat Washington DC – USA.
- VI. **Zuliani, N., Taccani, R., Microcogeneration system based on HTPEM fuel cell fuelled with natural gas: Performance analysis, Applied Energy, 2012, Vol. 97 pp. 802-808.**
- VII. Valle F, Marmiroli B., Amenitsch H., Taccani R. (2012). Electron microscopy and small-angle X-ray scattering analysis of the catalyst layer degradation. Associazione Termotecnica Italiana - Sez. Friuli Venezia Giulia, Trieste: pp.1- 7, In: 67° Congresso nazionale ATI - Trieste 2012. Settembre 2012, Trieste.
- VIII. Zuliani N., Taccani R. (2012). Micro Combined Heat And Power System Based On Htpem Fuel Cell And Li-Ion Batteries: Performance Analysis. ATI Sezione FVG - Formato elettronico, pp.-- -, In: 67° Congresso Nazionale ATI. 11-14 Settembre 2012, Trieste.
- IX. N. Zuliani, R. Taccani (2013). Micro combined heat and power system based on htpem fuel cell and li-ion batteries: analysis of performance under different operating strategies . Università degli Studi del Sannio - Università degli Studi di Napoli, pp.-- -, In: Microgen III. Aprile 15-17, 2013, Napoli,
- X. N. Zuliani, F. Valle, R. Taccani (2013). Degrado accelerato di celle a combustibile polimeriche: sistema di acquisizione dati e controllo. National Instrument , pp.0- 1, In: NI LabVIEW Days 2013. settembre 2013, Milano,
- XI. **Zuliani N., Taccani R., Energy simulation model and parametric analysis of a micro cogeneration system based on a htpem fuel cell and battery storage, Proceeding of ICAE2013, International Conference on Applied Energy, Pretoria 2013.**
- XII. F. Valle, N. Zuliani, B. Marmiroli, H. Amenitsch, R. Taccani (2013). Experimental analysis of catalyst degradation in High Temperature PEM Fuel Cells subjected to accelerated ageing tests. pp.1- 9, In: 5th International Conference Fundamentals & Development of Fuel Cells. 16-18 April 2013, Conference Center Karlsruhe, Germany.
- XIII. R. Radu, R. Taccani (2013). Monitoraggio e controllo di un sistema micro-cogenerativo con celle a combustibile. National Instruments Italy, pp.1- 6, In: NI Days 2013. 27/02/2013, Milano.

- XIV. **R. Radu, R. Taccani, M. Scagliotti, C. Valli (2013). HT PEM fuel cell system fed with biogas: experimental characterizations. ECOS 2013, pp.1- 9, In: 26th International Conference on Efficiency, Cost, Optimization, Simulation and Environmental Impact of Energy Systems (ECOS). July 16-19, 2013, Guilin, Guangxi, China.**
- XV. N. Zuliani, F. Valle, R. Taccani Performance degradation study on polybenzimidazole fuel cells subjected to different ageing tests, European Fuel Cell Conference, Roma 2013.
- XVI. **F. Valle, N. Zuliani, B. Marmiroli, H. Amenitsch, R. Taccani (2014), SAXS Analysis of Catalyst Degradation in High Temperature PEM Fuel Cells Subjected to Accelerated Ageing Tests, Fuel cells, Wiley-VHC.**

In bold letters the papers that have been attached to the thesis

ANNEX

1. R. Radu, N. Zuliani, R. Taccani, Design And Experimental Characterization Of A High Temperature Pem Fuel Cell Stack, Journal of Fuel cell Science and technology, 11/2011 vol. 8 pg 051007 1-5, ISSN 1550-624X.
2. R. Taccani, N. Zuliani, Effect of flow field design on performances of high temperature PEM fuel cells: Experimental analysis, International Journal of Hydrogen Energy, Volume 36, Issue 16, August 2011, Pages 10282-10287, ISSN: 0360-3199
3. Zuliani, N., Taccani, R., Microcogeneration system based on HTPEM fuel cell fuelled with natural gas: Performance analysis, Applied Energy, 2012, Vol. 97 pp. 802-808.
4. Zuliani N., Taccani R., Energy simulation model and parametric analysis of a micro cogeneration system based on a htpem fuel cell and battery storage, Proceeding of ICAE2013, International Conference on Applied Energy, Pretoria 2013.
5. R. Radu, R. Taccani, M. Scagliotti, C. Valli (2013). HT PEM fuel cell system fed with biogas: experimental characterizations. ECOS 2013, pp.1- 9, In: 26th International Conference on Efficiency, Cost, Optimization, Simulation and Environmental Impact of Energy Systems (ECOS). July 16-19, 2013, Guilin, Guangxi, China.
6. F. Valle, N. Zuliani, B. Marmioli, H. Amenitsch, R. Taccani (2014), SAXS Analysis of Catalyst Degradation in High Temperature PEM Fuel Cells Subjected to Accelerated Ageing Tests, Fuel cells, Wiley-VHC.